

A STUDY ON SMART FOOD WASTE RECYCLING SYSTEM  
USING BLACK SOLDIER FLY LARVAE

LEE WAI SENG

INNOVATION & DESIGN PROGRAMME  
NATIONAL UNIVERSITY OF SINGAPORE

2024

A STUDY ON SMART FOOD WASTE RECYCLING SYSTEM  
USING BLACK SOLDIER FLY LARVAE

LEE WAI SENG

A THESIS SUBMITTED FOR THE DEGREE OF  
BACHELOR OF ENGINEERING (ELECTRICAL ENGINEERING)  
INNOVATION & DESIGN PROGRAMME  
NATIONAL UNIVERSITY OF SINGAPORE

## DECLARATION

I hereby declare that this thesis is my original work and it has been written by me in its entirety.

I have duly acknowledged all the sources of information which have been used in this thesis.

Additionally, I disclose that a paraphrasing tool was employed to assist in constructing sentences and enhancing the clarity of the text, ensuring that adherence to academic integrity and the scholarly presentation of the work.



---

LEE WAI SENG

6 APRIL 2024

## **Acknowledgements**

The team would like to extend their appreciation to our project supervisor Dr Elliot Law, co-supervisors Ms. Wong Kah Wei and Mr. Adrian Fuhrmann, for their constructive guidance and sharing of valuable information and ideas while leading the team through this project. Their contributions have proven instrumental in fostering the development of fresh perspectives and steering us towards apt ideation procedures. Without their ongoing guidance and extensive expertise, our team would not have garnered the enriching learning experience or achieved success in our project.

# Table of Contents

Acknowledgements .....	4
Summary .....	8
List of Tables .....	10
List of Figures .....	11
1. Introduction/Background .....	13
1.1 Food Waste in Singapore and the issue.....	13
1.2 Current method of Processing Food Waste .....	15
1.3 Alternative methods of Processing Food Waste.....	16
1.3.1 Anaerobic Digestion .....	16
1.3.2 Insects .....	17
1.4 Why Insects.....	18
1.5 Why Black Soldier Fly Larvae.....	19
1.5.1 Circular Economy.....	20
1.5.2 Sustainability.....	21
1.5.3 Food Security.....	21
1.6 Current state of Black Soldier Fly Larvae .....	22
1.7 Our Vision .....	23
2. Our Solution.....	24
2.1 Project Objective.....	24
2.2 Target Venue.....	24
2.3 Value Proposition.....	25
2.4 Concept Design .....	26
2.5 Overall Design Requirements .....	27
2.6 Sub-systems .....	33
3. Electrical System Objective .....	34
3.1 Key Parameters for Considerations .....	34
3.1.1 Moisture Content of the substrate .....	35
3.1.2 Temperature in the substrate.....	35
3.1.3 Internal Air Temperature .....	36
3.1.4 Relative Humidity.....	36
3.1.5 Light Intensity.....	37
3.1.6 Gas Emission (Carbon Dioxide, CO <sub>2</sub> ) .....	37
3.1.7 pH Value.....	37
3.1.8 Mass of the Food Waste.....	38
3.1.9 Air Flow Rate .....	38

3.1.10 Larval Density per feeding container .....	38
4. Validation of Electronics Components .....	39
4.1 Methodology for Testing Selected Parameters .....	39
4.1.1 Moisture Content of the substrate .....	40
4.1.1.1 Results and analysis: Moisture Content of the substrate .....	41
4.1.2 Temperature in the substrate.....	43
4.1.2.1 Results and analysis: Temperature in the substrate .....	44
4.1.3 Internal Air Temperature .....	45
4.1.3.1 Results and analysis: Internal Air Temperature .....	45
4.1.4 Relative Humidity.....	46
4.1.4.1 Results and analysis: Relative Humidity .....	47
4.1.5 Light Intensity.....	48
4.1.5.1 Results and analysis: Light Intensity .....	50
4.1.6 Gas Emission (Carbon Dioxide, CO <sub>2</sub> ) .....	51
4.1.6.1 Results and analysis: Gas Emission (Carbon Dioxide, CO <sub>2</sub> ) .....	52
4.1.7 pH Value.....	53
4.1.8 Mass of the food waste .....	54
4.1.8.1 Results and analysis: Mass of the food waste.....	56
4.1.9 Air Flow Rate .....	58
4.1.9.1 Results and analysis: Air Flow Rate.....	59
5. Integration of Hardware and Software .....	60
5. 1 Experimental Phases and Laboratory Setting .....	60
5.1.1 Phase 1: Moisture Content & Temperature in the substrate .....	60
5.1.1.1 Results & Analysis: Moisture Content & Temperature in the substrate .....	62
5.1.2 Phase 1: pH value in the substrate .....	67
5.1.2.1 Results & Analysis: pH value in the substrate.....	68
5.1.2 Phase 2: Comprehensive Testing .....	70
5.1.2.1 Results & Analysis: Comprehensive Testing .....	72
5.1.3 Phase 3: Testing in the Constructed Reactor .....	72
5.1.3.1 Results & Analysis: Testing in the Constructed Reactor.....	90
5.2 Software Integration .....	90
6. Integration of Electronics.....	92
6.1 Overview of Electronics Integration .....	92
7. Future Works (Limitations & Recommendations for Improvement) .....	95
7.1 Exclusion of Light Sensor .....	95
7.2 Difficulties with CO <sub>2</sub> and Load Cells sensors Integration .....	95

<b>7.3 Adjustments for Mounting of pH Sensors .....</b>	<b>96</b>
<b>7.4 Sensor Maintenance and Harvesting: JST Connector Integration .....</b>	<b>97</b>
<b>References .....</b>	<b>100</b>
<b>Appendix .....</b>	<b>104</b>
<b>Appendix A: .....</b>	<b>104</b>
<b>Appendix B:.....</b>	<b>105</b>
<b>Appendix C:.....</b>	<b>107</b>
<b>Appendix D: .....</b>	<b>108</b>
<b>Appendix E:.....</b>	<b>109</b>

## **Summary**

The thesis titled "A Study on Smart Food Waste Recycling System Using Black Soldier Fly Larvae", introduces a novel approach to tackle Singapore's growing food waste dilemma with a focus on sustainability and efficient resource use. It explores the development and application of a compact reactor that employs Black Soldier Fly Larvae (BSFL) to turn food waste into useful products like animal feed and natural fertilizer. This study is set against the context of Singapore's food waste issue, where the majority of waste is not recycled but rather incinerated or dumped in landfills, leading to increased greenhouse gas emissions and the potential for landfills to reach capacity.

The thesis critiques the traditional methods of food waste disposal in Singapore, such as incineration and anaerobic digestion, pointing out their contributions to carbon emissions and their lack of effectiveness in resource recycling. Instead, it proposes using BSFL as a more sustainable and efficient option, capable of converting all food waste into usable products, thereby embracing the principles of a circular economy.

A significant part of the study focuses on the conceptualization, design, and trial of a BSFL reactor system intended for use directly at the sites where food waste is generated, like restaurants and food markets. The design aims for the reactor to be portable, easy to use, and versatile enough to fit different urban settings, encouraging the local processing of food waste and reducing the dependency on centralized disposal facilities. The thesis provides a detailed account of the reactor's design process, covering the technical specs, challenges faced, and the solutions devised to ensure the system's efficiency in breeding BSFL and converting food waste.

Additionally, the thesis thoroughly examines the reactor's components, with a particular emphasis on chassis and electronic design, each chosen for their effectiveness, durability, and user-friendliness. The study highlights the importance of a design that can be scaled and adapted to different operation

sizes and environments. The evolution of design is documented as a careful process of engineering and innovation, deeply rooted in the principles of sustainability and practical application.

Moreover, the study emphasizes the collaborative nature of the project, with advice and feedback from experts across fields like mechanical engineering, electronics, and waste management. This cross-disciplinary approach has greatly enriched the development of the reactor system, ensuring it is not only technologically sound but also meets the sustainability goals and industry requirements.

## List of Tables

<b>Table 1: Food Waste statistics over 5 years (2018-2022) Adapted from [1] .....</b>	<b>13</b>
<b>Table 2: Waste Statistics and Overall Recycling Adapted from [2] .....</b>	<b>14</b>
<b>Table 3: Design Requirement Table .....</b>	<b>27</b>
<b>Table 4: 10 Parameters .....</b>	<b>35</b>
<b>Table 5: Sensors .....</b>	<b>39</b>

# List of Figures

Figure 1: Tuas South Incineration Plant (TSIP). Adapted from [4] .....	15
Figure 2: Anaerobic Digestion Process. Adapted from [8] .....	17
Figure 3: Turning food waste into valuable materials. Adapted from [12].....	18
Figure 4: BSFL life cycle (Food waste). Adapted from [17] .....	20
Figure 5: Circular Economy Cycle .....	21
Figure 6: Current reactors in NUS.....	22
Figure 7: Our solution to deploy across Singapore .....	23
Figure 8: Lau Pa Sat hawker center. Adapted from [21].....	25
Figure 9: Operational Framework .....	26
Figure 10: EA building hallway in NUS .....	28
Figure 11: Lift in NUS .....	28
Figure 12: Hallways towards E2A building in NUS .....	29
Figure 13: E2A building slope in NUS .....	29
Figure 14: Container rack in laboratory (Only 11 containers on the rack) .....	30
Figure 15: Concept Ideas.....	31
Figure 16: CAD Design of reactor .....	32
Figure 17: One third design of reactor (Final Design) .....	33
Figure 18: Subsystems .....	34
Figure 19: Frass Samples .....	41
Figure 20: 60 grams of frass (0% water)	41
Figure 21: Graph of resistive sensor .....	42
Figure 22: Graph of capacitive sensor .....	43
Figure 23: Two different temperature conditions .....	44
Figure 24: Readings of DS18B20 sensor (with probe).....	44
Figure 25: Internal Air Temperature (Controlled Experiment) .....	45
Figure 26: Readings of DS18B20 sensor (without probe) .....	46
Figure 27: Standardized humidity environment (75%).....	47
Figure 28: Readings from DHT22.....	48
Figure 29: Position of the sensor.....	49
Figure 30: Pivoting .....	49
Figure 31: Readings from different positioning of sensor .....	50
Figure 32: Graph and readings of BH1750 .....	51
Figure 33: Carbon Dioxide Experiment.....	52
Figure 34: Graph of CO2 sensor .....	53
Figure 35: Calibration of pH sensors (with buffer solutions 4.0 and 7.0).....	54
Figure 36: CAD drawing of load cells bracket and bracket case.....	55
Figure 37: 3D printed load cells bracket and bracket case .....	55
Figure 38: Four load cells interconnected and mounted onto acrylic plate .....	56
Figure 39: Configuration of bottle and container in the cage (1264 grams) .....	57
Figure 40: Tare values .....	58
Figure 41: Readings recorded from the load cells .....	58
Figure 42: Combination of food waste, peanut skins, and larvae.....	61
Figure 43: Phase 1 setup configuration (Moisture and Temperature).....	62
Figure 44: Moisture readings .....	64
Figure 45: Temperature Readings .....	66

<b>Figure 46: Phase 1 setup configuration (pH) .....</b>	67
<b>Figure 47: pH value Readings.....</b>	69
<b>Figure 48: Combination of food waste, peanut skins, and larvae.....</b>	70
<b>Figure 49: Phase 2 setup configuration .....</b>	71
<b>Figure 50: Electronics Box .....</b>	73
<b>Figure 51: Arduino and protoboard shield .....</b>	74
<b>Figure 52: Micro SD card module connected to Arduino.....</b>	75
<b>Figure 53: Steps for preparing necessary cables .....</b>	76
<b>Figure 54: Connected all sensors to Arduino (exception of fans) .....</b>	77
<b>Figure 55: Connection of fans to socket.....</b>	77
<b>Figure 56: Capacitive Moisture Sensors .....</b>	79
<b>Figure 57: Temperature Sensors (DS18B20).....</b>	79
<b>Figure 58: Mounting of sensors (Moisture, temperature, and pH).....</b>	80
<b>Figure 59: Mounting of sensors at chimney, inlet (Temperature, Methane, and Relative Humidity)</b>	81
<b>Figure 60: Mounting of sensor at outlet (Temperature) .....</b>	82
<b>Figure 61: Back view of reactor.....</b>	83
<b>Figure 62: Back view of reactor (Zoom in).....</b>	83
<b>Figure 63: Vents for ventilation .....</b>	84
<b>Figure 64: Wire mesh installed onto the vents .....</b>	85
<b>Figure 65: Mixture of food waste and cocopeat .....</b>	85
<b>Figure 66: Weighing of food waste .....</b>	86
<b>Figure 67: Food waste and BSFL.....</b>	86
<b>Figure 68: Post loading configuration .....</b>	87
<b>Figure 69: Close-up of the BSFL in the container.....</b>	88
<b>Figure 70: Acceptable height of food waste.....</b>	89
<b>Figure 71: Not acceptable height of food waste .....</b>	89
<b>Figure 72: Flow Chart: Bioconversion process.....</b>	91
<b>Figure 73: Overview of sensors in pictorial diagram .....</b>	93
<b>Figure 74: Implemented and soldered an LED.....</b>	94
<b>Figure 75: Inclusion of LED in the pictorial diagram .....</b>	94
<b>Figure 76: Spacing constraints in between cages .....</b>	96
<b>Figure 77: Phase 1: Condition of sensors after experiment (Larvae on sensors) .....</b>	98
<b>Figure 78: Phase 2: Condition of sensors.....</b>	98
<b>Figure 79: Dupont head Connectors.....</b>	99
<b>Figure 80: JST Connectors .....</b>	99
<b>Figure 81: Total Food waste Calculation .....</b>	104
<b>Figure 82: Calculation of food waste generated from hawker centre .....</b>	105
<b>Figure 83: Sensors positions (Moisture and Temperature sensors) .....</b>	107
<b>Figure 84: Schematic Diagram.....</b>	108
<b>Figure 85 Chart for BSFL Bioconversion Process.....</b>	109
<b>Figure 86: Controllable and Influential Parameters .....</b>	110

## 1. Introduction/Background

### 1.1 Food Waste in Singapore and the issue

Food waste constitutes a significant proportion of Singapore's overall waste, and there has been a noteworthy rise of around 6.55% in the past five years, spanning from 2018 to 2022 (refer to Appendix A1 for calculation). Additionally, the recycling rate for food waste has remained relatively constant during this same period as shown in Table 1. In the year 2022, a substantial 813,000 tons of food waste were generated, highlighting a concerning trend in unsustainable consumption as seen in Table 2. To provide a clearer picture, this amount equates to approximately two bowls of rice per person every day. Unfortunately, despite the magnitude of this issue, only 18% of the total food waste generated underwent recycling initiatives during that same year as seen in Table 2. The remaining portion was directed to incineration plants for processing before ultimately finding its way to Singapore's sole landfill, the Pulau Semakau Landfill. This emphasizes the pressing need for increased efforts in waste reduction, recycling, and sustainable practices to address the environmental impact of food waste in the region.

*Table 1: Food Waste statistics over 5 years (2018-2022) Adapted from [1]*

Year	Food Waste Disposed of ('000 tonnes)	Food Waste Recycled ('000 tonnes)	Total Food Waste Generated ('000 tonnes)	Recycling Rate (%)
2022	667	146	813	18%
2021	663	154	817	19%
2020	539	126	665	19%
2019	607	136	744	18%
2018	637	126	763	17%

**Table 2: Waste Statistics and Overall Recycling Adapted from [2]**

2022 Waste Statistics and Overall Recycling Table				
Waste Type	Total Generated ('000 tonnes)	Total Recycled ('000 tonnes)	Recycling Rate	Total Disposed ('000 tonnes)
Ferrous metal	1,338	1,331	99%	7
Paper/Cardboard	1,064	394	37%	671
Construction & Demolition	1,424	1,419	99%	5
Plastics	1,001	57	6%	944
Food	813	146	18%	667
Horticultural	221	188	85%	32
Wood	419	298	71%	121
Ash & sludge	241	27	11%	213
Textile/Leather	254	5	2%	249
Used slag	169	166	99%	2
Non-ferrous metal	92	91	98%	2
Glass	73	11	14%	63
Scrap tyres	26	25	95%	1
Others (stones, ceramics, etc.)	249	30	N.A. <sup>1</sup>	219
<b>Overall</b>	<b>7,385</b>	<b>4,188</b>	<b>57%</b>	<b>3,197</b>

The consequences of food waste in Singapore reach beyond disposal considerations, with a significant environmental impact that amplifies the carbon footprint, exacerbates global warming, and contributes to climate change. Moreover, the implications for food security in a nation heavily reliant on importing more than 90% of its food supply are apparent [3]. Escalating food waste not only strains the environment but also poses a threat to food security, as the nation's heavy reliance on imports renders it vulnerable to disruptions in the global food supply chain. In light of these implications, there is an urgent need to adopt a comprehensive strategy that encompasses individual accountability, sustainable practices, and efficient waste management to tackle the intricate challenge posed by escalating food waste.

## 1.2 Current method of Processing Food Waste

Presently, non-recycled food waste undergoes the default processing method of incineration, followed by transporting the ashes and remnants to landfills. This method, implemented at Tuas South Incineration Plant (TSIP) as shown in Figure 1, Singapore's largest Waste-To-Energy plant, involves the reduction of waste by up to 90%, markedly decreasing its original volume both in landfills and within the country. On a daily basis, TSIP processes waste from around 600 refuse trucks, solidifying its role in Singapore's waste management system [4]. However, this conventional method faces sustainability challenges for three main reasons. Firstly, the extensive transportation to incineration plants and the incineration process contribute to increased carbon emissions, with about 15% of Singapore's greenhouse gas emissions in 2022 originating from incineration [5]. The annual transportation of food waste alone produces enough CO<sub>2</sub> to fill 39 million passenger buses. Secondly, despite incineration, the residual products (ash plus incombustible materials) ultimately contribute to landfill, projected to reach capacity by 2035, even though the initial plan was for it to last until 2045 [6]. Lastly, this method compromises our food security capabilities. Given Singapore's limited land resources and its dependence on importing 90% of its food, the allocation of land for waste storage and incineration restricts the already constrained space available for local food production, presenting obstacles to sustainable agriculture [7].



*Figure 1: Tuas South Incineration Plant (TSIP). Adapted from [4]*

## 1.3 Alternative methods of Processing Food Waste

### 1.3.1 Anaerobic Digestion

Anaerobic digestion is a biological process that occurs within a sealed, oxygen-free container known as a digester. In this process, organic materials, including food waste, are broken down by microorganisms like bacteria and archaea. The outcome is the conversion of food waste into biogas, mainly composed of methane and carbon dioxide, along with digestate [8]. While Singapore utilizes anaerobic digestion as an alternative method for recycling food waste, it is acknowledged that this might not be the most optimal approach. Despite its advantages, such as capturing biogas for renewable energy and obtaining digestate for soil conditioning and fertilization, there are notable drawbacks. The cost of construction is high, with estimates indicating an average cost of \$1.2 million dollars [9]. This is notably higher compared to alternative waste management methods, which typically incur lower initial investment costs. Challenges in certain locations primarily revolve around logistical constraints related to sludge disposal. Limited land availability, stringent environmental regulations, and community opposition in densely populated areas pose significant hurdles to establishing anaerobic digestion facilities. Additionally, the transportation of sludge to appropriate disposal sites can be logically complex and costly, particularly in regions with inadequate infrastructure. Moreover, while biogas itself is not inherently corrosive, it can contain trace amounts of corrosive gases such as hydrogen sulfide (H<sub>2</sub>S), which may pose risks to equipment and infrastructure if not properly managed. Therefore, the safe handling and storage of biogas are crucial considerations in anaerobic digestion facilities to mitigate potential corrosion issues [10]. These considerations underscore the need for a thorough evaluation of alternative methods in Singapore's approach to recycling food waste.

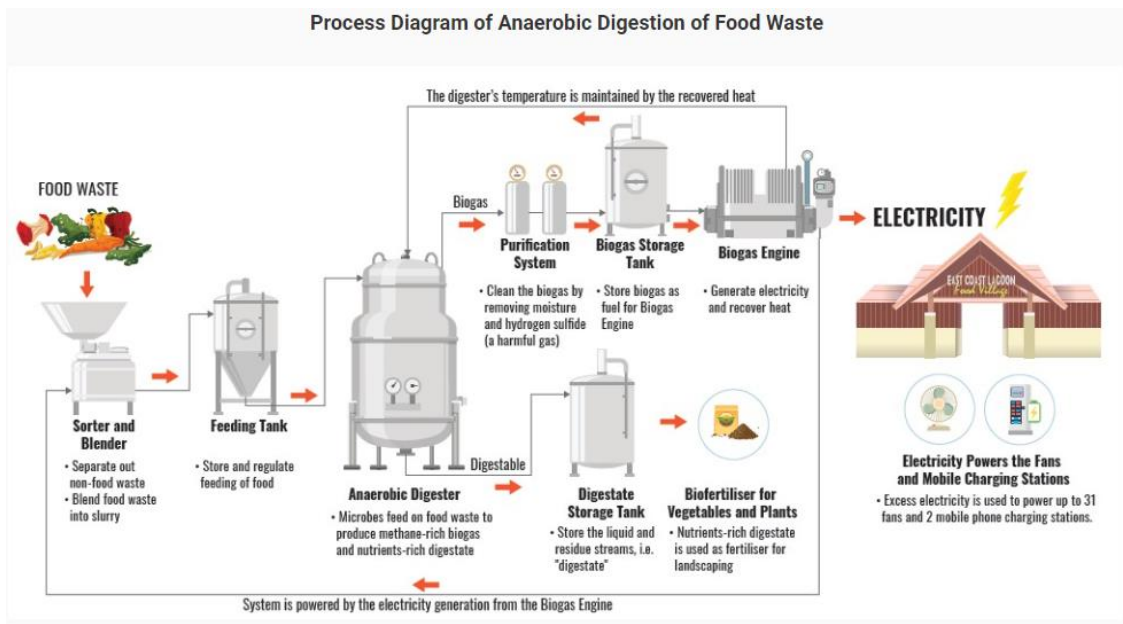


**Figure 2: Anaerobic Digestion Process. Adapted from [8]**

### 1.3.2 Insects

The exploration of sustainable food waste management has led to the recognition of insect bioconversion as a significant and innovative solution. Insects, such as black soldier flies (BSF) or mealworms, exhibit a natural proficiency in rapidly breaking down diverse food waste materials, yielding valuable nutrient-rich byproducts like larvae or frass [11]. This approach not only diverts food waste from landfills but also promotes recycling and resource recovery, providing sustainable alternatives for agriculture, including fertilizer and animal feed, as illustrated in Figure 3.

### How insects turn low value food waste into high value protein

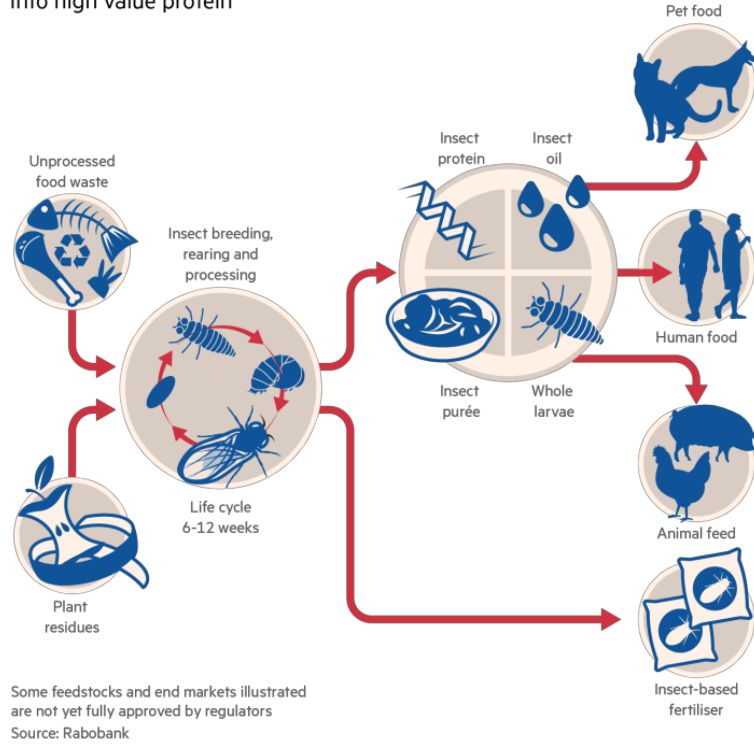


**Figure 3: Turning food waste into valuable materials. Adapted from [12]**

## 1.4 Why Insects

Integrating insects into our food waste processing strategy aligns with our sustainability goals and addresses crucial environmental challenges. Operating on circular economy principles, insects serve as an eco-friendly alternative to incineration. Their efficient bioconversion process transforms waste into valuable resources, diminishing our reliance on landfills and reducing overall environmental impact. The choice of insects extends beyond waste management, contributing to enhanced food security by producing byproducts like protein-rich animal feed and nutrient-rich fertilizers [10]. This comprehensive approach highlights the manifold benefits of insect bioconversion in waste management, emphasizing its pivotal role in environmental sustainability and local food security.

## 1.5 Why Black Soldier Fly Larvae

The choice of Black Soldier Fly Larvae (BSFL) larvae for our project is underpinned by their exceptional attributes that directly support our waste management objectives. Firstly, BSFL exhibits a remarkable ability for rapid organic matter consumption, ensuring an expeditious waste reduction process by processing up to four times their body weight daily [13]. Additionally, their versatility is highlighted in their capacity to digest a diverse range of food waste, including meats, dairy, and fats, setting them apart from other counterparts [14]. Most notably, the highly efficient conversion rate of BSFL, reaching 100%, guarantees that all processed food waste is transformed into biomass [15]. While mealworms excel and are adept at waste decomposition, they exhibit limitations, displaying selectivity in their food preferences by not consuming greasy food and highly acidic fruit, which are generally well-tolerated by BSFL [16]. This comprehensive conversion process aligns seamlessly with our commitment to sustainable waste management practices, leaving no remnants for disposal in landfills.

After the BSF eggs hatch, the resulting hatchlings are carefully maintained in a controlled and sheltered environment for five days until they reach the Five-Day-Old-Larvae (5-DOL) stage. This stage is crucial as it represents the primary feeding phase for BSFL, during which they accumulate fat reserves and protein essential for subsequent development [15]. Generally, BSFL can efficiently complete the composting process within approximately three weeks as shown in Figure 4. However, the precise timeline is subject to variations influenced by factors such as temperature, the type of food waste, and larval density [11]. Optimizing environmental parameters such as temperature, ensuring suitable moisture levels, and regulating larval density are crucial factors in enhancing the efficiency of BSFL digestion. These considerations allow for the maximization of BSFL's capacity to consume organic matter. Consequently, meticulous control of environmental parameters is imperative for achieving quicker processing times and fostering more sustainable waste management outcomes within project framework.

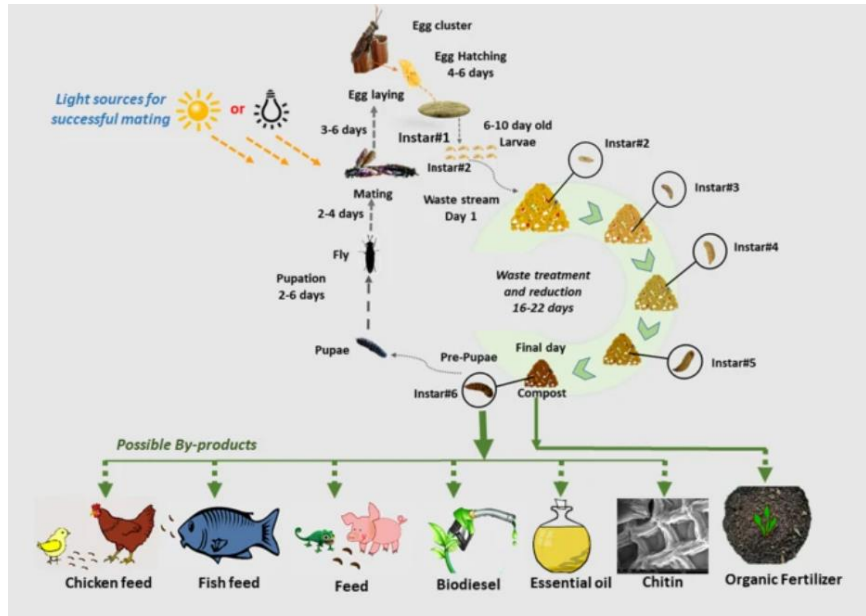


**Figure 4: BSFL life cycle (Food waste). Adapted from [17]**

### 1.5.1 Circular Economy

In the context of circular economy, the use of BSFL to treat food waste creates products that can be used to produce food. Starting with the feeding of food waste to the insect larvae, the process leads to the accumulation of shedding, and feces known as frass. Upon harvesting, the larvae can be dehydrated to create animal feed, while the frass serves as a nutrient-rich fertilizer for plants and crops [18]. As these plants and crops grow, they become a food source for both animals and humans, completing the cycle, as illustrated in Figure 5. This circular economy not only minimizes waste sent to landfills but also maximizes the value extracted from food waste.

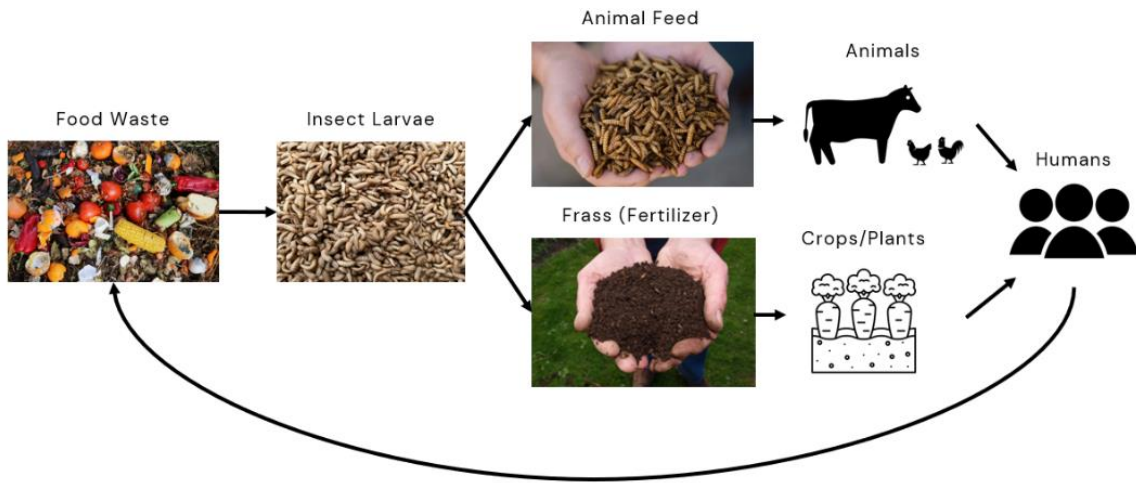


**Figure 5: Circular Economy Cycle**

### 1.5.2 Sustainability

The use of BSFL for food waste management contributes significantly to sustainability. By efficiently converting food waste into biomass, BSFL reduces the volume of waste destined for incineration and landfill disposal. This process aligns with sustainable practices, as it decreases the environmental impact associated with traditional waste disposal methods. The reduction in waste sent to incineration plants also contributes to the conservation of natural resources and minimizes carbon emissions, enhancing the overall ecological sustainability of our waste management approach.

### 1.5.3 Food Security

In addressing food security, the use of BSFL to treat food waste contributes to the promotion of local and sustainable food production. By converting food waste into valuable resources such as animal feed and fertilizers through BSFL bioconversion, such a solution contributes to the creation of a more resilient and self-sufficient food system. This approach reduces the reliance on external sources for food production inputs while simultaneously mitigating the impact of food waste on the environment. The improved efficiency in waste management enhances the overall stability and security of our local food supply chain.

## 1.6 Current state of Black Soldier Fly Larvae

Currently in Singapore, there are initiatives utilizing BSFL for food waste management, but predominantly, these initiatives are small-scale or laboratory-based, often featuring a centralized facility. Notably, the collaborative efforts between ETH Zurich, the National University of Singapore (NUS), and Nanyang Technological University (NTU) are actively engaged in researching and applying BSFL for food waste management and sustainable food production within urban systems [19]. The ongoing lab-scale research project involves specialized reactors designed to optimize the conditions for BSFL during their feeding period. Illustrated in Figure 6 below, these reactors incorporate sensors and equipment to monitor and facilitate adjustments to internal conditions.



*Figure 6: Current reactors in NUS*

## 1.7 Our Vision

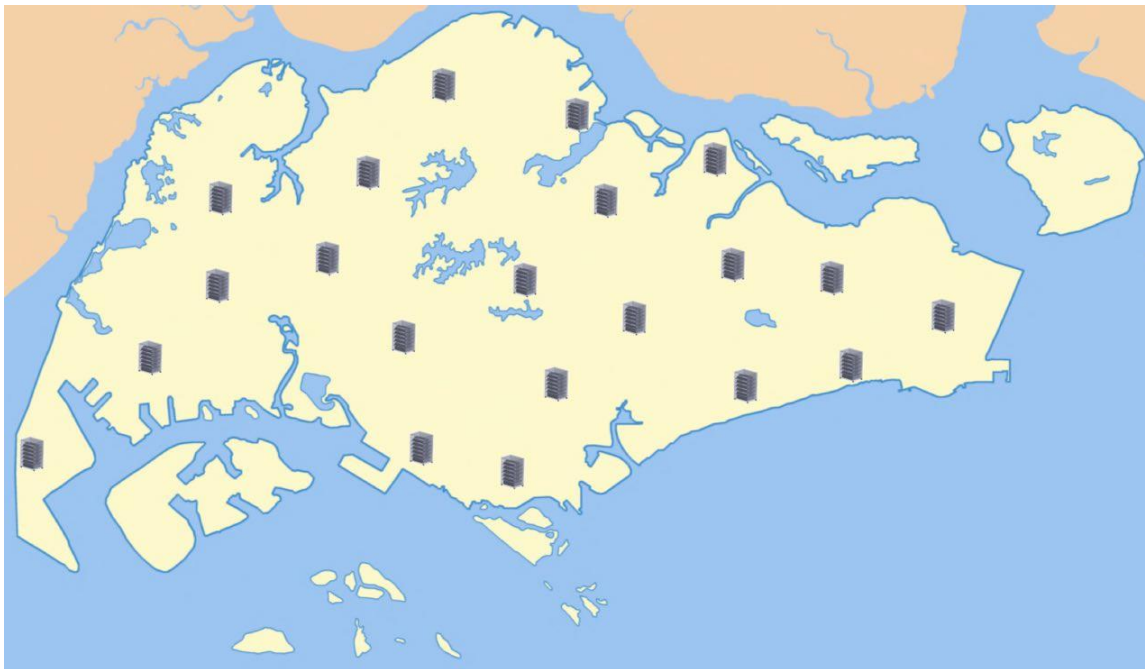


*Figure 7: Our solution to deploy across Singapore*

In order to integrate BSFL into food waste management effectively, we propose a decentralized deployment on a broader scale, deviating from a centralized facility model. Our vision is to establish multiple independent reactors strategically positioned in eateries and hawker centers across Singapore. This approach is designed to facilitate on-site food waste processing, ensuring simultaneous and efficient disposal without the need for extensive transportation volumes. This decentralized strategy aligns with our goal of enhancing sustainability and operational efficiency in food waste management practices. Furthermore, with the implementation of legislation mandating the allocation of space for on-site food waste treatment systems in new buildings since January 1, 2024, our decentralized approach not only complements regulatory requirements but also contributes significantly to Singapore's ongoing efforts in addressing food waste management comprehensively.

## **2. Our Solution**

### **2.1 Project Objective**

The primary goal of this project is to develop a scale-up version of a deployable reactor capable of on-site treatment processes with minimal human labor. Our objective is to enable food establishments in Singapore to leverage BSFL technology for the efficient processing of their food waste. This initiative serves as a crucial link between laboratory research and practical implementation for the consumer public's benefit.

Given the limited land availability in Singapore, a key focus is placed on maximizing the simultaneous processing of food waste while minimizing land usage. Incorporating automation into the reactor is a vital aspect of our approach, aiming to reduce the labor required for the process while maintaining optimal efficiency. This project strives to provide a sustainable solution to food waste management in the region, aligning with our commitment to innovation and environmental responsibility.

### **2.2 Target Venue**

This prompted us to focus on hawker centers, recognizing them as one of the primary sources of food waste generation. Given that there are approximately 110 hawker centers in Singapore as of 2022, we can deduce that these hawker centers alone account for roughly 30.1% of the total food waste generated in the country (refer to Appendix A2 for calculation) [20]. This figure underscores the substantial impact of hawker centers on the issue of food waste. Opting for a decentralized system and conducting bioprocessing on-site not only addresses this issue directly but also results in significant cost savings. The implementation of this approach is anticipated to lead to an 80-90% reduction in food waste mass, concurrently minimizing both transportation expenses and labor requirements.



*Figure 8: Lau Pa Sat hawker center. Adapted from [21]*

## 2.3 Value Proposition

Our project holds the potential to bring significant value to various stakeholders. Food establishments stand to benefit by having an alternative solution for managing their food waste. Instead of having to engage public waste collectors to collect their waste which will be sent to incineration plants, they can now derive value from the waste by utilizing the reactor and selling its byproducts. The primary beneficiaries of these byproducts are local farms, which can use the nutrient-rich frass as organic fertilizer, enhancing soil quality, and utilize the larvae as a sustainable and nutritious source of animal feed. Additionally, the government stands to gain by having a reduced burden of food waste to manage, leading to a decrease in the volume of waste sent to landfills or incineration facilities. This not only extends the lifespan of existing waste infrastructure but also lowers waste management costs. Furthermore, promoting the use of BSFL in animal feed production supports sustainable agriculture, potentially reducing the need to import food from other countries.

## 2.4 Concept Design

The operational concept of the reactor involves a systematic flow of processes as illustrated in Figure 9. Initially, staff from food establishments drain excess fluids from food waste and deposit them into designated bins. On the left of the flow chart, it represents the conventional treatment process, where these bins are transported to a central collection point for routine waste disposal. Conversely, the right side represents the innovative solution of recycling food waste using BSFL. In this process, the food waste is directed into the reactor, where both the food waste and BSFL coexist within a designated container. After completing one treatment cycle, during which the food waste undergoes a bioconversion process facilitated by BSFL, the subsequent step involves harvesting. This includes extracting the resulting high-protein biomass and frass, which have potential agricultural uses, followed by replacing the containers with clean ones.

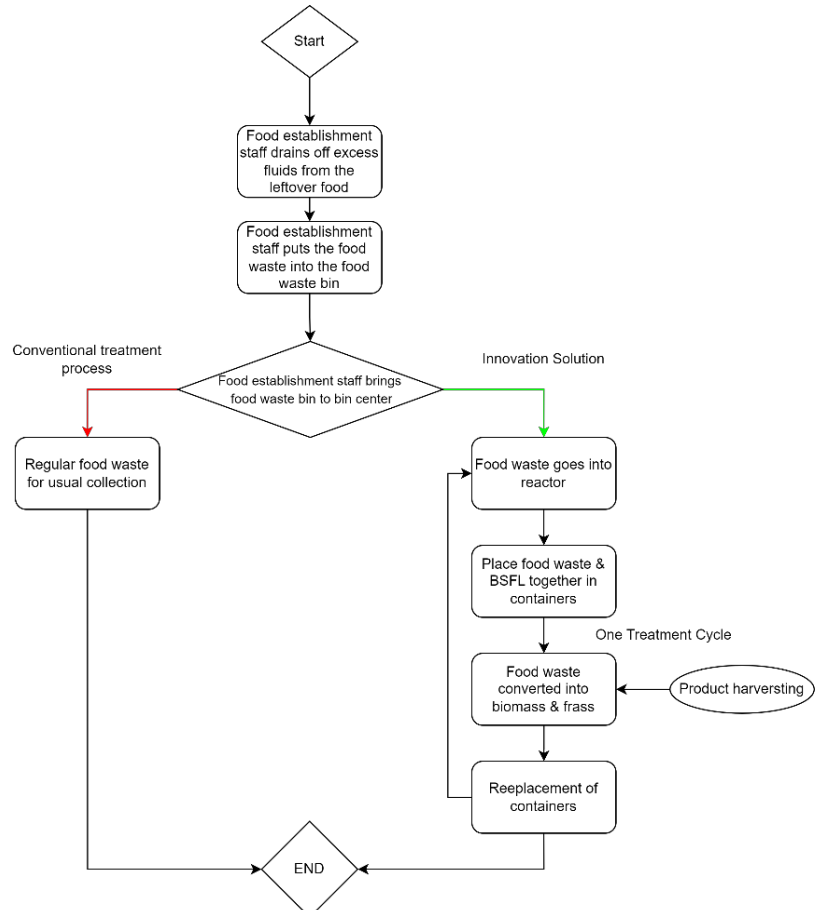


**Figure 9: Operational Framework**

## 2.5 Overall Design Requirements

**Table 3: Design Requirement Table**

Criteria	Requirements	Rationale
Size	Maximum Width of 85cm	Given that we have a decentralized application, our solution has to be portable. With the full derivation of the Size and Weight criteria in Section 6.2 – Sizing Constraints
	Maximum Depth of 120cm	
	Maximum Height of 200cm	
Weight	Maximum Weight of 400kg (when fully loaded with food waste and BSFL)	
Optimal Bioconversion Performance	Achieve moisture content of 70 – 80%	This is the ideal moisture content range of food waste for BSFL
	Achieve relative humidity of 40 – 70%	The mortality was 62%, 26% and 3% at a relative humidity of 25%, 40% and 70%, respectively
	Achieve environmental temperature of between 25 - 30°C	This is the optimum temperature range for the growth of BSFL
	Ensure Light Intensity of 0 Lux	Presence of light can affect the feeding rate of the BSFL which will affect its developmental growth
Reduction in Organic food waste mass	80 – 90% reduction in organic mass 50 – 80% volume reduction	Effective and sustainable means of food waste management by reducing cost and carbon footprint due to waste transportation as well as designated land for waste management facilities and landfill

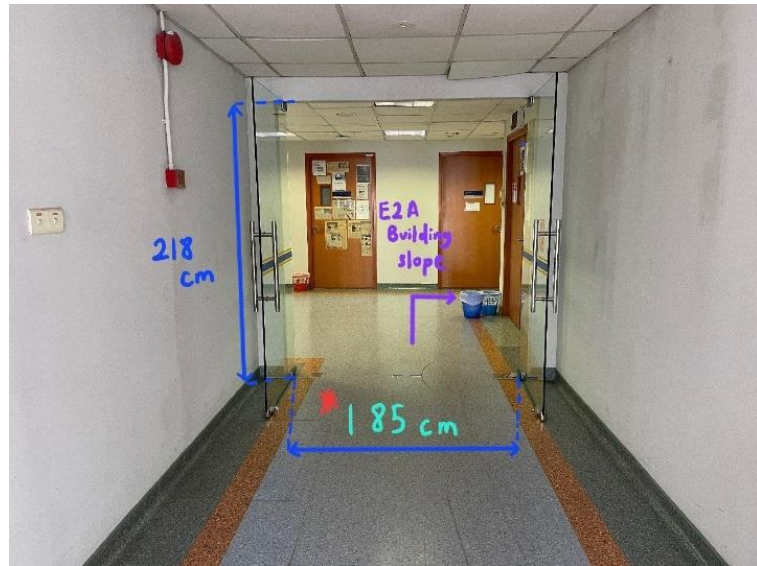
In establishing the comprehensive design parameters for our reactor, our goal was to accommodate a minimum of one day's worth of food waste. Through our investigation, focusing on the Utown food court at NUS, we found an average daily generation of 120 liters, equating to 188 kg of food waste. The subsequent challenge involved determining the reactor size for optimal portability, akin to a vending machine. Adhering to the Building and Construction Authority standards for pathways, doors, and lifts, we ensured that the dimensions aligned with the NUS environment, as illustrated in Figures 10 to 13.



Figure 10: EA building hallway in NUS



Figure 11: Lift in NUS



**Figure 12: Hallways towards E2A building in NUS**



**Figure 13: E2A building slope in NUS**

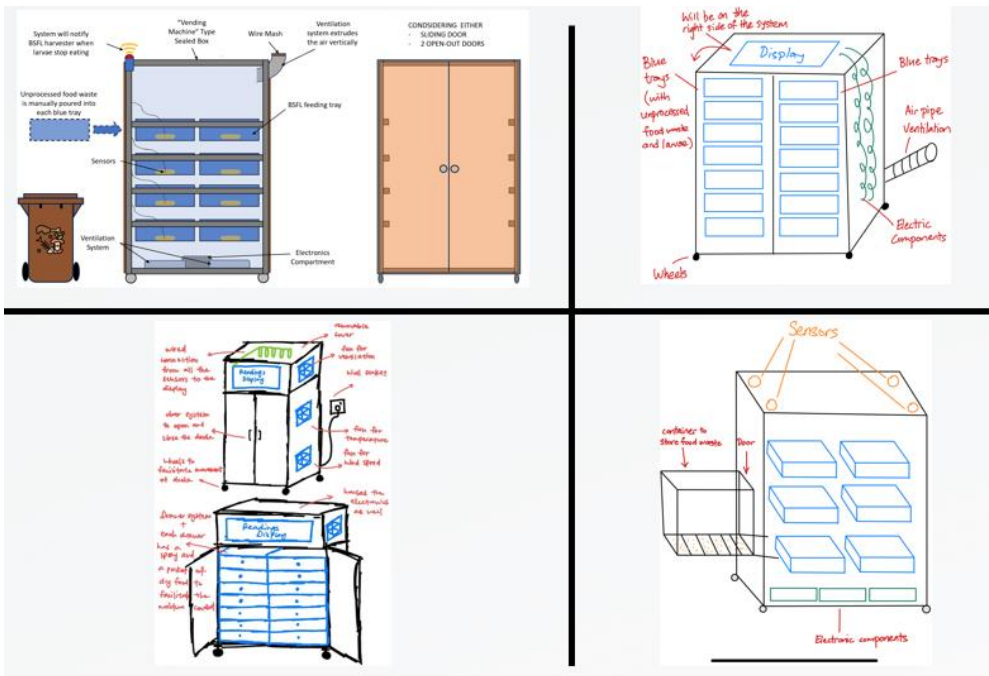
Currently, there are two distinct setups in place. The first configuration comprises three containers inside a box, specifically designed for bioconversion experiments in a controlled environment. This setup allows for the exploration of various parameters and control methods, as illustrated in Figure 6. Conversely, the second setup features multiple containers arranged on a rack, operating within uncontrolled environmental conditions that mirror the ambient lab surroundings, as illustrated in

Figure 14. Unlike the previous, this setup is not intended for experimentation, rather, its primary purpose is to sustain the BSF colony. These setups are situated within the NUS laboratory, which serves as the venue for the BSFL bioconversion research conducted by ETH Zurich, in collaboration with the Singapore-ETH Centre and the National University of Singapore, supported by funding from the National Research Foundation of Singapore.



***Figure 14: Container rack in laboratory (Only 11 containers on the rack)***

In our group, we looked to the existing reactor and rack system used in the laboratory as a starting point to brainstorm designs for our planned reactor, making sure to stay within the size and regulations provided by the BCA. After pooling our thoughts together, we noticed that most of our designs were based on using several bins to hold the food waste. We imagined these bins arranged at different heights within the framework, all encased by an external housing that would wrap around the whole setup.



**Figure 15: Concept Ideas**

Leveraging insights from our research and drawing inspiration from the laboratory equipment, we have concluded the design for the upcoming reactor implementation with the size of 120cm x 85cm x 200cm and a maximum weight of 400kg. The conceptual design is visually represented in Figure 15 below.

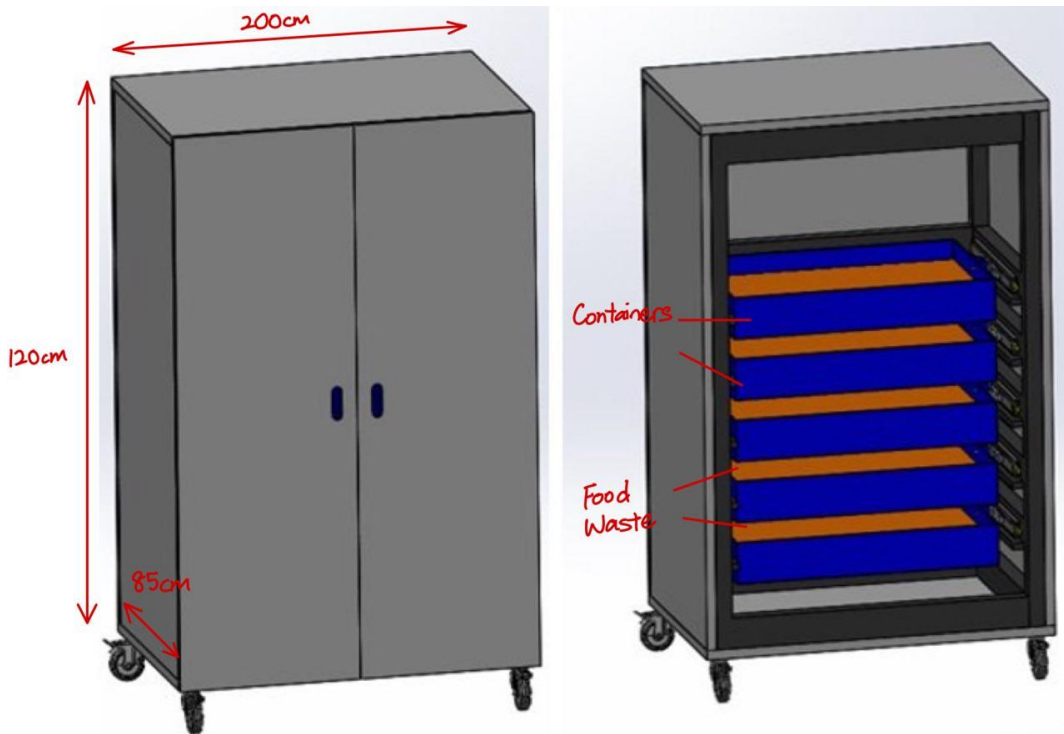


*Figure 16: CAD Design of reactor*

When revising the original design, we made crucial changes to better fit the project's limits and aims. The chassis size was greatly reduced because we chose to use lab containers and changed how many we needed. This brought the design down to a third of its starting size, now with six containers. To prevent damage from gases like methane that could build up inside, we positioned the electronics at the bottom of the structure, as illustrated in Figure 17. These changes were mainly due to the limited resources our group had. For instance, the number of larvae we could get from the lab was limited since they also needed them for their research, and they're not bred on a large scale. The workshop where we make the reactor parts also had its constraints, as it needed time to get and make the materials we needed while dealing with other projects as well. Given these obstacles, we downsized the reactor's design to a third of its size. This was not just to work around the scarcity of larvae and workshop capacity but also to make a reactor that's really useful for research. By doing this, we are making sure the reactor is not just another tool, but a significant aid for lab researchers to carry out studies and collect data to finetune the reactor's functioning. With this focused strategy, we are

aiming to add valuable insights to the progress of eco-friendly waste management, despite the limitations we're up against.

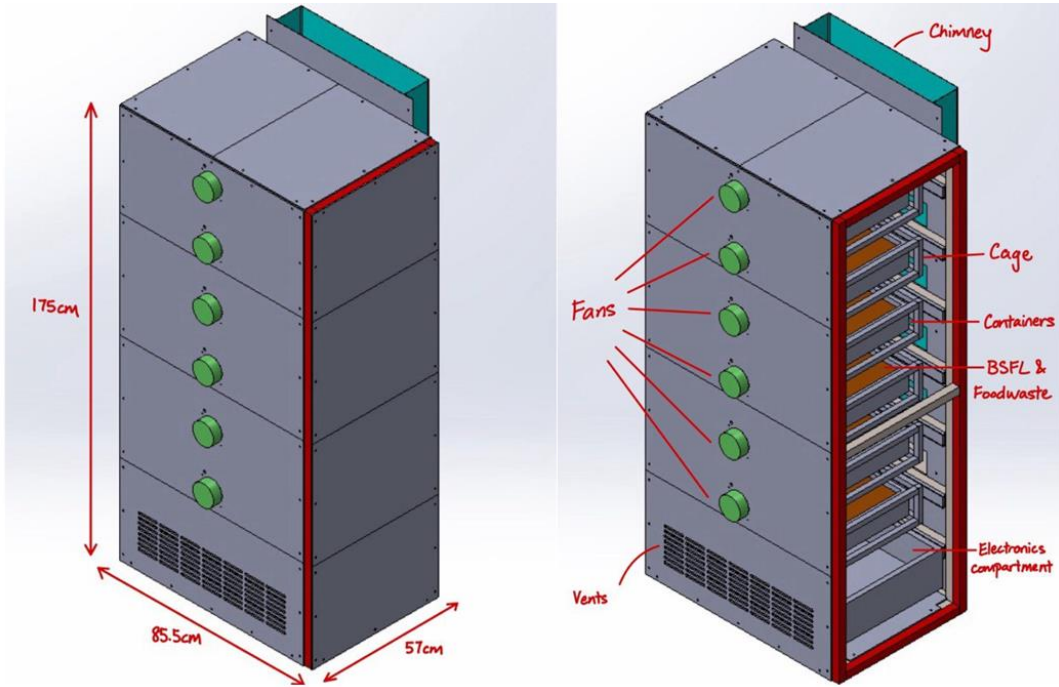


*Figure 17: One third design of reactor (Final Design)*

## 2.6 Sub-systems

Our project is organized into two main subsystems: electronics and mechanical. The electronics subsystem is further divided into three areas of work. The first one is data acquisition and processing which includes tasks like sensor selection, calibration, and data extraction. The second area, focused on software, manages system programming, and facilitates the automatic adjustment of internal conditions. The third area is responsible for overseeing the system's power supply and overall electronics integration. Concurrently, the mechanical subsystem is divided into two key areas of work. The first area concentrates on the design and construction of the chassis and container, while the second area investigates ventilation of our reactor. This structured approach ensures a thorough and efficient integration of both electronic and mechanical elements in our project, as illustrated in Figure

18. In the subsequent section, I will specifically concentrate on the electronic components and provide further information.

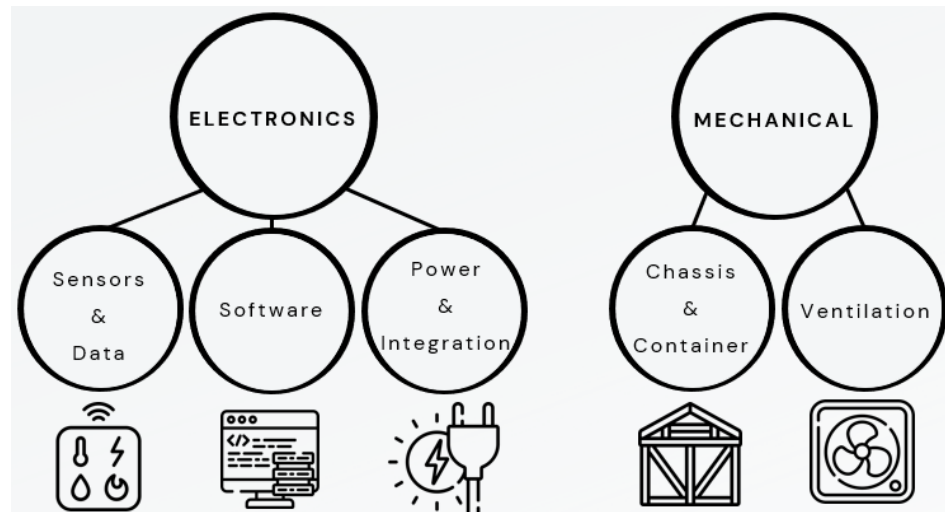


*Figure 18: Subsystems*

### 3. Electrical System Objective

To create an optimal rearing environment for BSFL during the bioconversion process, attention must be given to key parameters influencing their growth and development. This involves maintaining precise conditions within the reactor, including temperature, humidity, and substrate composition, to support the larvae's well-being [22]. Adequate and balanced nutrition, derived from the food waste substrate, is crucial for their optimal development. Strategic container design and placement facilitate efficient interaction between the larvae and food waste. Regular monitoring and adjustment of these parameters throughout the bioconversion process contribute to a thriving BSFL population. Implementing a systematic approach to these considerations ensures a sustainable and effective bioconversion process, maximizing the benefits of BSFL in waste management.

#### 3.1 Key Parameters for Considerations

Upon research, we have identified 10 parameters integral to fostering the well-being of BSFL. Our primary focus centers on the top six parameters, deemed crucial in ensuring the survival and thriving

of the larvae. Simultaneously, we acknowledge four additional parameters, although considered, are deemed to carry less significance in the context of the bioconversion process within our system. A breakdown of these parameters and their respective importance is presented in Table 3. This strategic identification lays the foundation of our subsequent focus on testing and optimizing the critical factors influencing the rearing environment for BSFL.

**Table 4: 10 Parameters**

Parameters	Target Values	Rational
Moisture Content of the substrate	60% - 80%	Survival + Separation
Temperature in the substrate	25 – 50%	Survival
Internal Air Temperature	25 – 30%	
Relative Humidity	70% - 85%	
Gas Emission (CO <sub>2</sub> , CH <sub>4</sub> , NH <sub>3</sub> )	-	Survival + Indication for harvesting & Monitor gas flow
pH Value of Substrate	6 - 8	Indication for harvesting
Light Intensity	0	Indication a significant influx of incoming light
Mass of the Food waste	-	Evaluate Bio-convertors effectiveness in reducing impact of GHG (Transportation)
Air Flow Rate	-	Collect Additional Information
Larval Density per feeding pod/ container	1.2 Larvae/cm <sup>2</sup> to 5 Larvae/cm <sup>2</sup>	Perform by the BSFL loader (Manual)

### 3.1.1 Moisture Content of the substrate

Excessive moisture can hinder larval thriving by limiting air circulation, creating anaerobic conditions. Additionally, BSFL are averse to a wet and clumpy substrate, introducing an unfavorable texture that discourages their feeding activities [22]. However, inadequate moisture content poses risks of dehydration in BSFL, putting their health and vitality at risk. Therefore, maintaining the optimal range of 60% to 80% is crucial [15].

### 3.1.2 Temperature in the substrate

Temperature range is intricately connected to bioconversion efficiency, as ideal substrate temperatures foster microbial activity essential for the breakdown of organic matter, enhancing the overall effectiveness of the bioconversion process. However, it is important to note that the BSFL are

sensitive to temperature variations in their substrate. If the substrate temperature falls below the optimal range, the BSFL's metabolic rate decreases, leading to slower growth and prolonged exposure to cold temperatures can even result in death [15]. Conversely, if the substrate temperature exceeds the optimal range, several issues may arise. Higher temperatures can accelerate the metabolic rates of the larvae, leading to increased activity and energy consumption. However, the larvae may experience heat stress at temperatures significantly above the optimal range, which can lead to dehydration, reduced feeding activity, and mortality. Additionally, extremely high temperatures can also promote the growth of harmful bacteria and fungi in the substrate, posing health risks to the BSFL population. Therefore, maintaining an optimal substrate temperature between 25°C to 50°C is crucial for promoting healthy growth and development of the BSFL, as well as ensuring optimal bioconversion efficiency [15].

### **3.1.3 Internal Air Temperature**

Monitoring and regulating the internal air temperature in the reactor enables precise environmental control. If the temperature becomes excessively high, the larvae may crawl away and search for cooler areas. Conversely, if it becomes too cold, the larvae may reduce their metabolism and eat less, slowing down their overall development [15]. Therefore, maintaining internal air temperature within the optimal range of 24°C to 30°C is crucial [15].

### **3.1.4 Relative Humidity**

Effective control of humidity is paramount, given the larvae's high sensitivity to dehydration, which can compromise their vitality and hinder overall growth. In excessively humid conditions, the larvae encounter respiratory challenges, as the pores in their exoskeleton become compromised, impeding their ability to breathe [23]. Therefore, maintaining an optimal relative humidity range of 70% to 85% is crucial [11].

### **3.1.5 Light Intensity**

In a shaded environment with minimal light, larvae exhibit a natural aversion to light and actively seek areas away from sunlight. When exposed to light, larvae tend to move deeper into the layer of food to escape [15]. This behavior underscores the significance of providing a dark and shaded setting for BSFL, aligning with their natural instincts and preferences. Therefore, maintaining a light intensity of zero lux is crucial.

### **3.1.6 Gas Emission (Carbon Dioxide, CO<sub>2</sub>)**

Carbon Dioxide, CO<sub>2</sub>, serves as an indirect indicator of microbial activity during the bioconversion process. Optimal CO<sub>2</sub> levels support efficient breakdown of organic matter by promoting favorable microbial conditions, contributing to the overall success of BSFL rearing. However, excessive CO<sub>2</sub> can lead to poor ventilation, hindering larvae development and potentially causing stress or mortality [22]. Monitoring CO<sub>2</sub> levels allows for adjustments to maintain an environment conducive to bioconversion while preventing conditions that might adversely affect BSFL health and development. Therefore, precise CO<sub>2</sub> measurement is crucial for optimizing the rearing environment and ensuring the well-being of the BSFL.

### **3.1.7 pH Value**

Measuring the pH value of the substrate is a crucial aspect of BSFL rearing and bioconversion processes. The optimal pH range for BSFL typically falls between 6 to 8 [15]. This range is vital as it ensures that the substrate maintains an environment conducive to the optimal growth and development of BSFL. The pH levels directly influence various factors essential for BSFL health and bioconversion efficiency, including microbial activity, nutrient availability, and overall substrate stability. Within the optimal pH range, beneficial microbial communities responsible for decomposing organic matter thrive, while essential nutrients remain readily available to the larvae. Moreover, maintaining pH within this range prevents substrate acidification or alkalization, which could compromise BSFL health and bioconversion effectiveness. In essence, by monitoring and managing

pH levels in the substrate, we can create and maintain an environment that maximizes BSFL performance and supports sustainable waste management practices.

### **3.1.8 Mass of the Food Waste**

By quantifying the rate at which BSFL consumes the food waste, we gain valuable insights into the efficiency of the bioconversion process. The rapid consumption of food waste by BSFL not only reduces the volume of waste destined for landfills but also accelerates the conversion of organic matter into valuable byproducts. Additionally, monitoring the mass of food waste allows us to gauge the optimal timing for harvesting BSFL larvae, maximizing their yield while ensuring efficient resource utilization. Consequently, this approach aids in promoting sustainable waste management practices and contributes to the overall reduction of greenhouse gas emissions linked to waste transportation and disposal.

### **3.1.9 Air Flow Rate**

The airflow rate within a reactor is vital for maintaining the health of BSFL and optimizing bioconversion efficiency. Sufficient airflow is necessary to supply oxygen to the larvae, aiding in respiration and upholding favorable environmental conditions within the reactor. Inadequate airflow may result in oxygen depletion, potentially suffocating the larvae and hindering their growth and development [24]. Hence, it is crucial to guarantee adequate airflow to support the living conditions of BSFL. Effective management of airflow not only fosters the well-being of the larvae but also enhances bioconversion efficiency, ultimately ensuring the success of insect farming endeavors.

### **3.1.10 Larval Density per feeding container**

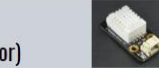
The population density of larvae within a specific container is crucial in the bioconversion process. This would assist in determining the optimal number of larvae for each container, ensuring efficient resource utilization while providing sufficient space and resources for their growth, development, and feeding activities. Adjusting larval density per feeding container can impact factors such as waste

processing rates, nutrient cycling, and overall production yields in insect-based systems. The process of monitoring and adjusting larval density will be performed by the BSFL loader manually.

## 4. Validation of Electronics Components

Understanding the importance of each parameter, we conducted a thorough investigation into different types of sensors capable of measuring them. Through rigorous experimentation, we assessed the accuracy and effectiveness of various sensors to determine their suitability for our reactor. The details of the sensors we tested are provided in Table 4. As we move forward to our final experiment in the reactor we have built, we will use these selected sensors to ensure accurate and reliable measurements.

**Table 5: Sensors**

Parameters	Component	
 Moisture Content of the substrate	Capacitive Soil Sensor	
 Gas Emission (CO <sub>2</sub> )	SGP30 (Air Quality Sensor, CO <sub>2</sub> Sensor)	
 Temperature in the substrate	DS18B20 waterproof version (Temperature Sensor)	
 Internal Air Temperature	DS18B20 (Temperature Sensor)	
 Relative Humidity	DHT22 (Temperature & Humidity Sensor)	
 PH Value	Analog pH Sensor (Meter Kit V2)	
 Weight of substrate	Load Cell & HX711 (Amplifier)	
 Light Intensity	BH1750 (Ambient Light Sensor)	
 Methane	MQ135 (Gas Sensor, CH <sub>4</sub> )	
 Ammonia	MQ2 (Gas Sensor, NH <sub>3</sub> )	

### 4.1 Methodology for Testing Selected Parameters

The experiments were conducted in the same laboratory at the National University of Singapore (NUS) mentioned previously, which serves as the venue for the BSFL bioconversion research conducted by

ETH Zurich, where ongoing lab-scale research projects are in progress, and we utilized the available resources in the laboratory to achieve our objectives and collect the intended data.

#### 4.1.1 Moisture Content of the substrate

Soil sensors function by assessing the moisture levels in the soil, offering crucial insights for efficient irrigation and soil management. These sensors commonly employ technologies such as capacitance or resistive sensing. When placed in the soil, the sensor measures electrical conductivity or resistance, indicating the soil's moisture levels [25]. In our application, we tested both capacitance and resistive soil sensors to measure the moisture content of the substrate, aiming to discern their comparative effectiveness in our experimental setup.

In the experimental setup, we tested two distinct dry frass samples, each treated differently to assess specific factors. One sample included cocopeat, a powdery substance introduced intentionally to serve dual purpose, including preventing larvae from escaping and reducing moisture levels within the substrate. Given the need to increase the moisture content from 20% to 80% in the cups used for the experiment, it was crucial to select an appropriate amount of frass. We settled on a standardized quantity of 60 grams for each sample after considering various factors such as experimental requirements and the need for consistent data collection. This amount was carefully chosen to strike a balance, ensuring that it was neither too little nor too much for the intended purpose. By maintaining uniformity across the samples, we could effectively compare the results and assess the moisture content using the sensors. Subsequently, both frass samples underwent a 48-hour drying process within an oven set at 80°C to eliminate any existing moisture content. This meticulous preparation allowed for accurate assessment of the sensor's performance in subsequent tests, where water was gradually added to increase the moisture content from 20% to 80% systematically. Figure 19 provides an illustration of this process, demonstrating how sensors were strategically inserted into the frass to measure moisture content. For more detailed information on the specific process of increasing the moisture content, please refer to Appendix B.



*Figure 19: Frass Samples*

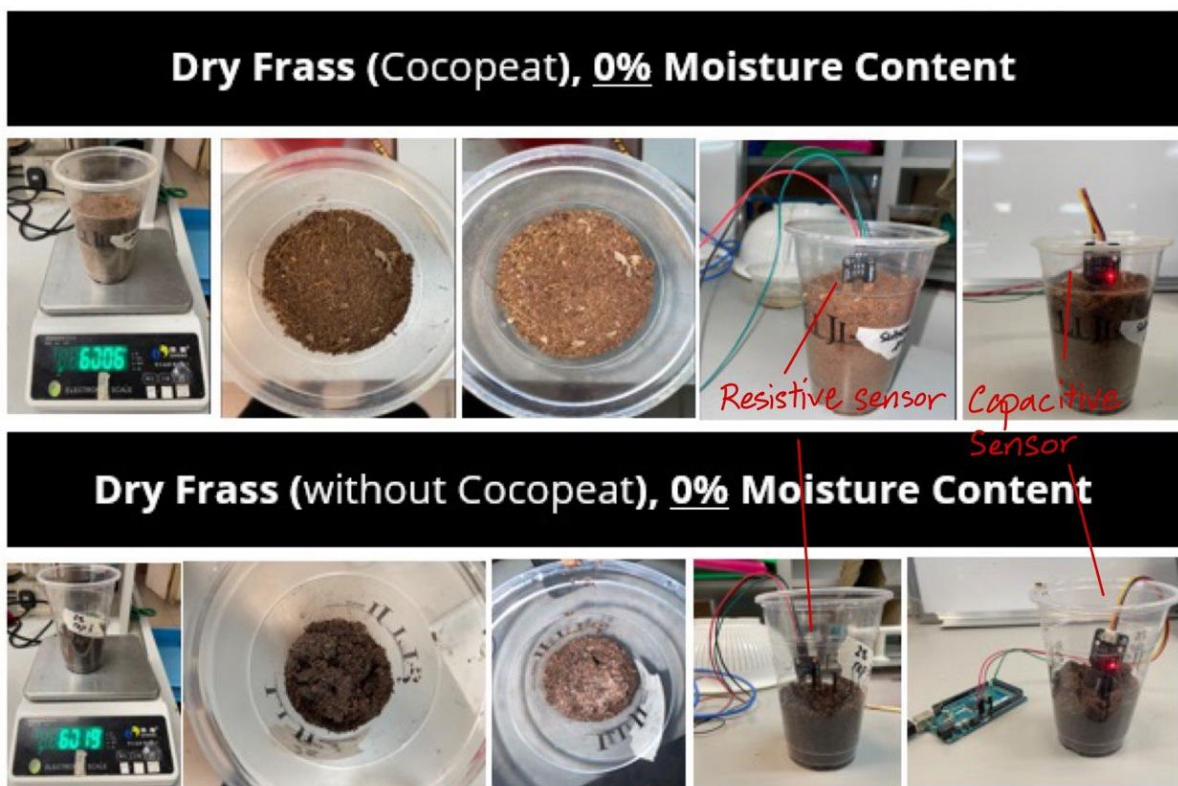


*Figure 20: 60 grams of frass (0% water)*

#### 4.1.1.1 Results and analysis: Moisture Content of the substrate

Upon analyzing the readings obtained from both the resistive and capacitive soil moisture sensors, our decision to integrate the capacitive sensor into our upcoming system is grounded in thorough analysis. The graphical representation of the resistive sensor illustrates a consistent linear relationship for both frass samples, with and without cocopeat, as illustrated in Figure 20. This suggests that as

moisture content increases, the voltage readings also increase, indicating a positive correlation. In contrast, the capacitive sensor's graph reveals an inverse linear relationship for both frass samples, as illustrated in Figure 21. It is important to note that the initial inverse correlation observed in the capacitive sensor graph is not indicative of inferior performance; rather, it highlights the need for calibration, as the analog readings are yet to be precisely calibrated. Following calibration adjustments, the accuracy and reliability of the capacitive sensor are to be enhanced, rendering it an optimal choice for our system. Research indicates that the resistive sensor, with exposed copper conductors over prolonged periods, is susceptible to measurement inaccuracies due to rust. Therefore, opting for the capacitive sensor is deemed more suitable for an accurate measurement. Moreover, to plot a straight line across the data points in the graphical representation of the resistive and capacitive sensor aids in visualizing the consistent linear relationship observed, providing clarity on the sensor's performance.

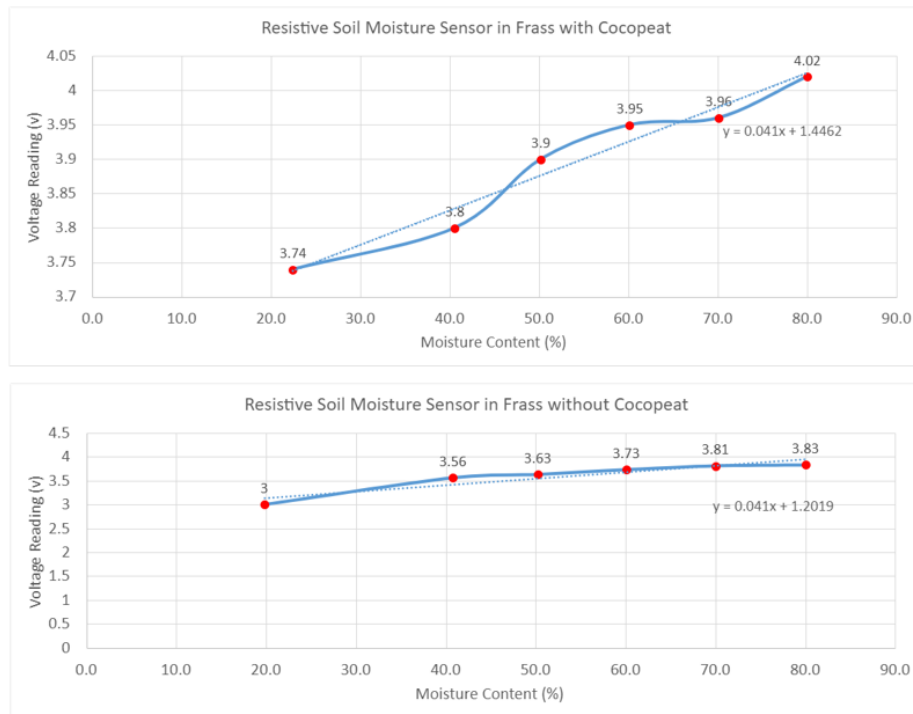


**Figure 21: Graph of resistive sensor**

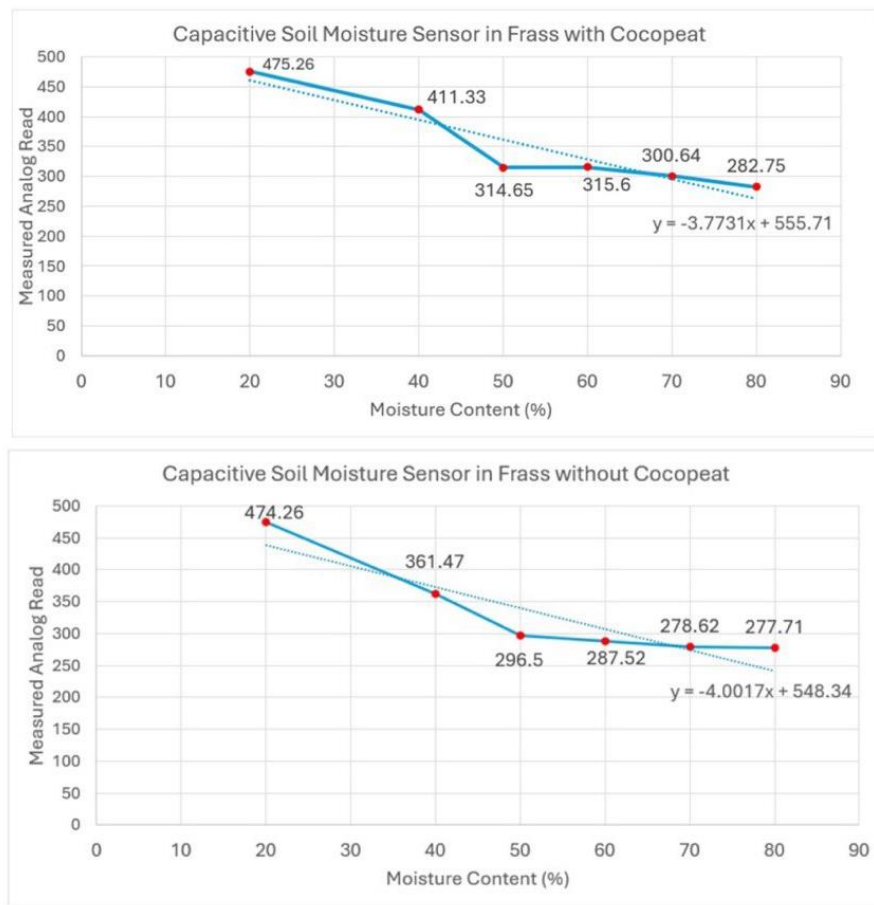


**Figure 22: Graph of capacitive sensor**

#### 4.1.2 Temperature in the substrate

The DS18B20 temperature sensor utilizes the One-Wire communication protocol, featuring a digital serial number for identification. Operating with a single data line, it converts temperature-sensitive electrical resistance into a digital signal, enabling accurate and high-resolution temperature measurements [26].

To monitor the substrate temperature, we utilized the sensor to be inserted directly into the substrate for accurate measurements. In the experimental validation, the accuracy of the sensor was assessed by comparing its readings with those obtained from a digital pocket thermometer, serving as a ground truth reference. The experiment involved testing the sensor's performance under two different temperature conditions, with assessments conducted at boiling water (100°C) and cold water at

(12.5°C), as illustrated in Figure 23. This rigorous evaluation aimed to verify the reliability of the DS18B20 sensor and determine if any calibration adjustments were necessary for optimal performance.

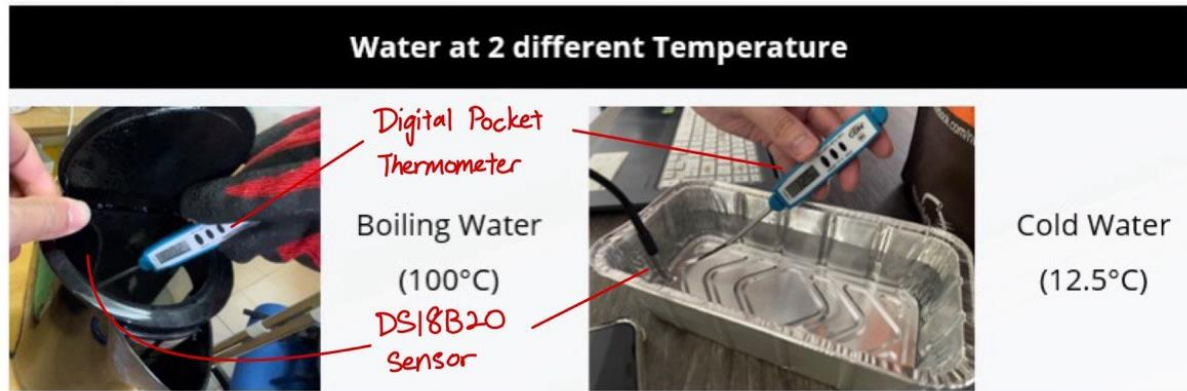


*Figure 23: Two different temperature conditions*

#### 4.1.2.1 Results and analysis: Temperature in the substrate

The readings obtained from the DS18B20 sensor were compared to the digital pocket thermometer to assess the sensor's temperature measurement accuracy. Figure 24 visually represents the results, indicating minimal discrepancies between the sensor readings and the digital pocket thermometer. This comparison demonstrates the effectiveness of the DS18B20 sensor in accurately measuring temperature, affirming its reliability for our intended applications.

Boiling Water in Kettle	Measurement	Cold Water in Container	Measurement
	96.25 C 96.37 C 96.50 C 96.56 C 96.62 C 96.69 C 96.75 C 96.81 C 96.81 C 96.81 C 96.81 C		13.31 C 13.38 C 13.38 C 13.25 C 13.31 C 13.31 C 13.38 C 13.31 C 13.31 C 13.31 C 13.31 C

*Figure 24: Readings of DS18B20 sensor (with probe)*

#### 4.1.3 Internal Air Temperature

To monitor the internal air temperature, we employed a variant of the DS18B20 temperature sensor.

The accuracy of this sensor was validated by comparing its readings with those obtained from an anemometer, which not only measured temperature but also monitored air flow speed, serving as a ground truth reference. The experimental setup involved testing the sensor's performance within an enclosed box, creating a controlled environment for precise evaluations, with the added element of fan activation to observe the impact on internal air temperature, as illustrated in Figure 25. This thorough assessment aimed to confirm the reliability of the DS18B20 sensor and ascertain if any calibration adjustments were required for optimal performance.

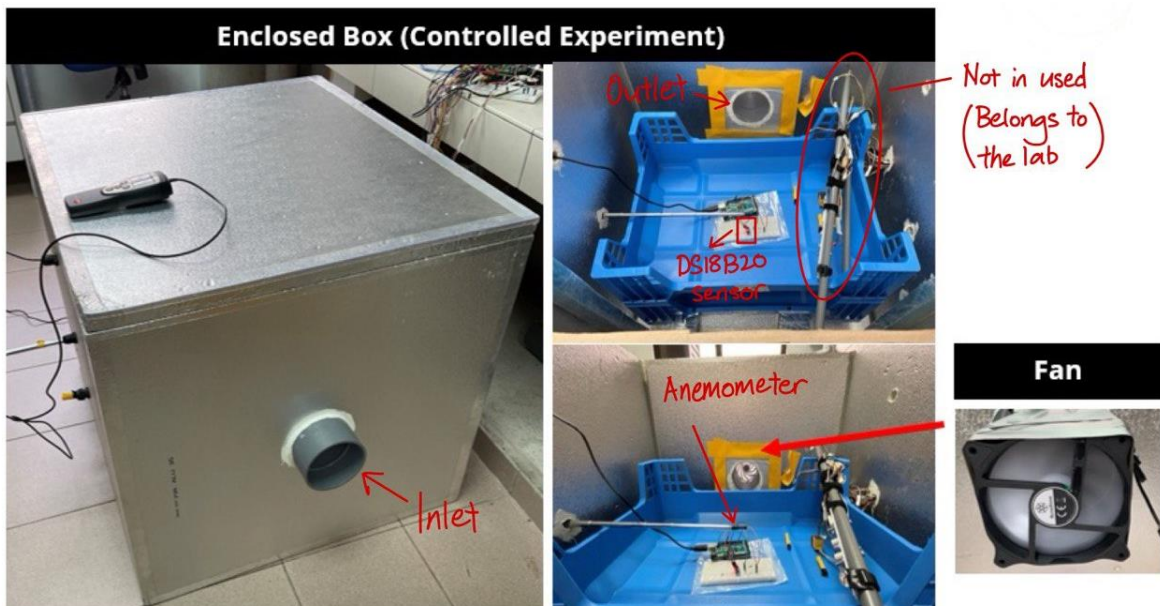


Figure 25: Internal Air Temperature (Controlled Experiment)

##### 4.1.3.1 Results and analysis: Internal Air Temperature

The temperature readings from the DS18B20 sensor were cross-referenced with the anemometer to evaluate the sensor's accuracy in measuring both temperature and air flow speed. As illustrated in Figure 26, when the fan was activated at approximately 2 minutes and 20 seconds, a gradual decrease in temperature was observed. This observation suggests that the sensor effectively captures data

swiftly, demonstrating its responsive performance within a short timeframe. This supports its potential use in our upcoming system.



**Figure 26: Readings of DS18B20 sensor (without probe)**

Considering that air flow can influence parameters like temperature and humidity within the system, it is imperative to prioritize testing and validation. The incorporation of a ventilation system becomes crucial for adjusting temperature and humidity, making it necessary to understand the calibration process within the system due to the interdependence of these variables.

#### 4.1.4 Relative Humidity

Both the DHT11 and DHT22 sensors utilize capacitive humidity sensing elements to measure humidity. These sensors work by detecting changes in the capacitance of a humidity-sensitive resistor in response to variations in humidity levels. The humidity-sensitive resistor's capacitance is affected by the absorption or release of water molecules in the air. This capacitance change is then converted into a digital signal and transmitted for further processing [27].

In the assessment of relative humidity, we conducted experiments utilizing the two sensors. To verify the accuracy of these sensors, it was essential to establish a standardized humidity environment, determining the exact humidity level for calibration. To achieve this, we employed saturated sodium

chloride (NaCl), commonly known as salt, in our experiment. The process involved combining salt with water to create a consistently stable relative humidity of 75% [28]. This was accomplished by placing a bowl of saltwater within a sealed container alongside the sensors, as illustrated in Figure 27. The experiment was maintained for approximately 6 hours to ensure environmental stability and precision during our testing.



*Figure 27: Standardized humidity environment (75%)*

#### 4.1.4.1 Results and analysis: Relative Humidity

After the 6-hour testing period, data retrieved from the DHT22 sensor indicated a relative humidity of approximately 74.70%, as illustrated in Figure 28. Although this value deviates slightly from the target of 75%, the DHT22 sensor has an acceptable margin of error of  $\pm 2\%$ , which could explain this discrepancy. Despite this, the data suggests that the DHT22 sensor is accurate enough for integration into our forthcoming system for relative humidity measurement. Additionally, the recorded data exhibited a narrow range, with values ranging from 74.70% to 74.80%, indicating consistent performance and reliable readings within this range. On the contrary, challenges were encountered with obtaining data from the DHT11 sensor. These issues may stem from connection errors or code-related problems, necessitating additional time and effort to address and ensure the sensor's reliability and accuracy.

### Obtain data from the DHT22 sensor connected to an Arduino



*Figure 28: Readings from DHT22*

#### 4.1.5 Light Intensity

The BH1750 light intensity sensor operates based on the principle of illuminance measurement. It employs a photodiode to convert incoming light into an electrical current, generating a proportional digital output. This digital output corresponds to the illuminance level, allowing the sensor to provide accurate measurements of light intensity in various settings [29].

An experiment was conducted to assess the sensor's accuracy, involving its placement in two different positions to capture readings and identify potential variations, as illustrated in Figure 29. As illustrated in Figure 30, the experimental setup involves lifting the cover at an approximate angle of 10 degrees on the left, while on the right, a protractor is positioned at the pivot point opposite the box, enabling precise measurement of the angle following the elevation of the cover. This experiment aimed to ascertain consistent and accurate measurements of light intensity in our system. Additionally, experiments were conducted at lifting angles of 5 and 15 degrees to comprehensively assess the sensor's performance across varying conditions.

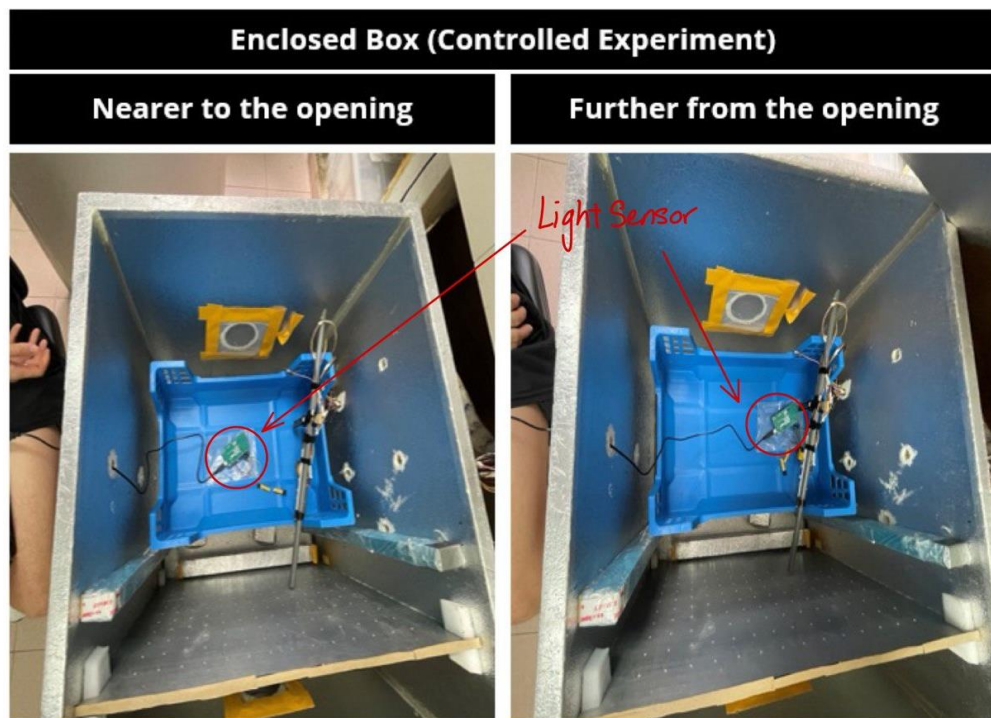


*Figure 29: Position of the sensor*

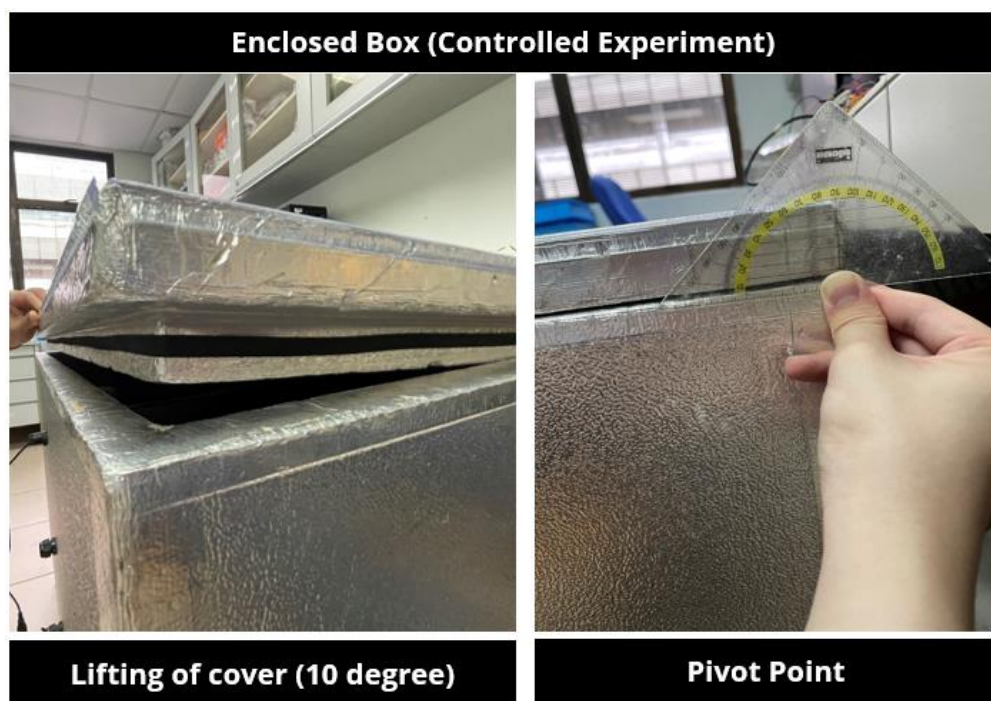


*Figure 30: Pivoting*

#### 4.1.5.1 Results and analysis: Light Intensity

The results revealed that the sensor readings remained consistent, regardless of whether the sensor is nearer or further away from the box's opening, implying that it has minimal differences in readings, as illustrated in Figure 31. However, it is crucial to acknowledge the possibility of experimental error contributing to this consistency. While the majority of experiments yielded similar readings of 3.33 when positioned both near and further from the opening. Experiment 3 notably recorded a higher reading of 4.17. This deviation could be indicative of potential sources of error, such as procedural inconsistency and environmental conditions to Experiment 3. Therefore, while the overall trend suggests minimal variation in sensor readings, the presence of outliers like Experiment 3 highlights the importance of rigorous experimental controls to mitigate the impact of potential errors on data accuracy and reliability.

Enclosed Box (Controlled Experiment)						
	Lifting box's cover (Angle)	Exp 1 (lux)	Exp 2 (lux)	Exp 3 (lux)	Exp 4 (lux)	Exp 5 (lux)
<b>Nearer to the opening</b>	5	0	0	0	0	0
	10	0.83	0.83	1.67	0.83	0.83
	15	3.33	3.33	4.17	3.33	3.33
<b>Further from the opening</b>	5	0	0	0	0	0
	10	0.83	0.83	0.83	0.83	0.83
	15	3.33	3.33	4.17	3.33	3.33

*Figure 31: Readings from different positioning of sensor*

The experiment was replicated five times, involving the repeated lifting of the cover within a range of 5° to 50°. The graph depicting the results demonstrates a consistent pattern across all five experiments, as illustrated in Figure 32. Analyzing the data presented in the table reveals that a slight lift of the box's cover by approximately 10° corresponds to a sensor reading of 0.83 lux, indicating an open box. Notably, when the cover is lifted by around 5°, the sensor fails to provide any readings. This discrepancy suggests the need for sensor calibration to enhance accuracy before integration into the

system. In summary, the sensor exhibits sensitivity in detecting incoming light, justifying its potential inclusion in our system for determining the system's status—whether it is open or closed.

The sudden increase in sensor readings at angles greater than 30 degrees could be due to a combination of factors such as the angle of incidence of light and the geometry of the box. Up to an angle of 30 degrees, the gradual increase in sensor readings suggests that the amount of light entering the box is proportional to the angle of lift. However, beyond 30 degrees, there appears to be a more pronounced increase in sensor readings. This could be because at higher angles, the opening of the box allows for a larger area of direct exposure to light sources, resulting in a greater influx of light into the box. Additionally, the geometry of the box at angles greater than 30 degrees might lead to reflections or refractions of light within the box, further increasing the sensor readings. Therefore, the sudden increase in sensor readings beyond 30 degrees could be attributed to the combined effect of increased direct exposure to light and potential light interactions within the box.

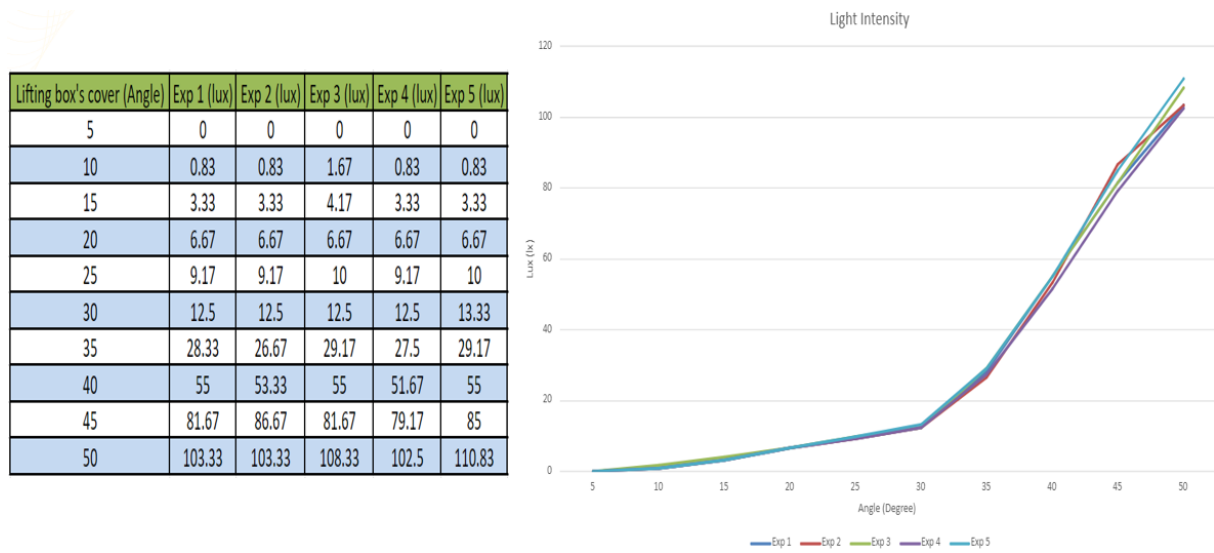


**Figure 32: Graph and readings of BH1750**

#### 4.1.6 Gas Emission (Carbon Dioxide, CO<sub>2</sub>)

In the evaluation of carbon dioxide levels, we utilized the MH-Z16 NDIR CO<sub>2</sub> sensor. The experiment involved placing the sensor alongside a CO<sub>2</sub> reference device in a glass jar, serving as the ground truth

for comparison, as illustrated in Figure 33. The MH-Z16 NDIR CO<sub>2</sub> sensor operates on the principle of non-dispersive infrared technology (NDIR), where it measures the concentration of CO<sub>2</sub> in the air by detecting infrared radiation absorbed by carbon dioxide molecules [30]. This rigorous testing aimed to assess the accuracy and reliability of the MH-Z16 sensor in capturing precise CO<sub>2</sub> measurements within our system.

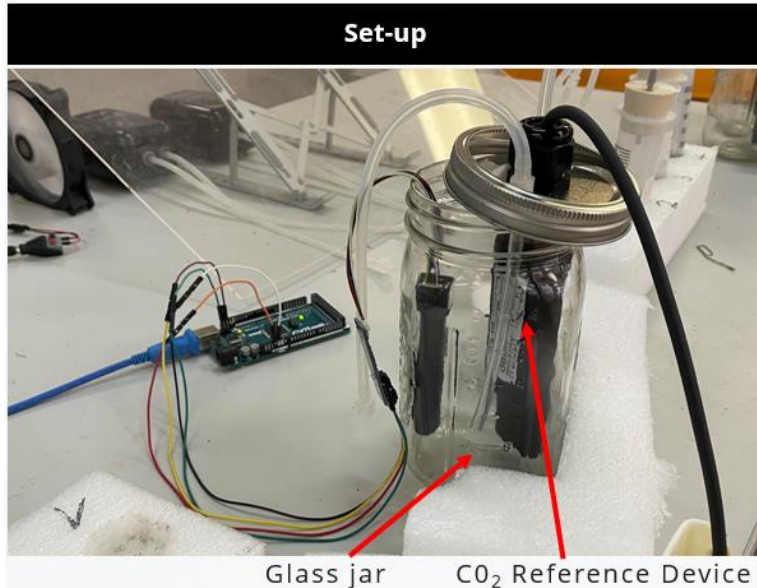
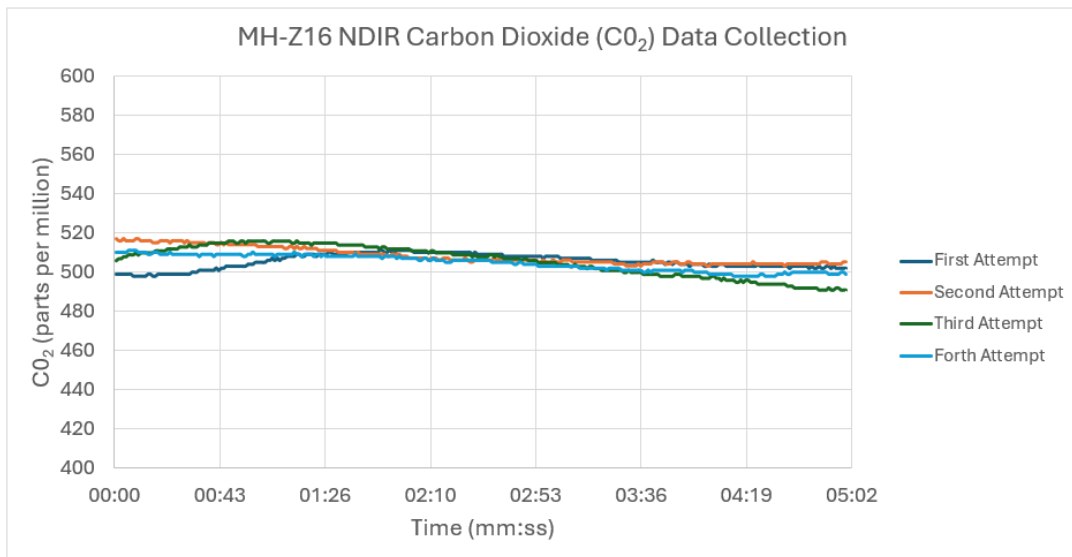


*Figure 33: Carbon Dioxide Experiment*

#### 4.1.6.1 Results and analysis: Gas Emission (Carbon Dioxide, CO<sub>2</sub>)

The sensor readings were compared with the reference device, indicating a slight discrepancy between them. The graph depicts consistent results, demonstrating minimal variation within the sensor itself, despite conducting the experiment four times to ascertain its accuracy, as illustrated in Figure 34. This supports its potential use in our upcoming system. Notably, the average number indicated in the reference sensor stands at 499ppm.



Sampling Rate: 1Hz  
Duration: 5 Minutes

**Figure 34: Graph of CO<sub>2</sub> sensor**

#### 4.1.7 pH Value

Calibrating the pH value sensor before use is crucial to ensure accurate and reliable measurements of pH levels [31]. pH calibration involves adjusting the sensor's response to match known pH values using buffer solutions, as illustrated in Figure 35. This process compensates for any deviations or inaccuracies in the sensor's readings, which can arise due to factors such as sensor drift, environmental conditions, or manufacturing variations. By calibrating the pH sensor, we can verify its accuracy and reliability, thereby ensuring the validity of pH measurements in our experiments or applications. This step is particularly important in scientific research, environmental monitoring, and industrial processes where precise pH measurements are essential for making informed decisions and drawing meaningful conclusions. Therefore, calibrating the pH value sensor before use is a fundamental practice that helps to ensure the quality and integrity of pH data.

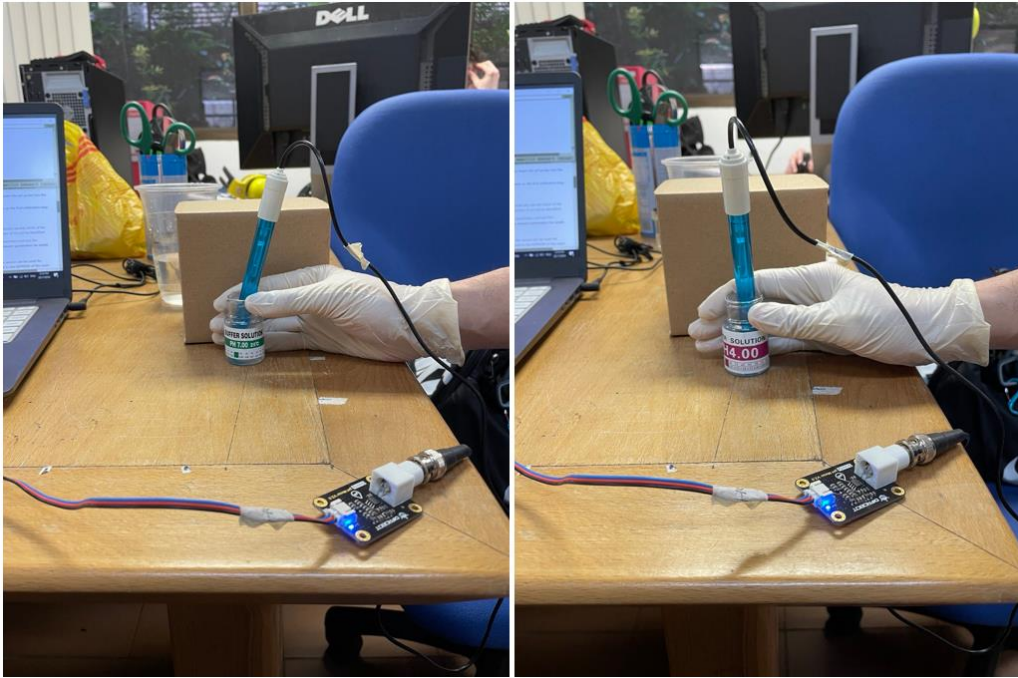


**Figure 35: Calibration of pH sensors (with buffer solutions 4.0 and 7.0)**

#### 4.1.8 Mass of the food waste

To accurately quantify the mass, we utilize four load cells interconnected in a single circuit. Each load cell has a capacity to measure up to 50kg, allowing for a collective measurement of up to 200kg when all four are connected. This setup enables precise monitoring of the amount of food waste processed by the BSFL. When four load cells are connected, an amplifier serves several crucial purposes. Firstly, it amplifies the small electrical signal produced by each load cell in response to applied force, ensuring that it reaches a level suitable for accurate measurement by data acquisition systems. Secondly, the amplifier helps in reducing electrical noise that could interfere with the signal, thus ensuring reliable measurements. Thirdly, it facilitates the completion of the Wheatstone Bridge configuration, necessary for precise balancing and proportional voltage output corresponding to the applied force. Additionally, amplifiers often include features for calibration adjustment, enabling users to fine-tune the system for optimal performance and ensure consistent and accurate measurements across various load cells and operating conditions. Overall, the amplifier plays a critical role in ensuring the accuracy, reliability, and stability of measurements obtained from multiple load cells connected in a circuit.

In order to ensure the load cells provide accurate readings, it is crucial to mount them on a flat and stable surface. This ensures that the measurements obtained are reliable and consistent. To achieve this, we utilized computer-aided design (CAD) software to design a custom bracket specifically tailored for the load cells, as illustrated in Figure 36. This bracket was then fabricated using 3D printing technology, allowing for precise and secure mounting onto an acrylic plate, as illustrated in Figure 37. Once mounted, the load cells effectively function as a weighing scale, enabling us to accurately measure the mass of the food waste. This meticulous approach to mounting the load cells ensures that our data collection process is reliable and contributes to the overall accuracy of our experiments.

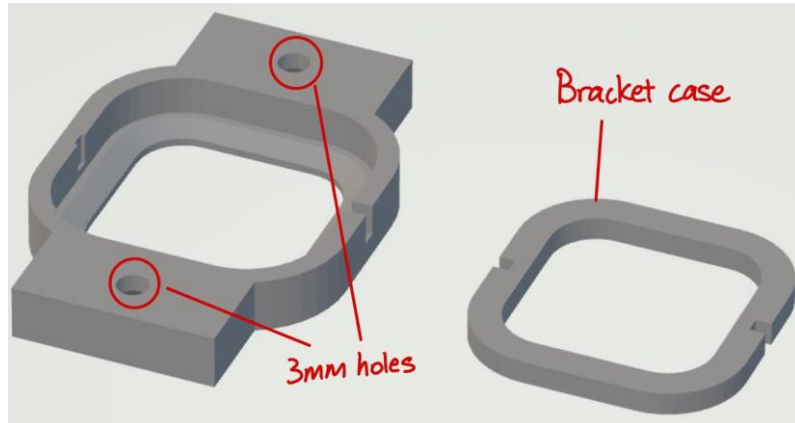


*Figure 36: CAD drawing of load cells bracket and bracket case*



*Figure 37: 3D printed load cells bracket and bracket case*

We attached the load cells to the acrylic plate, which we then fastened onto the cage, as illustrated in Figure 38. The load cells are equipped with rubber feet, which play a crucial role in stabilizing the setup. When the container is placed on the load cell assembly, these feet ensure that the entire weight of the container is evenly distributed across all four load cells. This distribution is essential for obtaining precise measurements from the load cells, enabling us to accurately assess the container and its contents.

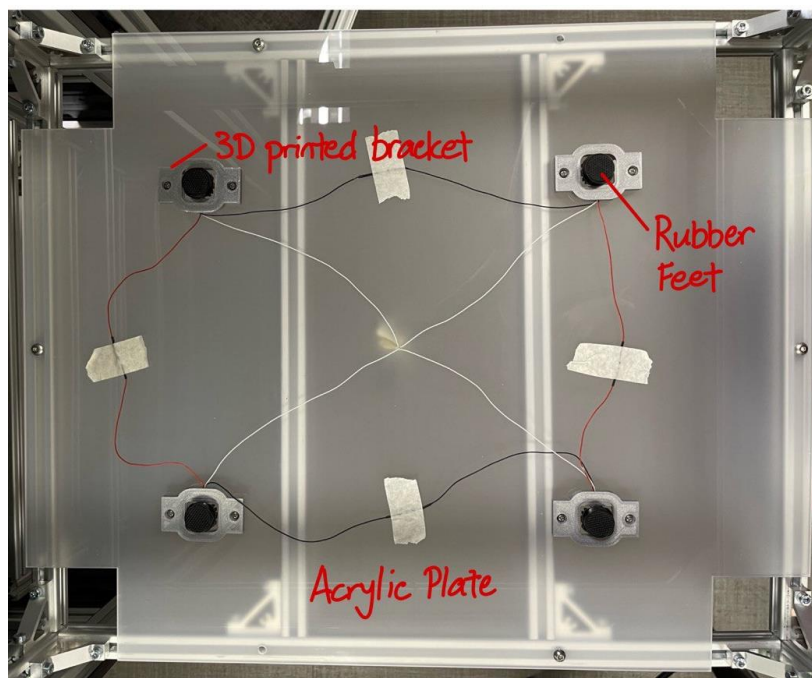


**Figure 38: Four load cells interconnected and mounted onto acrylic plate**

#### 4.1.8.1 Results and analysis: Mass of the food waste

After mounting the load cells onto the acrylic plate, we conduct functionality tests to ensure accurate readings. To perform this test, we measured the weight of a tray along a bottle, resulting in a combined weight of 1264 grams. The calibration factor, which adjusts raw readings, is determined by dividing the tare value by the total weight. This calculated factor is then integrated into the code to fine-tune the load cell readings, ensuring that the displayed weight values are accurate and calibrated. This

calibration process is crucial for obtaining precise measurements and ensuring the reliability of the weight data collected from the load cell.

This configuration displays how the bottle is positioned inside the container to acquire readings from the load cells, as illustrated in Figure 39. To enhance the precision of the tare value, we conducted ten readings and calculated their average to derive the calibration factor, as illustrated in Figure 40. This process ensures accurate calibration and reliable measurements from the load cells.

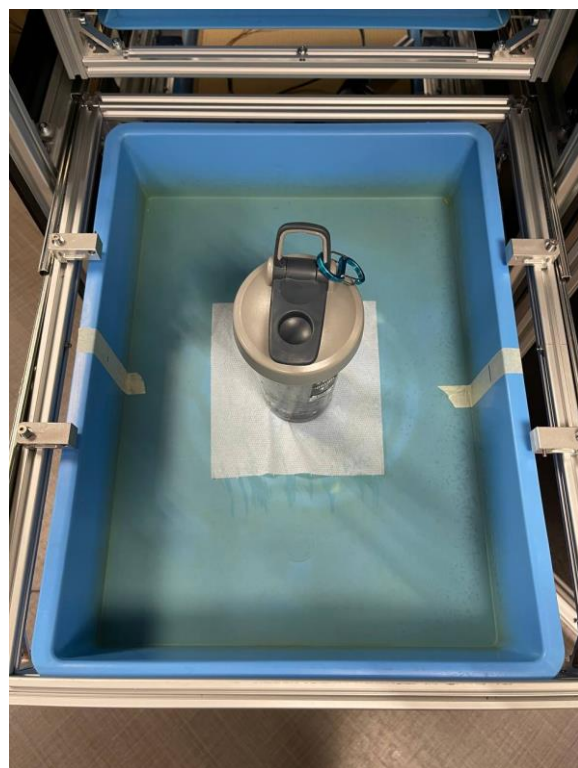


*Figure 39: Configuration of bottle and container in the cage (1264 grams)*

Trial Number	Tare Value
1	-44995
2	-44890
3	-44895
4	-45071
5	-45537
6	-43777
7	-45537
8	-44840
9	-44696
10	-44329
Average	-44856

Calibration Factor: Tare Value / Known weight = -44856 / 1264 = -35.48734

*Figure 40: Tare values*

The results show the accuracy of total weight measurement, aligning closely with the known weight of 1264 grams, with readings ranging from 1263 to 1265 grams, as illustrated in Figure 41.

Trial Number	Reading Value (grams)
1	1264.7
2	1265.4
3	1265.2
4	1264.8
5	1264.4
6	1263.8
7	1265.1
8	1265.5
9	1264.9
10	1264.5

*Figure 41: Readings recorded from the load cells*

#### 4.1.9 Air Flow Rate

Controlling the internal environment of the BSFL reactor is pivotal for maintaining the optimal conditions required for larvae growth and waste bioconversion. One key aspect of this environmental control is managing the air flow rate within the reactor, which is critical for ensuring sufficient oxygen supply and maintaining appropriate temperature levels. The integration of modern cooling fan

technology, specifically the use of a standardized CPU fan with a 4th wire for "controlled input" or Pulse Width Modulation (PWM) input signal, plays a vital role in this process.

These 4 wired fans, crucial for the operation of cooling fan assemblies with an internal motor driver circuit, allow for the precise adjustment of the fan's rotational speed without altering the input voltage. By utilizing PWM control, the reactor can dynamically adjust the cooling rate and air flow based on the current needs of the BSFL and the internal conditions of the reactor. This flexibility ensures that the fan operates quietly and conserves energy when maximum speed is not necessary, contributing to a more sustainable and efficient bioconversion process.

To monitor and optimize the reactor's air flow, the system incorporates a method for measuring the fan's rotational speed (RPM). This is achieved by counting the number of pulses generated by the fan within a specific timeframe, with the understanding that each revolution corresponds to two pulses. This measurement is crucial for calibrating the air flow rate, ensuring that the BSFL reactor maintains an environment conducive to efficient waste processing and larvae development.

#### **4.1.9.1 Results and analysis: Air Flow Rate**

The results from the experiments on air flow rate management within the BSFL reactor, utilizing a standard CPU fan with PWM control, revealed insightful data on the fan's performance at various duty cycles. By manipulating the PWM input through an Arduino, a direct correlation between duty cycle increments and fan rotational speed was established. At a 10% duty cycle, the fans operated at their lowest recorded speeds, which ranged from 1440 to 1620 RPM across different units, indicative of the minimal air flow rate necessary for maintaining basic metabolic processes within the reactor. As the duty cycle was systematically increased, the RPMs exhibited a proportional rise, peaking at a duty cycle of 100%, which yielded RPM values in the range of 5130 to 5160. This increment in air flow rate is significant for the BSFL reactor operation as it aligns with the need to intensify cooling and oxygenation when the biological activity and thermal load are at their highest. The results also point towards minor variability between individual fan units, which underscores the necessity for precise

calibration in practical applications. This variability necessitates a responsive system capable of adapting to the unique performance characteristics of each fan to maintain a consistent and suitable environment for the larvae. Collectively, the experiment validated the efficiency of using PWM signals to control fan speed, which enables the reactor to adjust air flow rates dynamically, ensuring optimal conditions for the growth and productivity of the BSFL within the reactor.

## 5. Integration of Hardware and Software

### 5. 1 Experimental Phases and Laboratory Setting

We devised our experimental plan, which consists of three distinct phases aimed at systematically evaluating and refining our bioconversion system. In Phase 1, our focus was on determining optimal sensor placements for key parameters such as moisture levels, temperature, and pH value. Moving on to Phase 2, to integrate all sensors and conducted comprehensive tests on each parameter, excluding weight of substrate and light intensity, using the standalone reactor already present in the laboratory. As we transitioned to Phase 3, our goal was to assess all parameters within our constructed reactor, providing crucial insights into creating ideal conditions for supporting BSFL within our system. In addition to these planned phases, we recognized the opportunity to gain further insights into the scope outlined by conducting two experiments with a standalone reactor currently in laboratory use. By methodically progressing through these phases and incorporating additional experiments, we aimed to deepen our understanding of the bioconversion process and optimize the efficiency of our system design.

#### 5.1.1 Phase 1: Moisture Content & Temperature in the substrate

In the initial phase of experimentation, our primary objective was to identify the most effective positioning for sensors within the container. This phase aimed to ascertain the optimal locations for measuring crucial parameters such as moisture level, temperature and pH value using specialized sensors. To facilitate this experiment, we utilized the combination of 8kg of food waste, 300g of

peanut skins, and an initial population of 10,000 larvae (5 DOL) within the container, as illustrated in Figure 42. The addition of peanut skins served a similar purpose to cocopeat, as discussed earlier. Its purpose is to prevent larvae from escaping and also to reduce moisture level within the substrate. This setup allowed us to simulate real-world conditions and gather accurate data for analysis and further refinement of our bioconversion system.



*Figure 42: Combination of food waste, peanut skins, and larvae*

In our setup to determine optimal sensor locations, as illustrated in Figure 43, we adopted a meticulous approach aimed at ensuring accuracy and stability. Sensors were attached to aluminum profile bars using masking tape, which served as a temporary securing method. These profile bars were then firmly affixed to the container using tape to prevent any potential displacement, maintaining an upright position for precise data collection (refer to Appendix C for better visualize on how we positioned the sensors). Notably, we utilized an Arduino and micro-SD module to store the data generated throughout this experiment, which spanned a duration of 5 days. Initially, we focused

on measuring moisture levels and temperature, reserving pH analysis for later stages. It is important to note that in this first experiment of Phase 1, we started by testing moisture content and temperature before moving on to pH testing. This experiment specifically targeted the measurement of moisture levels and temperature, with the pH value analysis slated for subsequent stages. Through this systematic setup, our objective was to acquire dependable data to guide our decision-making processes and optimize the efficiency of our bioconversion system.

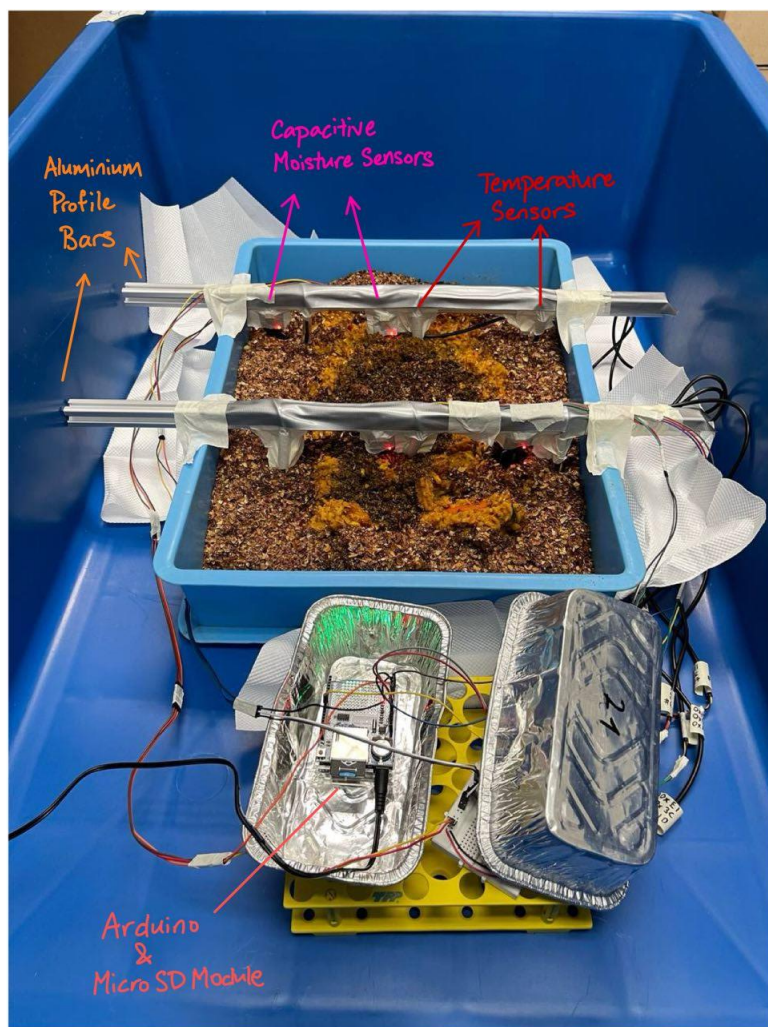
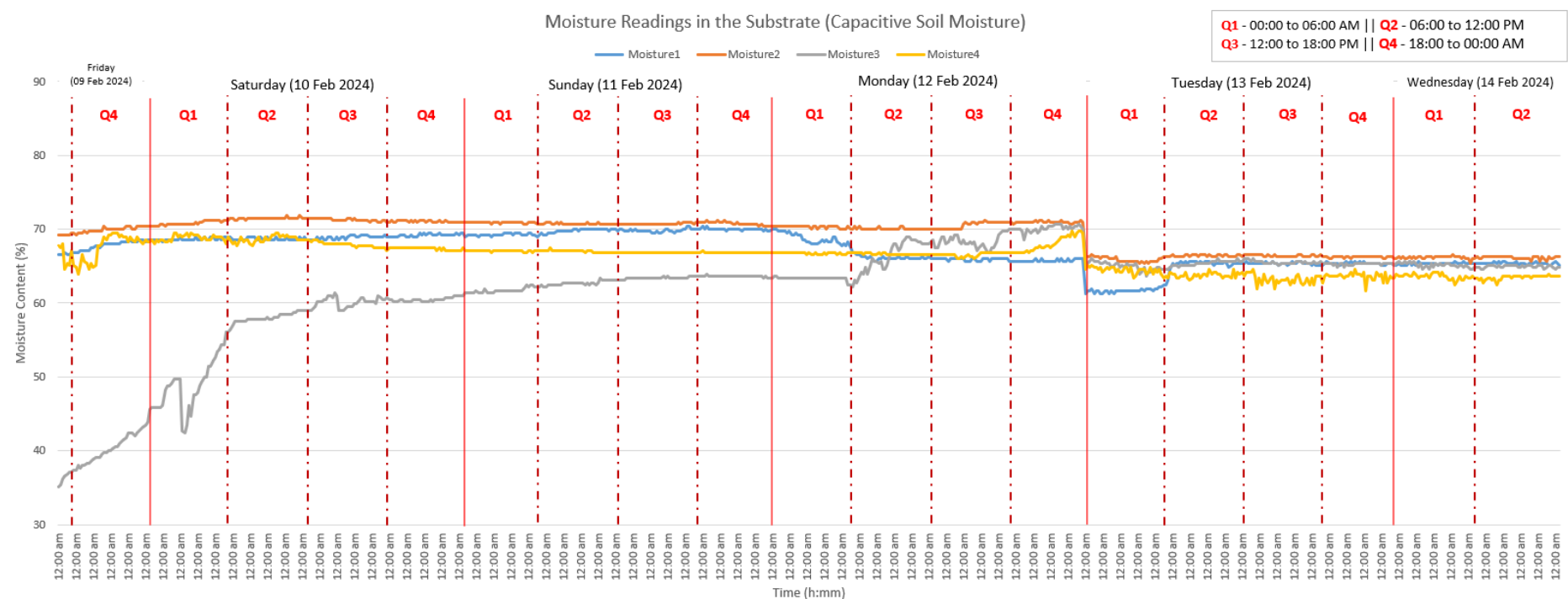


Figure 43: Phase 1 setup configuration (Moisture and Temperature)

#### 5.1.1.1 Results & Analysis: Moisture Content & Temperature in the substrate

During the initial phase of our substrate moisture evaluation, readings from sensors 1, 2, and 4 displayed a uniform moisture range between 65% and 70%, while sensor 3 differed, registering

moisture levels from 40% to 60%, suggesting an irregularity possibly due to calibration discrepancies, sensor placement, or the physical makeup of the substrate. By day two, the readings from sensor 3 adjusted to mirror those of its counterparts, signaling a normalization of moisture distribution within the substrate. Yet, an abrupt dip in the recorded moisture levels by all sensors was detected at midnight on the third day, a trend that could be linked to changing environmental factors or inherent characteristics of the substrate. In the subsequent period of observation, the sensors' data stabilized, reflecting a consistent moisture environment. For a definitive interpretation and to finetune our monitoring infrastructure, further detailed analysis is imperative to investigate the sharp decrease noted on the third night and pinpoint the underlying causes of observed data variances. To refine the monitoring system's precision and tailor irrigation practices to actual conditions, it is essential to reassess the calibration of the sensors, particularly sensor 3, integrate a detailed analysis that includes environmental data review, cross-reference the moisture changes with irrigation records, and undertake an in-depth evaluation of the substrate's composition. This strategy will bolster the reliability of our findings and contribute to informed irrigation decisions.



**Figure 44: Moisture readings**

Throughout the observation period, the substrate's temperature was diligently recorded, revealing distinct patterns. Initial measurements indicated that most sensors-maintained temperatures within the range of 27 to 31 degrees Celsius, indicative of a stable thermal environment. An exception was noted in sensor 6, which registered erratic temperature swings from 28.5 to 36 degrees celsius, signaling possible calibration inconsistencies.

As the monitoring progressed into the second day, sensor 6 showed a gradual return to expected temperature levels, albeit consistently recording slightly elevated readings relative to the other sensors. This could reflect the sensor's specific micro-environment or proximity to heat sources not affecting the other sensors. The third day marked a period of pronounced temperature volatility across all sensors, hinting at dynamic thermal processes occurring within the substrate. These variations might be attributable to the biological heat generated by the metabolic activity of the BSFL population as they engage in bioconversion processes or could be reflective of the larvae's thermal adaptation strategies.

Given the intricate relationship between temperature and the efficiency of bioconversion, understanding the causative factors behind these observed fluctuations is imperative. Consequently, an extended investigation involving cross-referencing sensor data against environmental conditions, BSFL activity levels, and potential changes in the substrate's properties is essential to elucidate the precise mechanisms at play. This detailed analysis will not only aid in verifying the sensor's functionality and placement but also in fine-tuning the bioconversion environment to optimize the BSFL's productivity, as evidenced by the trends depicted in Figure 45.

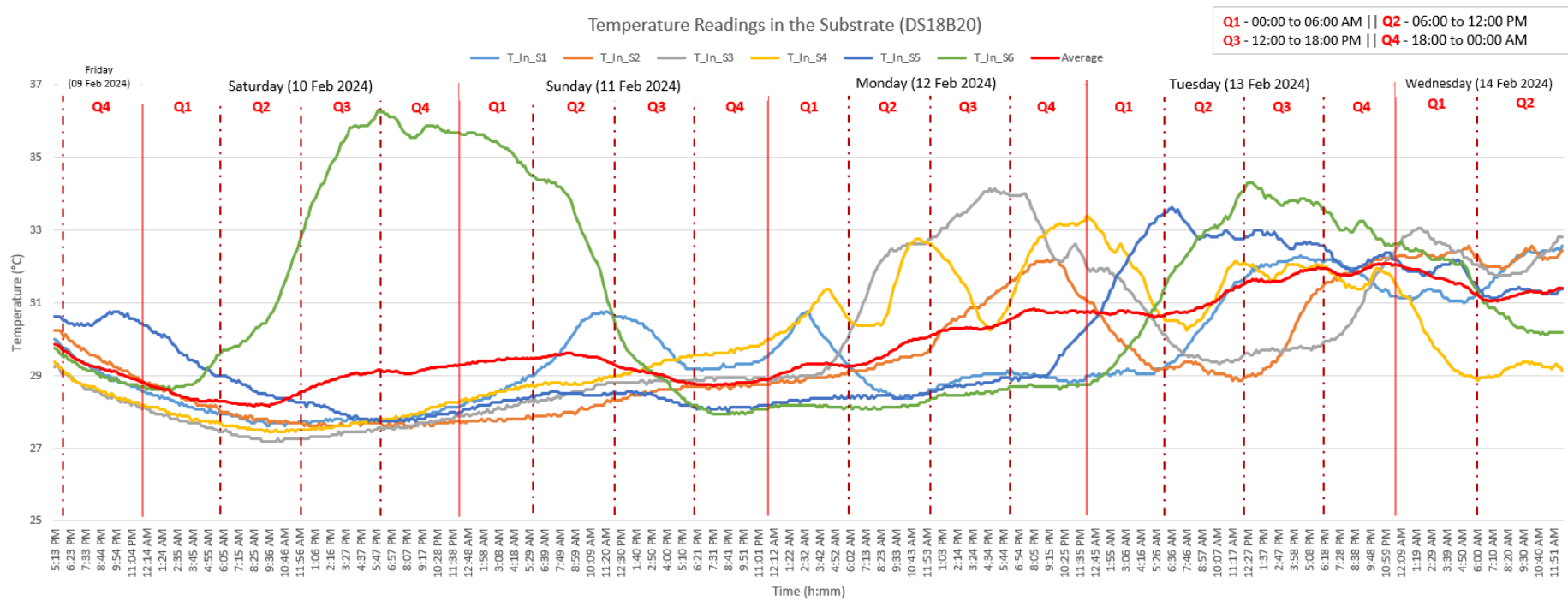


Figure 45: Temperature Readings

### 5.1.2 Phase 1: pH value in the substrate

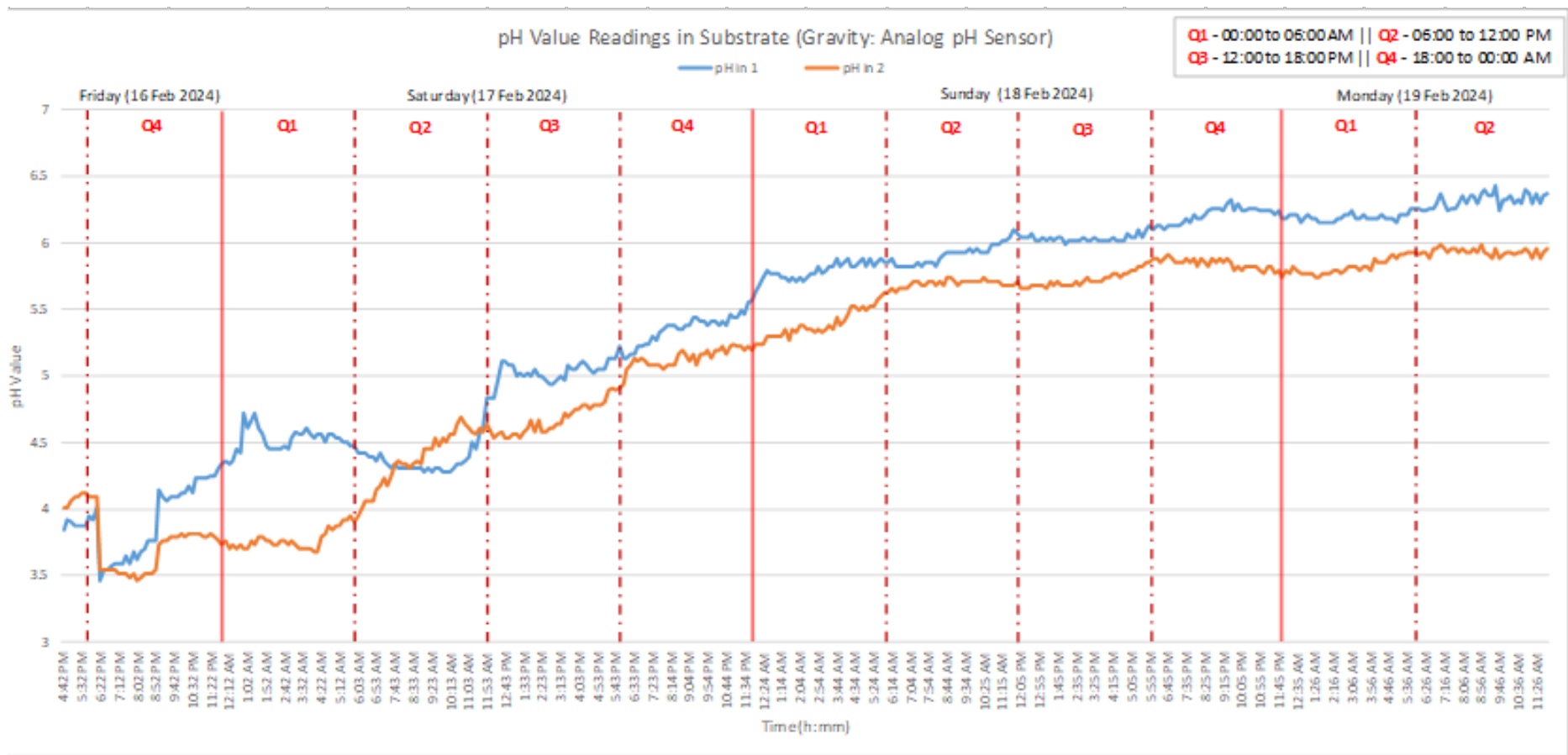
In the progression from the initial experiment of Phase 1 to the subsequent experiment, which marks the beginning of second part of the experiment, our focus shifted assessing the pH sensors. This transition occurred following the completion of the first experiment, where we measured moisture content and temperature in the substrate. As we transitioned to the second experiment, we continued to use the same batch of BSFL, which were about 10 DOL. The setup for this experiment is illustrated in Figure 46. The decision on the placement of the pH sensor was informed by insights provided by Adrian, whose expertise and research experience were invaluable in guiding our experimental approach. Adrian's input was crucial in ensuring a diverse range of testing conditions for the pH sensors, ultimately enhancing the comprehensiveness and effectiveness of our experimental procedures.



Figure 46: Phase 1 setup configuration (pH)

### 5.1.2.1 Results & Analysis: pH value in the substrate

Figure 45 presents the pH value trends within the substrate, as monitored by two analog pH sensors. Our methodology initially included a third sensor; however, due to anomalies in its output during the preliminary phase, which persisted despite calibration efforts, it was deemed unreliable and thus excluded from the data set. The retained sensors, pH 1 and pH 2, showed an increasing trend in pH values over the monitoring period, which lasted for four days. The readings started at a pH near 4, indicating a highly acidic substrate environment, and gradually increased, moving towards neutral pH levels. This gradual alkalinization could suggest microbial activity or chemical changes within the substrate, such as the breakdown of organic materials or ammonia volatilization. Notably, pH 1 consistently read slightly higher than pH 2, suggesting spatial variability in the substrate's pH or minor differences in sensor sensitivity. To corroborate our findings and strengthen the accuracy of our substrate pH profile, we continued to exclude data from sensor 3, focusing on the consistent and calibrated readings from the two primary sensors. Such an approach underscores our commitment to data integrity and reflects our ongoing efforts to refine the substrate monitoring process to provide reliable, actionable insights.



**Figure 47: pH value Readings**

### 5.1.2 Phase 2: Comprehensive Testing

In Phase 2 of our experiment, it involved integrating all sensors and conducted comprehensive tests on each parameter. These tests were carried out in a controlled environment to gain further insights. As mentioned earlier in Phase 1, while we gathered data on moisture content and temperature in the substrate, we encountered uncertainties regarding the reliability of these measurements. As a result, determining the optimal sensor's locations for the parameters became challenging. To address this issue, Phase 2 aims to further investigate and refine the locations of sensors within the system. This phase is crucial for enhancing the precision and effectiveness of our bioconversion system by ensuring that sensor's locations are optimized for accurate monitoring and control of all these parameters.

To maintain consistency and minimize external variables that could influence our data collection, we have replicated the identical setup tested in Phase 1. This involves using the combination of 8kg of food waste, 300g of peanut skins, and an initial population of 10,000 larvae (5 DOL) within the container, as illustrated in Figure 48.

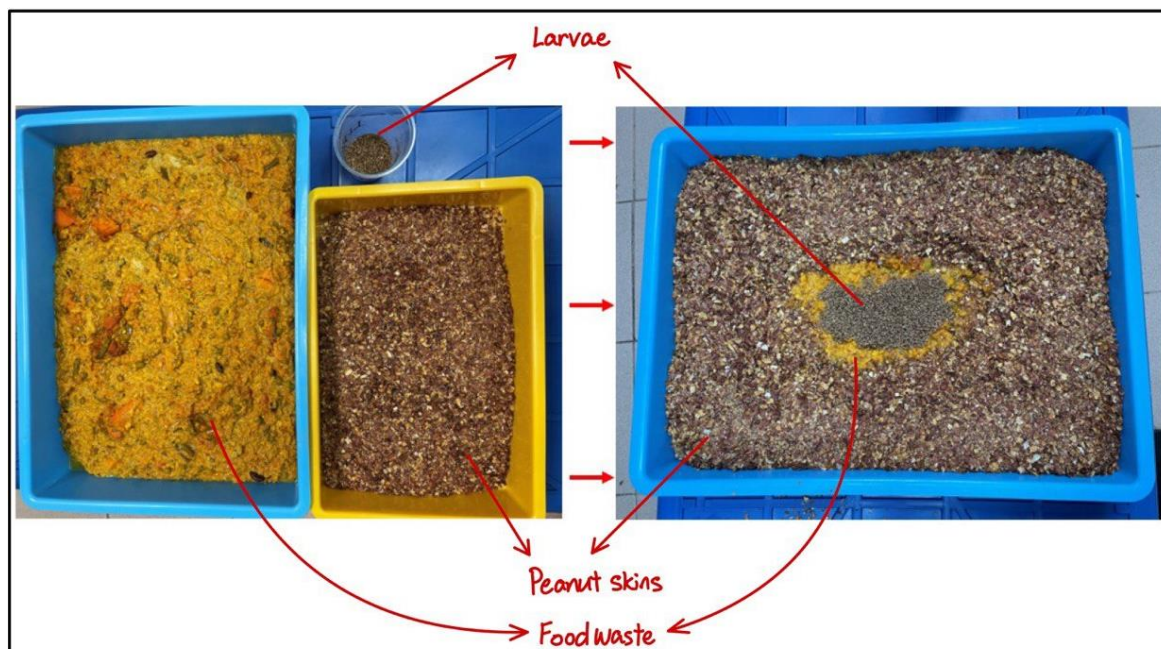


*Figure 48: Combination of food waste, peanut skins, and larvae*

Figure 49 illustrates the experimental setup designed for the precise measurement and regulation of environmental variables within a reactor system. Central to the setup is a reactor containing substrates, monitored for optimal processing conditions. The system integrates an array of sensors, including a relative humidity sensor (DHT22) and a CO<sub>2</sub> sensor (SGP30), vital for assessing the atmospheric conditions necessary for the substrates' stability. Temperature is monitored using two DS18B20 sensors, ensuring a consistent thermal environment. The Arduino and SD card module serve as the brain of the operation, recording data for further analysis and a step-down buck converter is used to manage the power supply to the system's components.

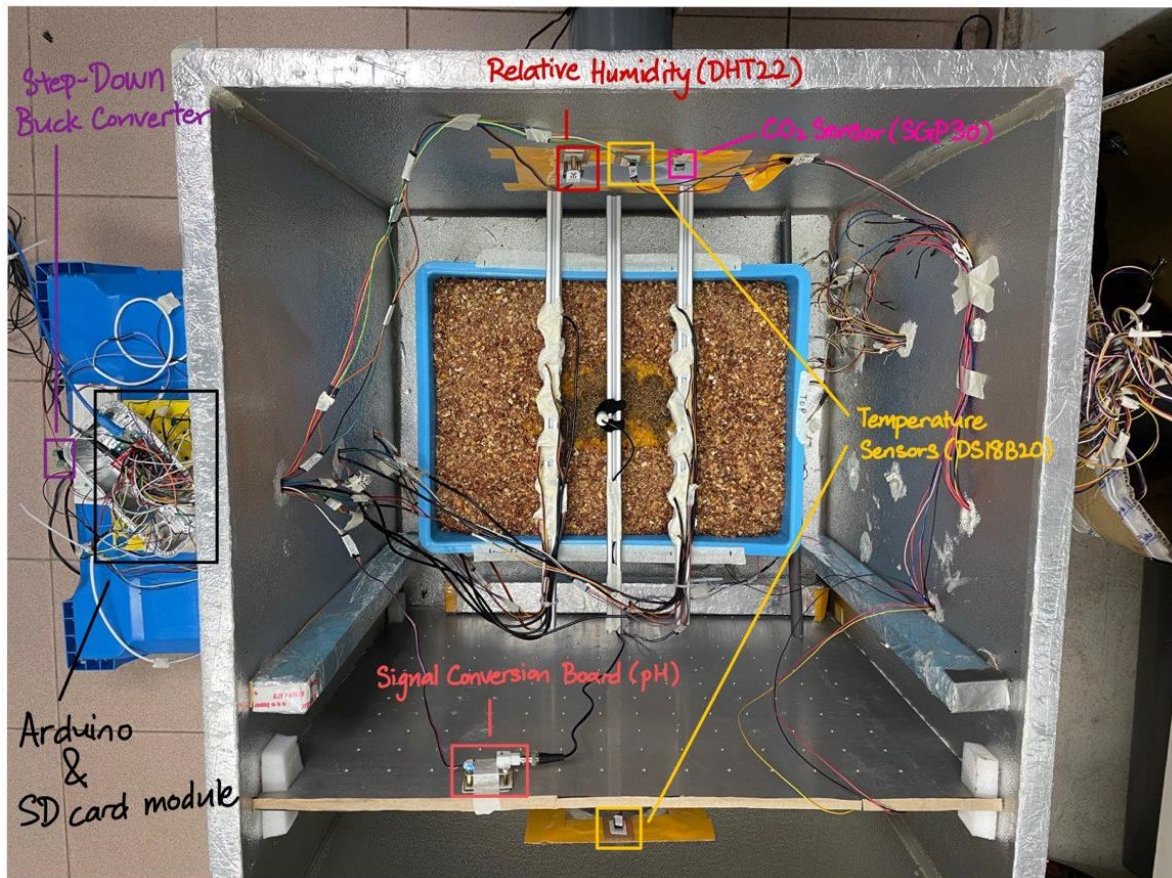


Figure 49: Phase 2 setup configuration

#### **5.1.2.1 Results & Analysis: Comprehensive Testing**

Unfortunately, due to unforeseen circumstances, we encountered challenges in collecting data during Phase 2 of the experiment. Despite our efforts to execute the planned tests, various unexpected factors hindered our ability to obtain the necessary data. These circumstances may have included technical difficulties such as connectivity issues, sensor malfunctions, or other unanticipated issues that arose during the experimental process. As a result, we were unable to gather the intended information during this phase of the study. Moving forward, it will be essential to address and overcome these challenges to ensure the successful execution of future experimental phases and the attainment of comprehensive data to fulfill our research objectives.

#### **5.1.3 Phase 3: Testing in the Constructed Reactor**

Phase 3 of our experiment involved a full integration of both hardware and software components, signaling the commencement of testing within our constructed reactor. With the reactor assembled, our next step was to install the sensors within the reactor. Drawing on insights from previous experiments, we meticulously positioned sensors to ensure optimal placement, thereby enabling accurate data collection.

For the purpose of establishing connections with multiple sensors to an Arduino housed within an electronics box, we have prepared 11 multi-strand cables, each measuring between two to three meters in length. These cables are designed to facilitate robust and reliable communication between the sensors and the microcontroller. The electronics box, a repurposed BPA-free plastic container originally intended for food storage, has been modified to serve as a protective housing for the electronic components. To tailor the electronics box for this setup, we installed four cable glands, ensuring secure cable entry points that maintain the enclosure's defense against environmental factors such as dust and moisture. Moreover, to address the heat generated by the Arduino during operation, we have drilled four 2mm holes in the lid of the box for ventilation, enhancing the system's thermal management and ensuring the stability of the internal temperature, as illustrated in Figure

50. This setup is indicative of a cautious approach to electronics design, where the protective measures are well-considered, pointing towards the enclosure's potential use in an outdoor or industrial setting where such precautions are necessary.

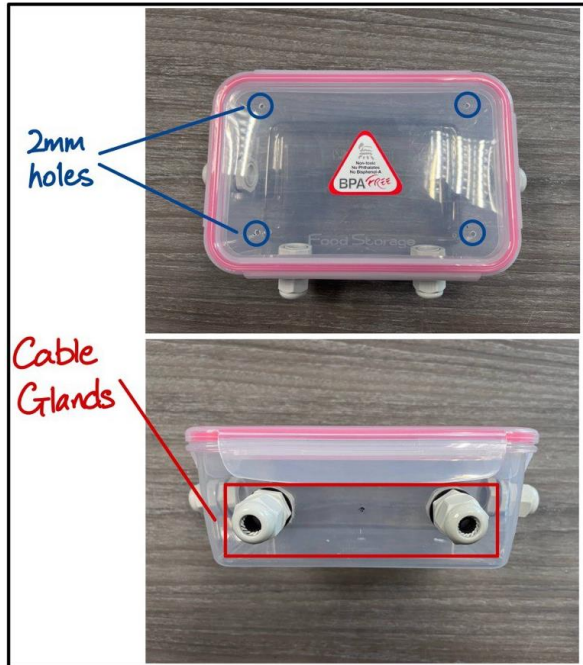


**Figure 50: Electronics Box**

We utilized a protoboard shield that has been securely soldered with terminal pins and then mounted onto an Arduino Mega—a microcontroller board that is favored for its ample pinout, accommodating complex projects, as illustrated in Figure 51. The shield aligns with the Arduino's header pins, enabling an electrical connection between the shield and the microcontroller. Notably, the protoboard is equipped with yellow, green, and red wires, which have been meticulously placed using wire wrapping techniques to establish connections without soldering. This method allows for durable yet easily modifiable circuits, ideal for iterative prototyping and testing. This setup serves as a testament to the versatility and adaptability of the Arduino Mega and its associated protoboard shield, providing a robust platform for custom electronic designs.

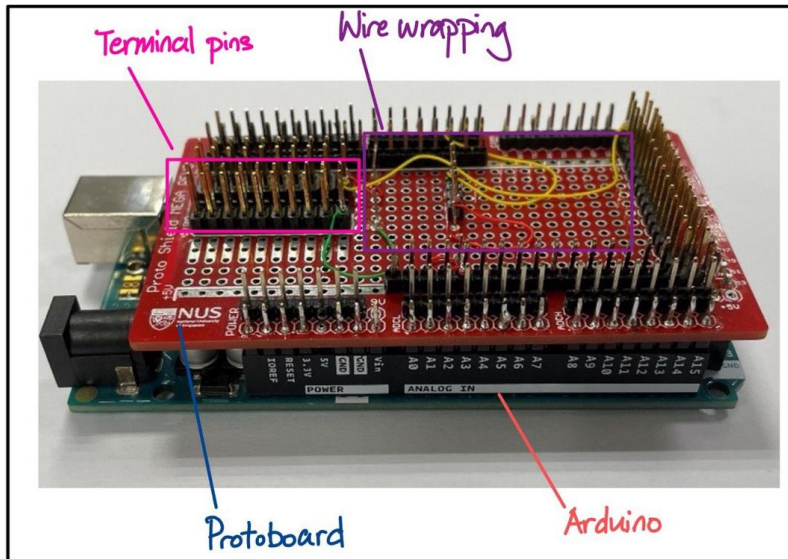


**Figure 51: Arduino and protoboard shield**

In this setup, the micro-SD card module is connected to an Arduino via a series of jumper wires, for the purpose of testing connectivity as well as collecting and storing data, as illustrated in Figure 52. This configuration illustrates a practical application of the module, which, through the Serial Peripheral Interface (SPI) bus, provides the Arduino with expanded data logging capabilities. The array of jumper wires is used to connect the various SPI pins on the Arduino to the corresponding pins on the micro-SD card module, establishing a communication channel that allows the microcontroller to write to and read from the SD card. This arrangement is instrumental in applications that require the long-term storage of data, such as environmental monitoring systems, where data points are collected at regular intervals and need to be archived for future analysis. The modularity and flexibility of this system are exemplified by the use of a prototyping shield, which provides convenient access to the Arduino's pins and facilitates the quick reconfiguration of the circuit if needed.

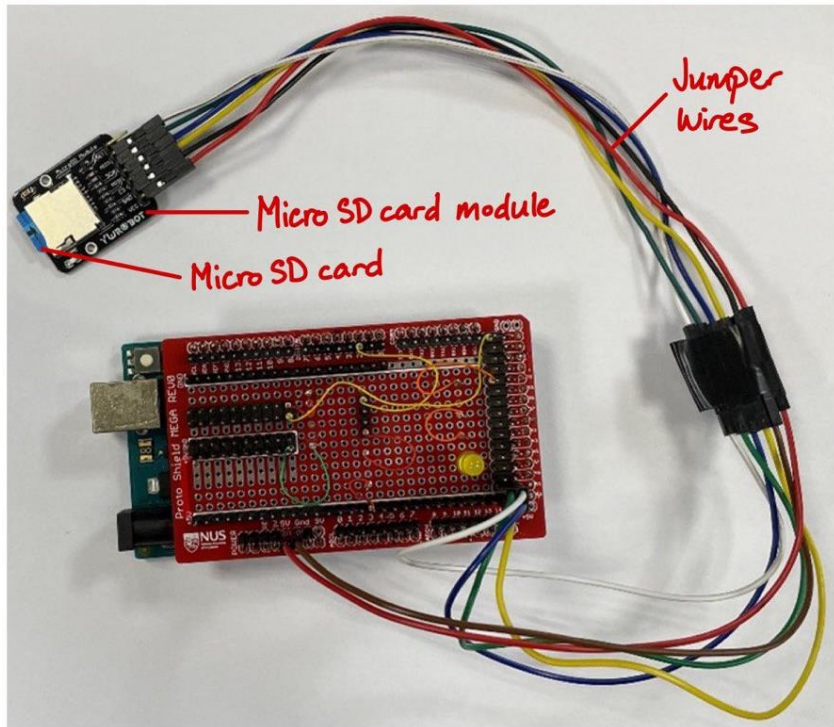


*Figure 52: Micro SD card module connected to Arduino*

To facilitate the connections of our sensors, a precise and systematic approach was adopted for preparing the necessary cables, as illustrated in Figure 53. Initially, the wires were measured and cut to the required lengths. Each wire then underwent a stripping process to remove the insulation from the ends, exposing the conductive material. Next, female Dupont terminals were affixed to the exposed ends of the wires. To ensure a robust electrical connection, solder was applied to the junction of the wire and the terminal using a heated soldering iron, which allowed the solder to flow into the terminal sleeve, solidifying upon cooling. The mechanical stability of the connection was further reinforced by employing a crimping tool, which securely fastened the terminal to the wire. This procedure was meticulously repeated for each wire intended for sensor connection. After all connections were established, they were inspected and tested with a multimeter to ensure integrity and continuous conductivity. Where necessary, cables were grouped and labeled to maintain organized and efficient sensor installation, thereby ensuring the reliability of the connections for accurate data transmission and sensor performance.

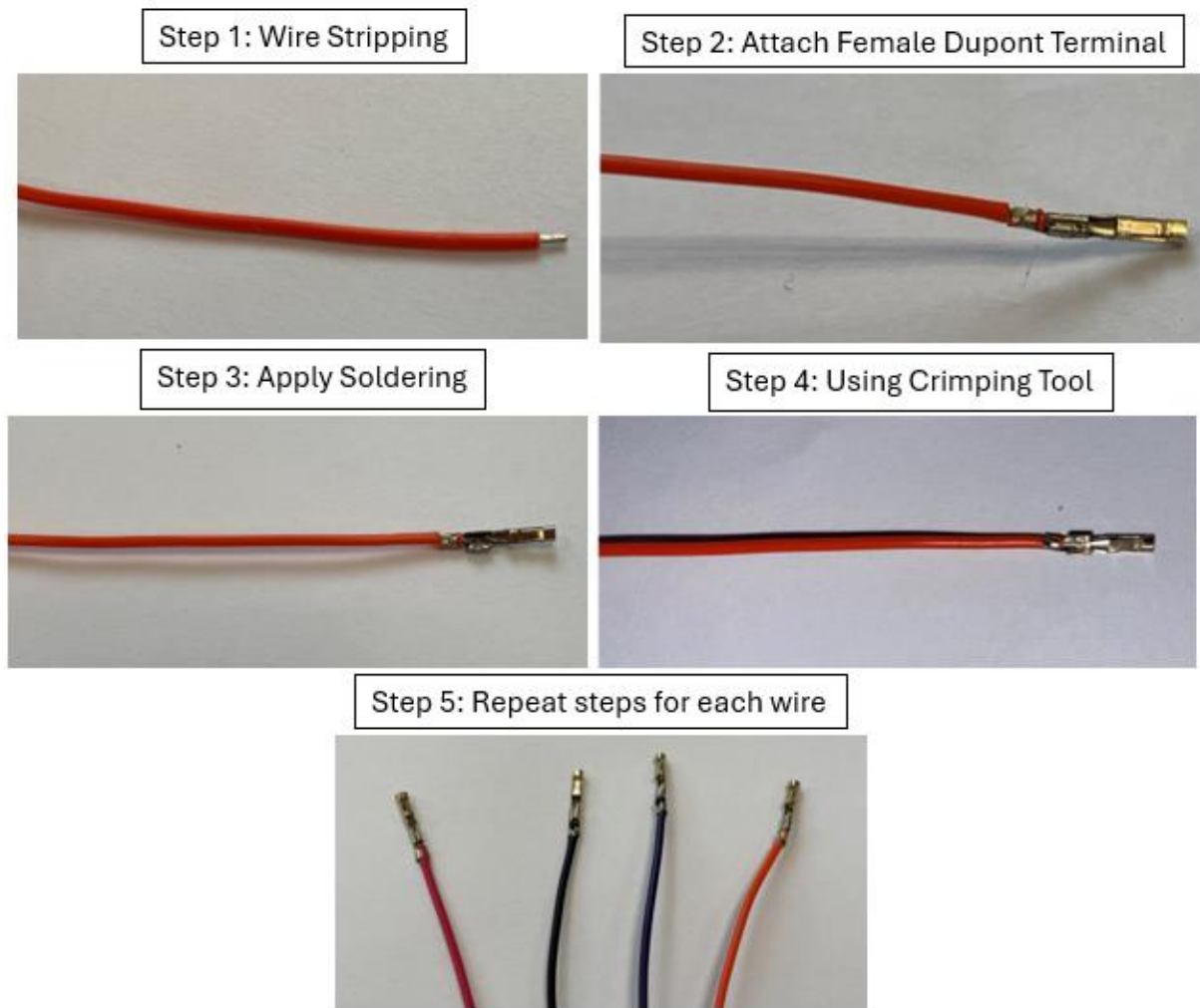


*Figure 53: Steps for preparing necessary cables*

In the comprehensive setup as illustrated in Figure 54, all the sensors are connected to an Arduino board equipped with a protoboard, less the fans. Additionally, the setup includes a step-down buck converter, which is essential for regulating the power supplied to the components, ensuring that each receives the correct voltage for safe and effective operation. The array of multi-strand cables, each wire corresponding to a different sensor, forms a network of connections that manage the flow of data and signals back to the microcontroller. With the completion of the hardware assembly, the project now transitions to the integration phase, focusing on the incorporation and mounting of the sensors into the reactor for operational.

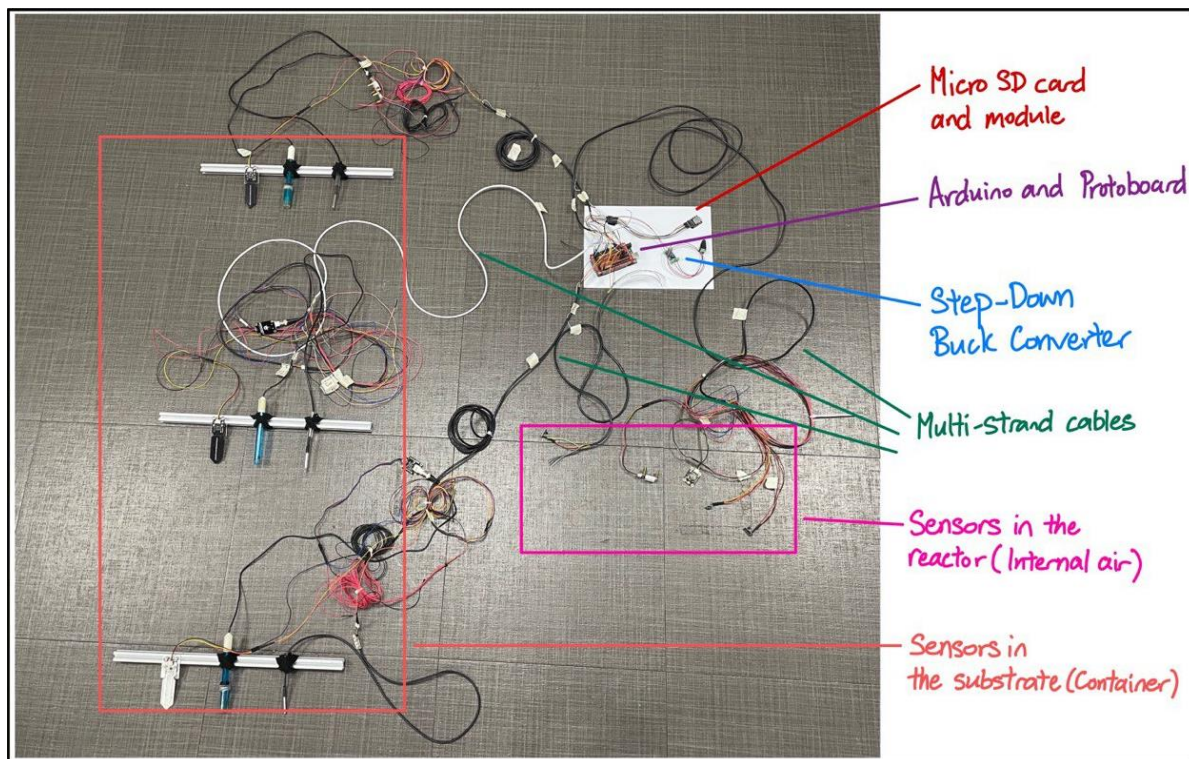


**Figure 54: Connected all sensors to Arduino (exception of fans)**

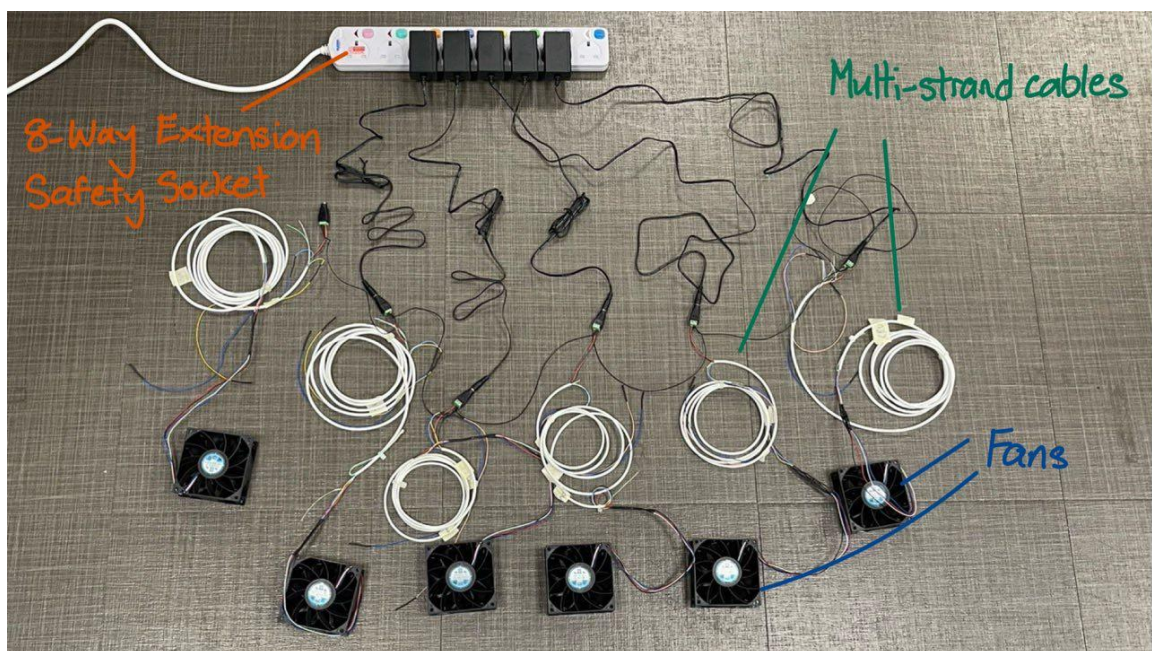


**Figure 55: Connection of fans to socket**

In order to gather thorough data, we strategically positioned sensors in the top, middle, and bottom containers within the reactor. This choice was driven by the necessity to grasp potential variations in moisture levels, temperature, and pH value in the substrate. Since we were uncertain about the extent

of differences between containers, it was crucial to collect data from various points within the reactor. This systematic method allowed us to gather a thorough understanding of the bioconversion process in our reactor and determine the necessity of measuring these parameters in all containers. Therefore, we have used three sensors for each parameter, covering moisture levels, temperature, and pH values in the substrate.

To begin, we initiated the process by mounting sensors into the substrate. Initially, we fabricated 3mm acrylic pieces measuring 4.5cm x 3.5cm to accommodate the moisture sensors. Utilizing the mounting holes provided with the sensor, we employed 2mm screws and nuts to firmly affix the sensor onto the acrylic base, as illustrated in Figure 56. Following this, for the temperature sensors, we fabricated 4.5cm hollow tubes to regulate its height and ensure better fixation onto the aluminium profile bar, as illustrated in Figure 57. As for the pH sensors, their size negated the need for fabrication, as they could be directly affixed onto the aluminium profile bars.

To mount these sensors, we used 3mm screws and nuts to secure the acrylic base of the moisture sensor onto the profile bars, while opting for velcro strips to secure temperature and pH sensors, as illustrated in Figure 58. This decision was made to enable easy adjustment of the sensor height, allowing for more precise readings. By adjusting the height, we could ensure that the sensors were positioned optimally within the substrate, enhancing the accuracy of our data collection process. This approach also facilitated the removal and repositioning of sensors as needed during experimentation, providing flexibility in our setup.

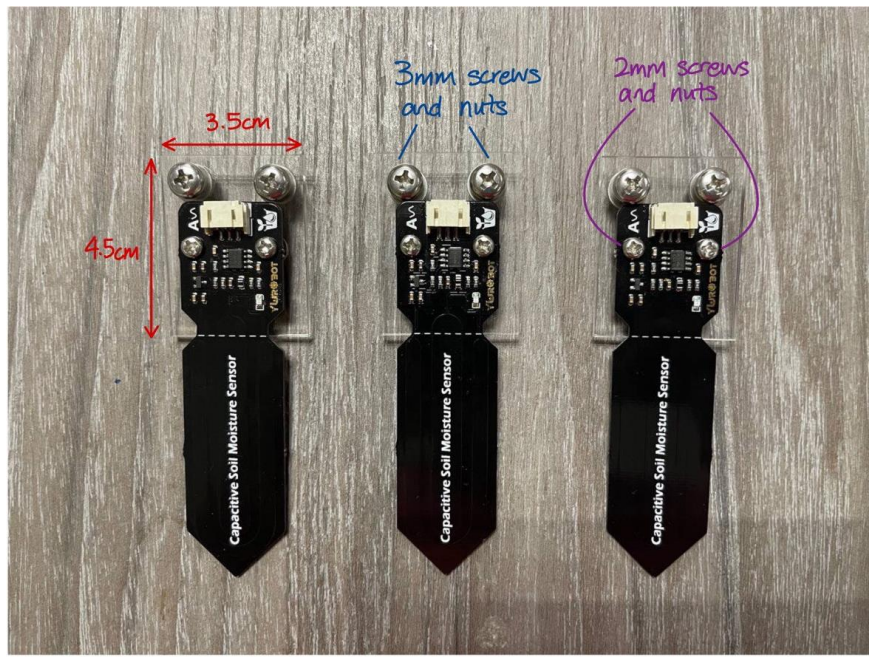


Figure 56: Capacitive Moisture Sensors

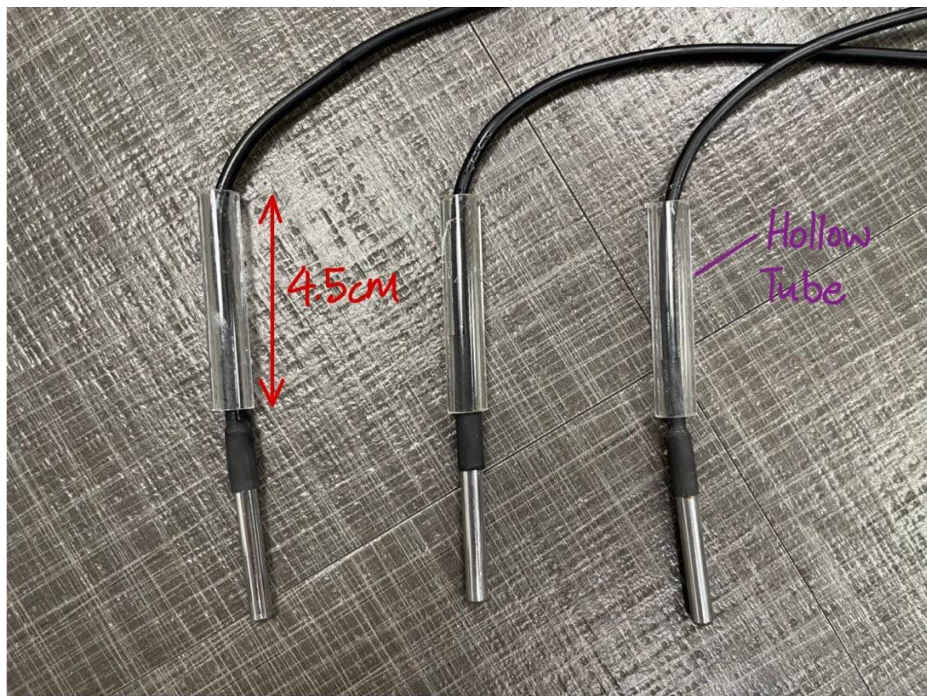
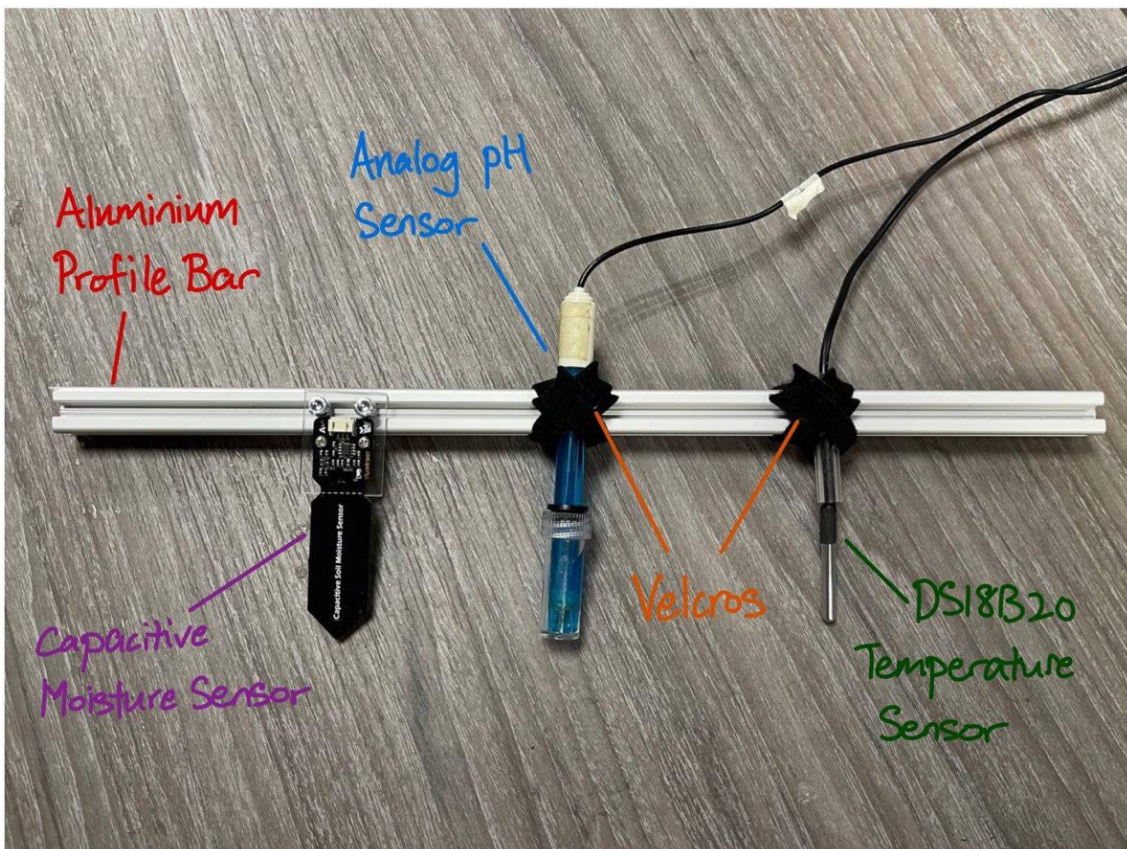


Figure 57: Temperature Sensors (DS18B20)



*Figure 58: Mounting of sensors (Moisture, temperature, and pH)*

We proceeded with installing sensors to monitor internal air parameters within the reactor, including internal temperature, methane levels, and relative humidity, strategically positioning them at both the inlet and outlet of the reactor. To mount these sensors, we decided to use the same dimensions of acrylic plates that we used for mounting the moisture sensor. However, mounting the sensors presented a challenge as we were unsure of the optimal position due to the absence of data from Phase 2. Without this data, we faced uncertainty regarding whether the sensors were positioned too low, too high, or even off-center within the reactor. Despite this challenge, we took measures to ensure accurate data collection. Each sensor was mounted onto a 4.5cm x 3.5cm acrylic plate, and a spacer was placed on the sensor to prevent interference with the data readings. This spacer maintained a consistent distance between the sensor and the substrate, reducing the risk of data inaccuracies. Notably, the temperature sensor lacked its own mounting holes, but we found that

securing it directly onto the acrylic plate with double-sided tape did not affect its performance, eliminating the need for spacers. Overall, we installed one temperature, methane, and relative humidity sensor at the chimney, serving as the outlet of the reactor, and another temperature sensor near the bottom fan, designated as the inlet. This setup was designed to offer more accurate readings across different points within the reactor. The mounting of these sensors is illustrated in Figures 59 and 60 for reference.

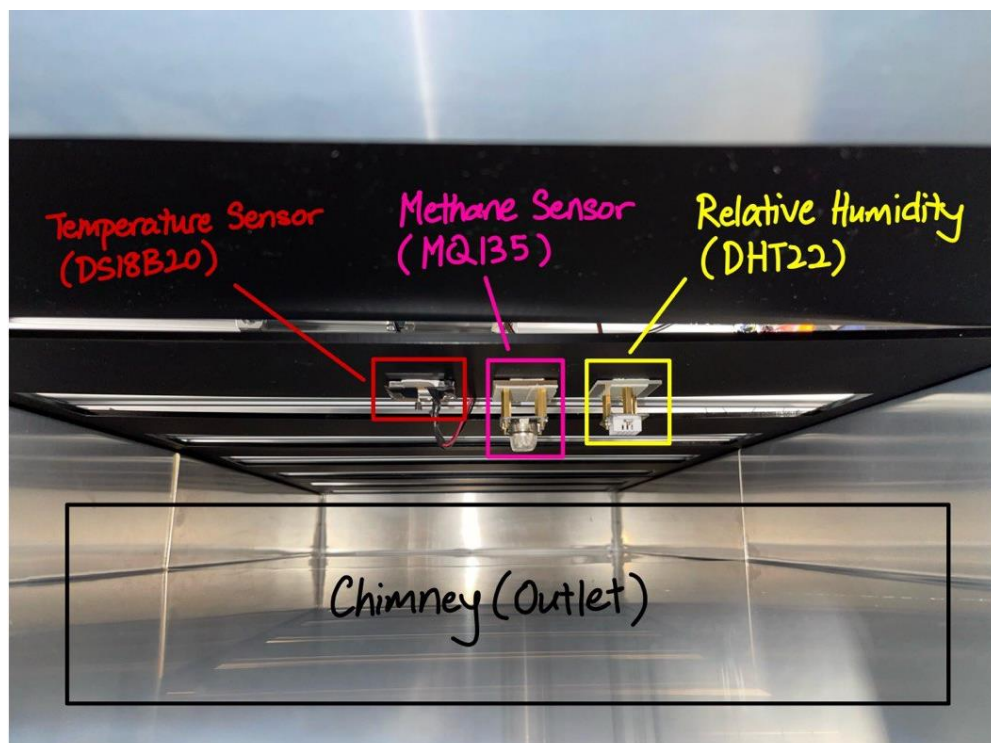
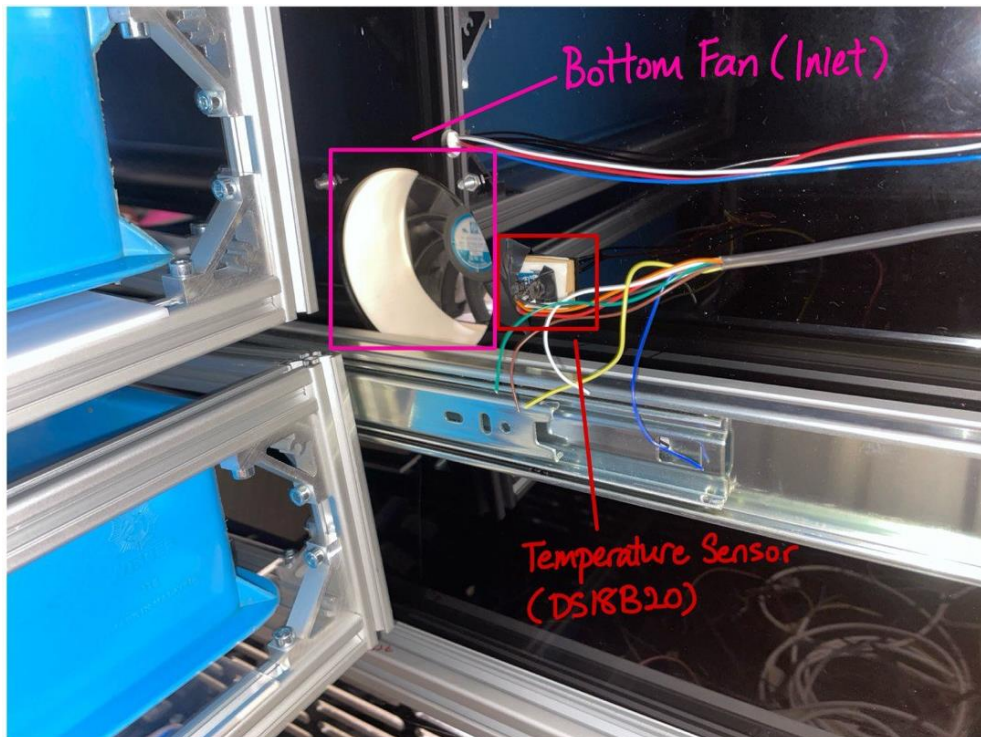


Figure 59: Mounting of sensors at chimney, inlet (Temperature, Methane, and Relative Humidity)



*Figure 60: Mounting of sensor at outlet (Temperature)*

As illustrated in Figures 61 and 62, provides a back view of the reactor, showcasing the installation and arrangement of all sensors to ensure their proper functioning. Our aim was to establish a streamlined setup that would facilitate efficient data collection and analysis. However, upon installation, we encountered challenges with cable management. Despite our initial planning, the arrangement of wires did not align as expected, resulting in a tangled mess of cables, particularly after connecting them to the Arduino unit housed within the electronics box. This unforeseen complication prompted us to revisit our cable management strategy and explore alternative solutions to organize the wiring effectively.

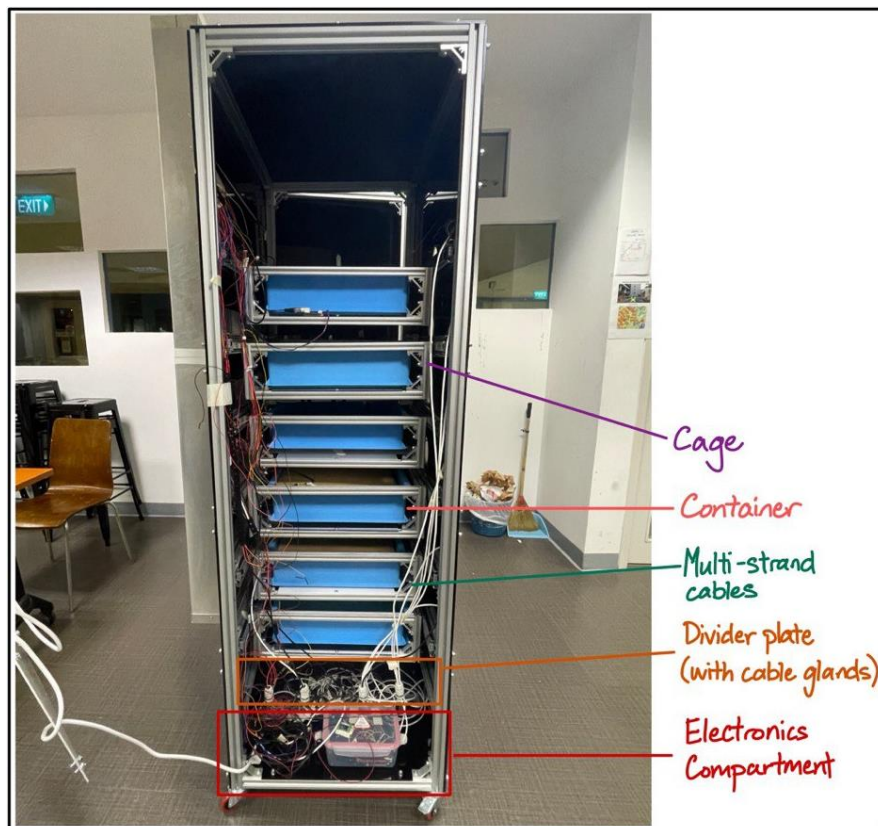


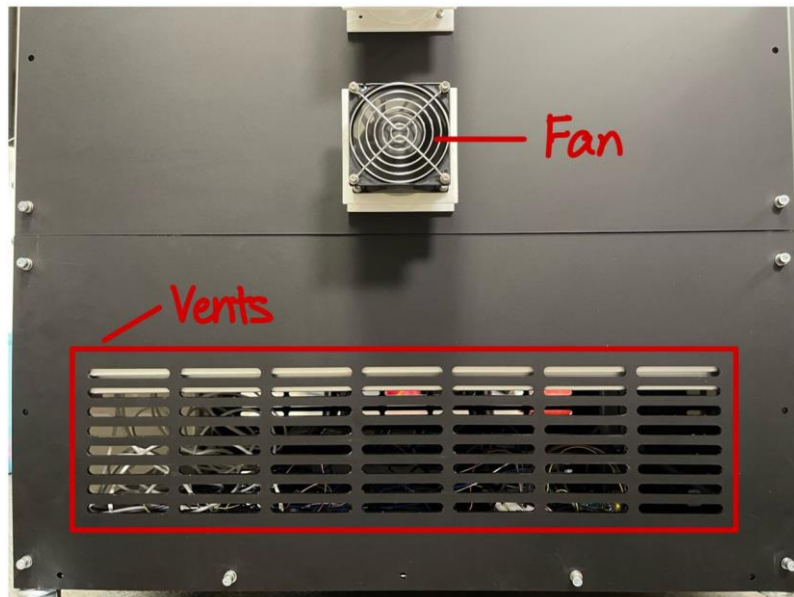
Figure 61: Back view of reactor



Figure 62: Back view of reactor (Zoom in)

To enhance the system's efficiency and maintain a controlled environment, ventilation openings have been incorporated, as illustrated in Figure 63. This addition aims to facilitate smooth airflow within the system, crucial for regulating temperature and humidity levels. However, the introduction of these vents brought to light a potential vulnerability, the risk of insects gaining access to the reactor, attracted by the stored food waste.

Insects infiltrating the system could compromise the quality of the composting process and potentially affect the reactor's operational efficiency. To address this concern, we implemented an additional safeguard by installing wire mesh over the vents. This modification, illustrated in Figure 64, serves a dual purpose: it maintains the intended ventilation benefits while effectively barring insects from entering the reactor. The wire mesh is designed to be fine enough to prevent the smallest of insects from passing through, yet sufficiently permeable to allow air to circulate freely, ensuring that the reactor's internal environment remains optimal for composting processes. This integration of ventilation and protective measures underscores maintaining a hygienic, efficient, and uncontaminated waste processing system.



*Figure 63: Vents for ventilation*

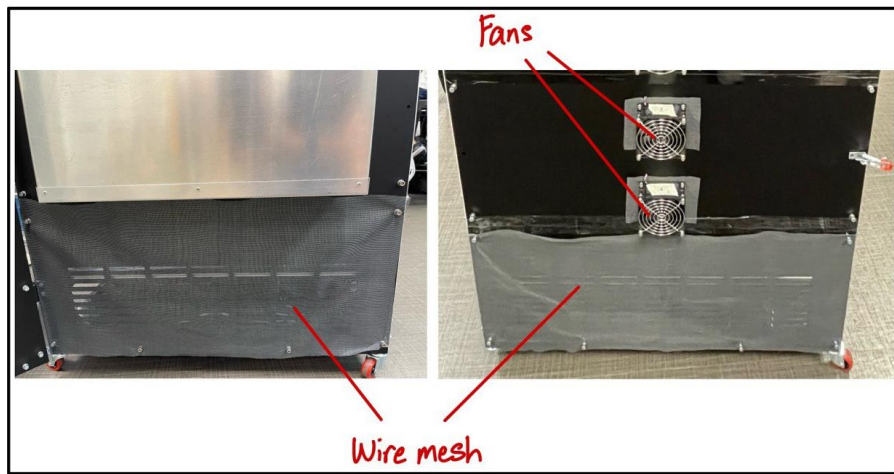


**Figure 64: Wire mesh installed onto the vents**

For this experiment, we utilized a total of 40.17 kilograms of food waste, distributed across multiple containers. Each container was loaded with a precise quantity of 6.695 kilograms of food waste, including a mixture of food waste and cocopeat, as illustrated in Figure 65 and 66. Additionally, we introduced 9280 BSFL into each container to facilitate the bioconversion process, as illustrated in Figure 67.



**Figure 65: Mixture of food waste and cocopeat**

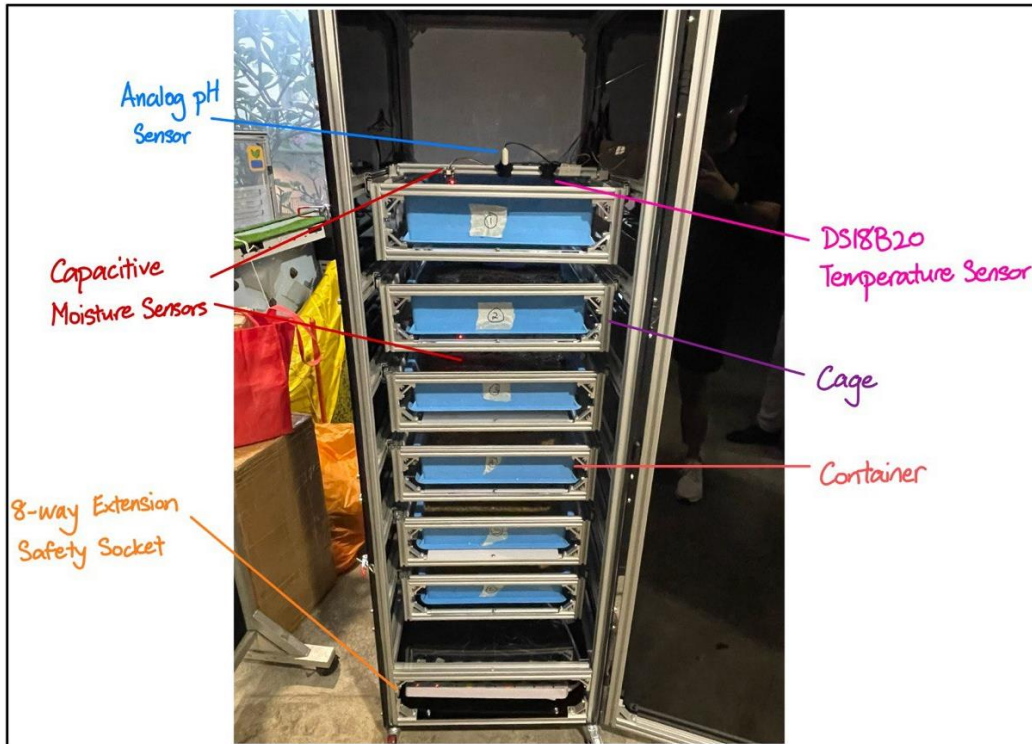


**Figure 66: Weighing of food waste**



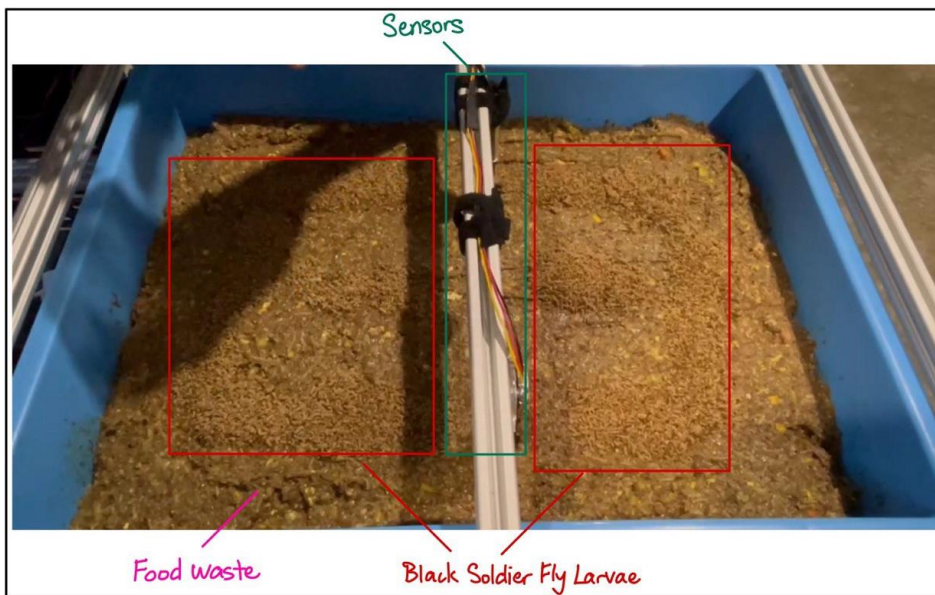
**Figure 67: Food waste and BSFL**

Figure 68 illustrates the reactor post loading, where food waste and larvae have been systematically placed into their respective containers within the reactor. This stage marks the beginning of the bioconversion process involving BSFL in its third phase, poised for detailed observation and analysis.



*Figure 68: Post loading configuration*

Figure 69 provides a detailed close-up of the experimental setup for BSFL, highlighting two specific locations, outlined in red, where the larvae have been placed for observation.



*Figure 69: Close-up of the BSFL in the container*

Figures 70 and 71 highlight inconsistencies in sensor output, pointing to an insufficient substrate depth in the test vessels. The experiment's design necessitates that sensors be deeply embedded in the food waste to accurately gauge environmental parameters. However, the top and bottom containers, with substrate depths of merely 2 to 3 centimeters, did not allow the sensors to be fully inserted in, compromising the precision of the data gathered. This partial insertion proves inadequate for closely observing the conditions within the BSFL environment. On the other hand, the middle tray's substrate depth of approximately 4 centimeters afforded almost complete sensor immersion, leading to a more reliable data set. Nonetheless, the validity of this setup remains to be confirmed post-harvest when the collected data can be thoroughly analyzed. To enhance the rigor of subsequent experiments, it will be imperative to normalize the depth of the food waste across all containers. This will ensure comprehensive sensor coverage and reliable data acquisition, thus preserving the validity of the research outcomes.

Acceptable height: 4cm

Middle Tray



*Figure 70: Acceptable height of food waste*

Not acceptable height: 2-3cm

Top Tray

Bottom Tray

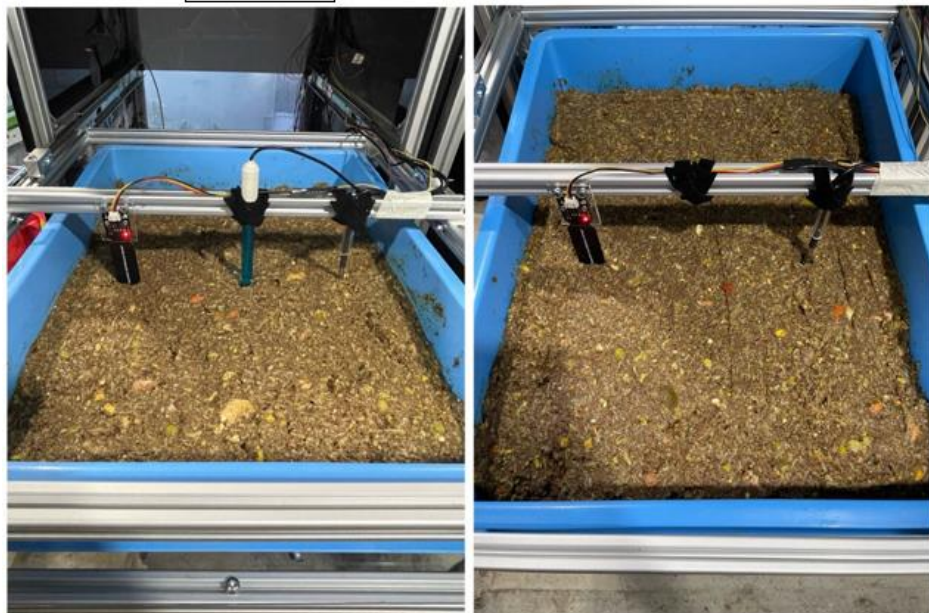


*Figure 71: Not acceptable height of food waste*

#### **5.1.3.1 Results & Analysis: Testing in the Constructed Reactor**

In the initial stages of our experimentation within the constructed reactor, we regretfully cannot present any data at this juncture. However, we anticipate providing detailed results and analysis in subsequent stages of our research. This phase serves as the foundation upon which we will gather essential data to evaluate the performance of our bioconversion system within the constructed reactor. As we progress, we will diligently document our findings, including any challenges encountered and adjustments made, to ensure a comprehensive understanding of our system's behavior. Through thorough analysis and interpretation of the data collected, we aim to draw meaningful conclusions regarding the efficacy and functionality of our system, paving the way for further optimization and refinement in subsequent experiments.

## **5.2 Software Integration**

The integration of software into our system will incorporate a detailed flow chart, as illustrated in Figure 72, showing the entire bioconversion process from initiation to completion. Prior to commencing the bioconversion process, it is imperative to load food waste and BSFL into all containers while ensuring that all sensors and the ventilation system (fans) are operational before closing. During the bioconversion process, the system diligently monitors various parameters such as substrate temperature, internal reactor's temperature, and relative humidity in real-time to ensure they remain within predefined threshold values for creating an optimal environment conducive to BSFL growth. Any deviations from these thresholds prompt the system to adjust the airflow speed accordingly until the desired values are attained. While data is stored on an SD card for subsequent analysis, the system's immediate response to sensor readings constitutes real-time control and management of the bioconversion process. The monitoring continues until the system determines that it is time for harvesting, which involves assessing additional parameters such as substrate moisture content, pH value, and gas emissions produced by the larvae. In the event of any anomalies, the system alerts for assistance and initiates a rechecking of all sensors to verify readiness for harvesting. Upon

confirmation of readiness, the system ceases airflow adjustments and awaits the harvesting process, during which the ventilation is turned off and the contents of all containers are unloaded into a single collection container, marking the conclusion of the bioconversion process. This comprehensive software integration not only streamlines the bioconversion process but also ensures data accuracy and reliability, facilitating informed decision making for optimal system performance.

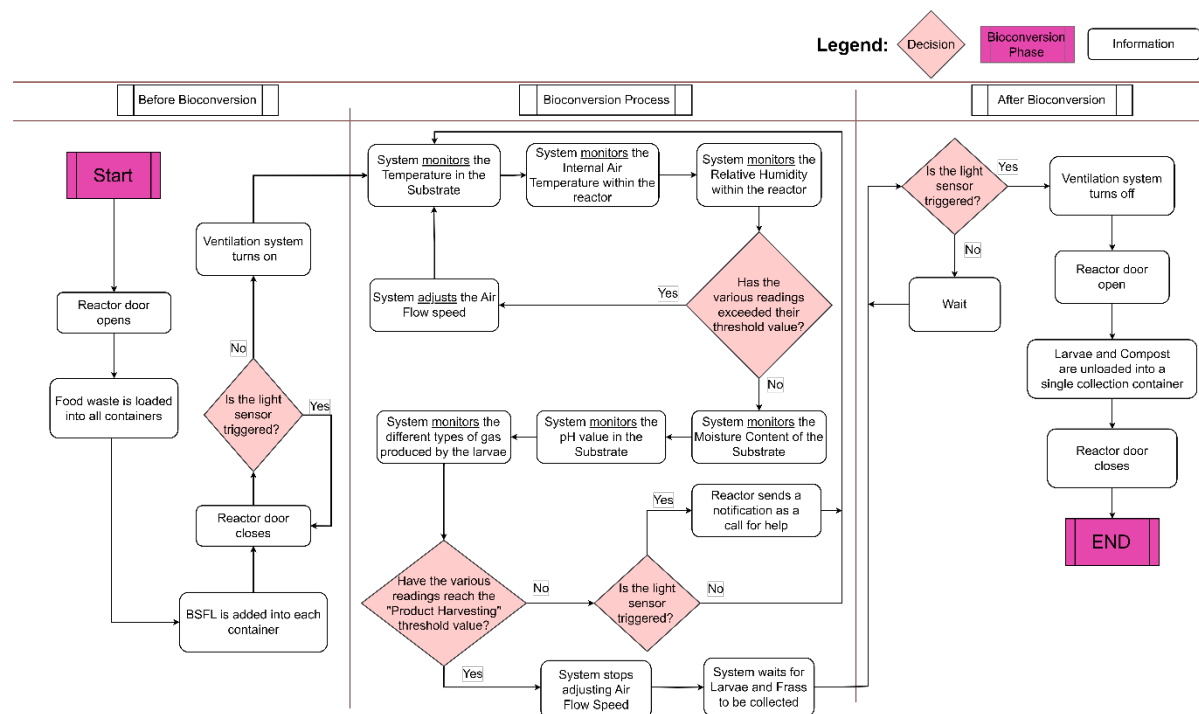


**Figure 72: Flow Chart: Bioconversion process**

## 6. Integration of Electronics

### 6.1 Overview of Electronics Integration

In Figure 73, it shows an overview of a pictorial diagram which offers a visual representation of the electronics network within a system, featuring a range of sensors all coordinated by a microcontroller, Arduino. The assortment of sensors present includes devices for measuring environmental variables—moisture levels are monitored by a capacitive moisture sensor, pH levels by an analog pH sensor, and air composition by an MQ4 gas sensor. Temperature and humidity data are collected by a DHT22 sensor, and a DS18B20 waterproof sensor is in place for temperature readings in moist conditions. A four-load cell array, interfaced with an HX711 signal amplifier, provides weight measurement capabilities. Data recording is managed by an SD card module. The power requirements for these components are met by a 12V 2.5A power adapter, and an 8-way extension safety socket efficiently channels electricity throughout the setup, including providing direct power to the fans. The inclusion of a buck converter within the setup underscores its function in reducing voltage to appropriate levels for the delicate electronics. For researchers aiming to replicate and maintain this assembly, this diagram would serve as a reference, detailing the intricate electrical connections that enable the functionality of the entire system.

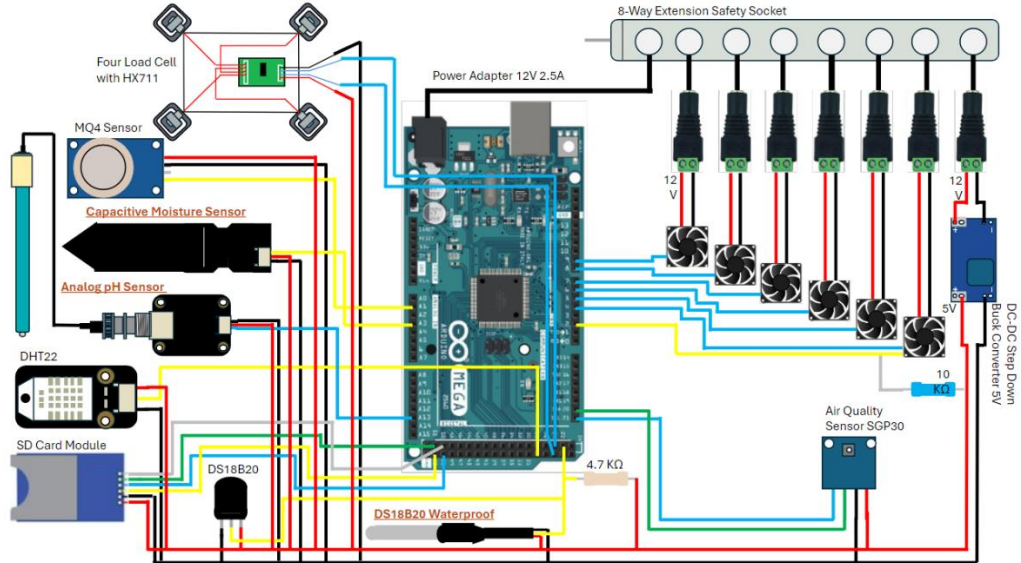


**Figure 73: Overview of sensors in pictorial diagram**

In response to the challenges encountered during the second phase of our experiment, where we lacked immediate data availability at harvest time, we have implemented an LED indicator into our Arduino protoboard circuit to be used in Phase 3, as illustrated in Figure 74. This LED serves as a diagnostic tool, designed to illuminate and signal a potential issue in data collection. With this modification, if the LED lights up, it alerts us that there is a malfunction that needs to be addressed, indicating that the sensors may not be recording data as expected. This proactive approach enhances our monitoring capability, allowing for quicker identification and resolution of issues, thus improving the reliability of our data acquisition process.

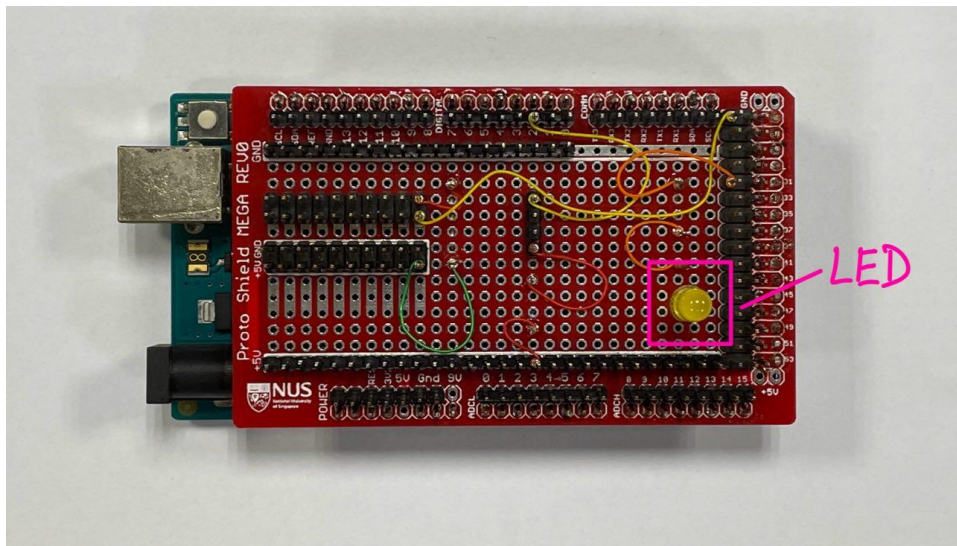


**Figure 74: Implemented and soldered an LED**

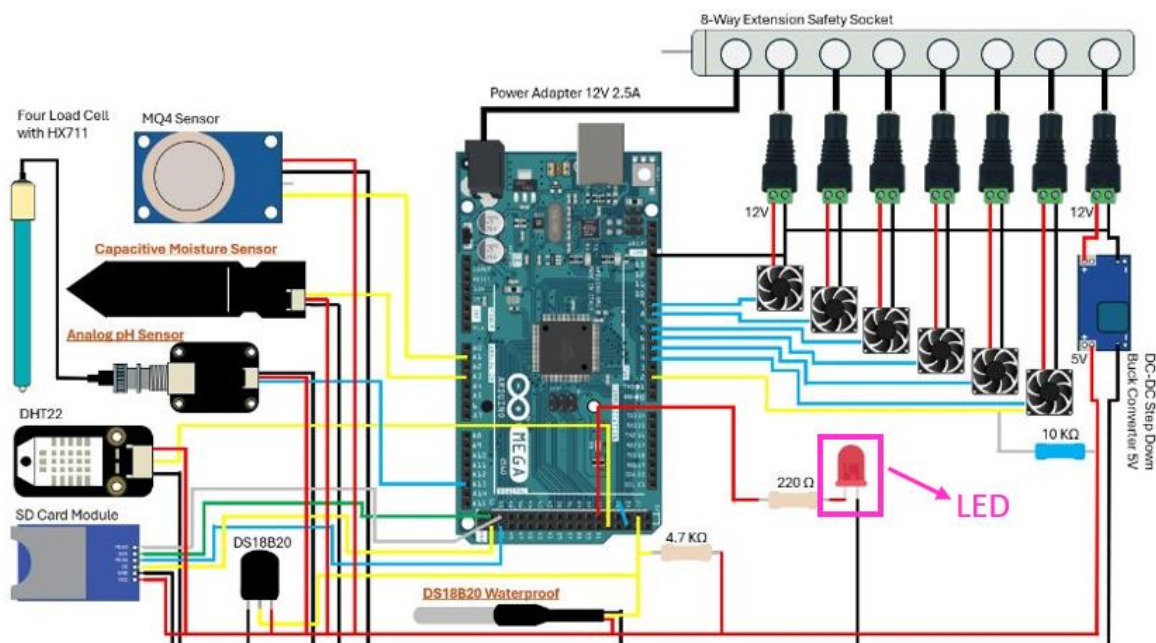


**Figure 75: Inclusion of LED in the pictorial diagram**

## **7. Future Works (Limitations & Recommendations for Improvement)**

### **7.1 Exclusion of Light Sensor**

The circuit design deliberately omitted the inclusion of a light sensor. The initial concept revolved around using the sensor as an alert mechanism for significant fluctuations in light intensity within the reactor, which could indicate changes in operating conditions. However, this feature was contingent on the implementation of a wireless data transmission system, which would enable remote monitoring capabilities. With such a system, users could receive notifications about light levels without the necessity for physical inspection. The light sensor's function was to provide real-time updates and trigger alerts when the light exceeded predetermined thresholds, enhancing the system's autonomy, and reducing the need for constant on-site supervision. This aspect of the design remains a consideration for future iterations, where wireless connectivity could streamline the operational workflow and offer improved convenience and efficiency.

### **7.2 Difficulties with CO<sub>2</sub> and Load Cells sensors Integration**

In the process of integrating all the sensors into our system, we encountered unexpected technical difficulties, particularly with the Carbon Dioxide (CO<sub>2</sub>) and the load cells sensors. These issues were displayed primarily in the data acquisition stage, where the readings for CO<sub>2</sub> concentrations and weight measurements were not captured as intended, which led to disruptions in the overall functionality of the code. The complexity of integrating these sensors proved to be a significant obstacle. Consequently, we chose to exclude these sensors from the third phase of our project. Resolving these issues demanded an in-depth analysis of our programming and electronic configurations, a task that extended beyond our initial time estimates. This development highlighted the complexities inherent in multi-sensor systems and the extensive troubleshooting often necessary in advanced research projects.

### 7.3 Adjustments for Mounting of pH Sensors

During the process of mounting the pH sensors into the containers, we encountered spacing constraints within the structure of the cages. As illustrated in Figure 76, the restrictive vertical spacing within the framework of the cage system was too compact, precluding the placement of pH sensors in the middle and bottom containers. Such a configuration would result in blockages, hindering the movement or operation within the cage. This prompted a reevaluation of the configuration of the cages level to ensure adequate room for sensor installation. Future modifications will need to address this by either adjusting the height between the cages or reconfiguring the sensor mounting approach to seamlessly integrate into the existing reactor.

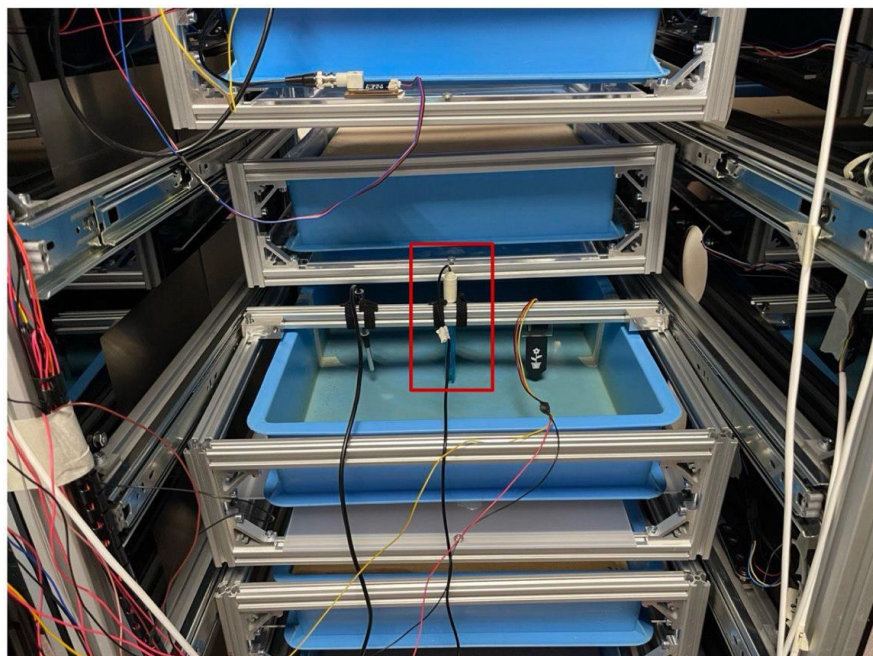


*Figure 76: Spacing constraints in between cages*

## 7.4 Sensor Maintenance and Harvesting: JST Connector Integration

We have discovered that during the operation of our container system, which utilizes a drawer mechanism for access, the attached wires and sensors are inadvertently dragged along. These sensors, crucial for monitoring substrate levels within the containers, are affixed to the cages. This issue complicates the process of smoothly sliding the containers in and out of the reactor, as we must vigilantly prevent the cables from entangling with adjacent cages or racks. Despite ensuring adequate slack for the sensors to allow full extension of the containers, retracting them poses its own challenge. The loose cables risk entanglement with the cages or racks and may come into contact with the lower levels of food waste stored within the containers.

Moreover, during the sensor retrieval phases of 1 and 2, we observed complications arising from their exposure to food waste. After spending approximately two weeks submerged in this environment, the sensors become coated with food waste, as illustrated in Figures 77 and 78. Additionally, the attraction of larvae to the sensors necessitates their removal for thorough cleaning before the sensors can be reused.

To address these operational challenges, we propose an innovative solution: the adoption of JST connectors. This upgrade would enable the easy detachment and reattachment of sensors from the cages, facilitating their maintenance and cleaning. Implementing JST connectors would streamline the process, ensuring that the sensors continue to operate effectively post-maintenance. This modification not only promises to alleviate the current handling and maintenance issues but also enhances the overall efficiency and hygiene of the system. Figure 79 shows the Dupont head connectors presently employed in the experimental setup, while Figure 80 presents the JST connectors, which are suggested as enhancements to the current system.



*Figure 77: Phase 1: Condition of sensors after experiment (Larvae on sensors)*

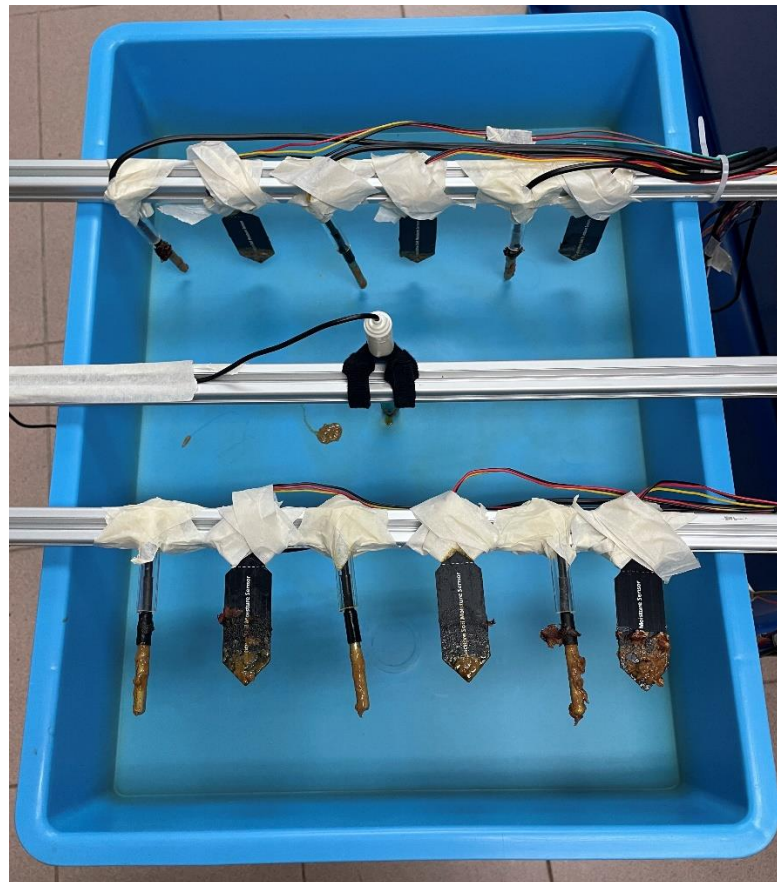


*Figure 78: Phase 2: Condition of sensors*

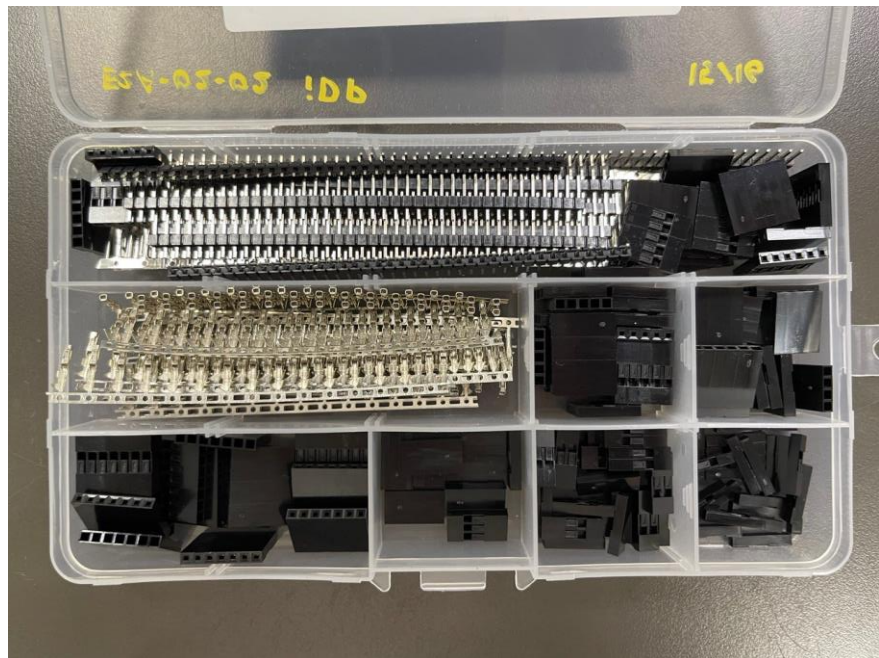


*Figure 79: Dupont head Connectors*

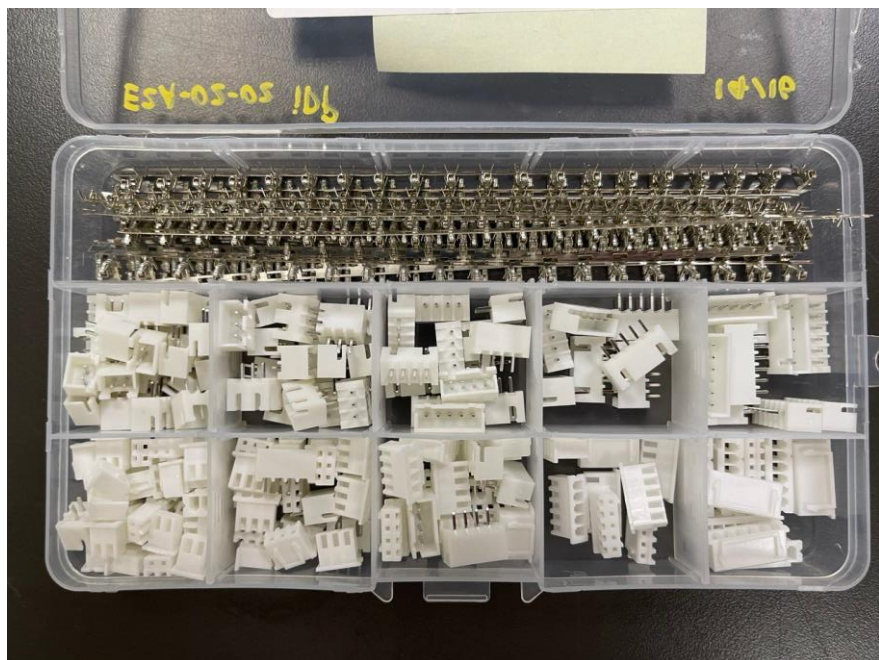


*Figure 80: JST Connectors*

## References

- [1] "Food Waste Management," National Environment Agency, <https://www.nea.gov.sg/our-services/waste-management/3r-programmes-and-resources/food-waste-management#:~:text=Food%20waste%20accounts%20for%20about,waste%20was%2018%20per%20cent>. (accessed Nov. 13, 2023).
- [2] "Waste statistics and overall recycling," National Environment Agency, <https://www.nea.gov.sg/our-services/waste-management/waste-statistics-and-overall-recycling> (accessed Nov. 13, 2023).
- [3] "Food waste," Towards Zero Waste Singapore, <https://www.towardszerowaste.gov.sg/foodwaste/#:~:text=Food%20waste%20is%20one%20of,around%2051%2C000%20double%20decker%20buses>. (accessed Nov. 13, 2023).
- [4] "The science behind incineration," Towards Zero Waste Singapore, [https://www.towardszerowaste.gov.sg/science\\_behind\\_incineration/](https://www.towardszerowaste.gov.sg/science_behind_incineration/) (accessed Nov. 13, 2023).
- [5] L. Hong, S'pore study on fitting incineration plants with carbon capture tech set to be completed by Q2 2024, <https://www.straitstimes.com/singapore/environment/s-pore-study-on-fitting-incineration-plants-with-carbon-capture-tech-to-be-completed-by-q2-2024> (accessed Nov. 13, 2023).
- [6] "Zero waste nation," Towards Zero Waste Singapore, <https://www.towardszerowaste.gov.sg/zero-waste-nation/> (accessed Nov. 13, 2023).
- [7] "Singapore: Food security vs land scarcity," Synergia Foundation, <https://www.synergiafoundation.org/insights/analyses-assessments/singapore-food-security-vs-land-scarcity#:~:text=Due%20to%20scarce%20agricultural%20land,a%20small%20number%20of%20countries>. (accessed Nov. 13, 2023).

[8] "News releases," National Environment Agency,  
<https://www.nea.gov.sg/media/news/news/index/food-waste-at-east-coast-lagoon-food-village-to-be-turned-into-energy-and-fertiliser-under-pilot-project> (accessed Nov. 13, 2023).

[9] Anaerobic digestion cost - plus gate fees and other rules of thumb. IPPTS Anaerobic Digestion Community Website. (2023a, June 18). <https://anaerobic-digestion.com/anaerobic-digestion-cost-gate-fees/#:~:text=Capital%20Cost,is%20roughly%20%241.2%20million%20dollars> (accessed Apr. 02, 2024).

[10] E. Larry E, E. Fayet, B. Krishna Kakumanu, and D. Lawrence C, Anaerobic Digestion, <https://citeseerx.ist.psu.edu/document?repid=rep1&type=pdf&doi=c8170c5d8da9065a5ec76ba8937bad7ab8c84b4f> (accessed Nov. 13, 2023).

[11] S. Anusha Siddiqui et al., "Black soldier fly larvae (BSFL) and their affinity for organic waste processing," Waste Management, <https://www.sciencedirect.com/science/article/pii/S0956053X22000010#s0015> (accessed Nov. 13, 2023).

[12] Insects creep up on the human diet, <https://www.ft.com/content/252c7358-8fcd-46e4-b500-4b06922d7f6c> (accessed Nov. 13, 2023).

[13] "Why BSFL?" Oberland Agriscience, [https://www.oberlandagriscience.ca/why-bsfl#:~:text=Black%20soldier%20fly%20larvae%20\(Hermetia,better%20than%20conventional%20protein%20sources](https://www.oberlandagriscience.ca/why-bsfl#:~:text=Black%20soldier%20fly%20larvae%20(Hermetia,better%20than%20conventional%20protein%20sources) (accessed Nov. 13, 2023).

[14] "Nutritional value of black soldier fly larvae," Kimmy Farm, <https://kimmyfarm.com/en/nutritional-value-of-black-soldier-fly-larvae> (accessed Nov. 13, 2023).

[15] B. Dortmans, S. Diener, V. Bart, and C. Zurbrügg, *Black Soldier Fly Biowaste Processing: A Step-by-Step Guide*. Dübendorf: eawag, 2017.

[16] “The Forbidden Foods: What not to feed worms in your compost bin,” Uncle Jim’s Worm Farm, <https://unclejimswormfarm.com/what-to-not-feed-worms/> (accessed Nov. 13, 2023).

[17] D. Purkayastha and S. Sarkar, Sustainable waste management using black soldier fly larva: a review, <https://link.springer.com/article/10.1007/s13762-021-03524-7> (accessed Nov. 13, 2023).

[18] Y. L. Foo, “A Primer on the Black Soldier Fly Market in Asia,” Mana Impact, <https://www.manaimpact.com/post/a-primer-on-the-black-soldier-fly-market-in-asia#:~:text=BSF%20solutions%20have%20the%20potential,based%20animal%20feed%20for%20live stock>. (accessed Nov. 13, 2023).

[19] C. Tan, “Researchers develop blueprint for Sustainable Food System using black soldier flies,” Researchers develop blueprint for sustainable food system using black soldier flies, <https://www.straitstimes.com/singapore/researchers-develop-blueprint-for-sustainable-food-system-using-black-soldier-flies> (accessed Nov. 13, 2023).

[20] “Hawker culture,” ROOTS, <https://www.roots.gov.sg/ich-landing/ich/hawker-culture> (accessed Apr. 3, 2024).

[21] Culinary Culture, [https://singaporemagazine.sif.org.sg/Stories/Data/Stories/Culinary-Culture\\_2021Issue1](https://singaporemagazine.sif.org.sg/Stories/Data/Stories/Culinary-Culture_2021Issue1) (accessed Nov. 13, 2023).

[22] S. Muhammad et al., “Effect of different environmental conditions on the growth and development of Black Soldier Fly Larvae and its utilization in solid waste management and pollution mitigation,” Environmental Technology & Innovation, <https://www.sciencedirect.com/science/article/pii/S2352186422001985#fig2> (accessed Nov. 15, 2023).

[23] Mindworkz, “Q&A: What are the best humidity levels for farming Bsfs?,” Insect School, <https://www.insectschool.com/production/what-are-the-best-humidity-levels-for-farming-the-black-soldier-fly/> (accessed Nov. 16, 2023).

[24] ScienceDaily. (2021, December 13). Air flow key to ensuring black soldier fly larvae thrive as a sustainable food source. ScienceDaily. <https://www.sciencedaily.com/releases/2021/12/211213133259.htm> (accessed Apr. 3, 2024).

[25] Last Minute Engineers, How Soil Moisture Sensor Works and Interface it with Arduino, <https://lastminuteengineers.com/soil-moisture-sensor-arduino-tutorial/> (accessed Nov. 17, 2023).

[26] T. Agarwal, DS18B20 temperature sensor: Pin Diagram, Working & Its Applications, <https://www.elprocus.com/ds18b20-temperature-sensor/> (accessed Nov. 17, 2023).

[27] N. kalaburgi, Working of DHT sensor - dht11 and DHT22, <https://nerdyelectronics.com/working-of-dht-sensor-dht11-and-dht22/> (accessed Nov. 17, 2023).

[28] Dht22 accuracy test and calibration with Arduino, <https://engineer2you.blogspot.com/2018/10/dht22-accuracy-test-and-calibration.html> (accessed Mar. 29, 2024).

[29] T. Agarwal, BH1750 ambient light sensor - specifications & applications, <https://www.elprocus.com/bh1750-specifications-and-applications/#:~:text=BH1750%20uses%20an%20ADC%20to,a%20clock%20for%20internal%20logic.> (accessed Nov. 17, 2023).

[30] Grove - CO2 Sensor: Seeed studio wiki, [https://wiki.seeedstudio.com/Grove-CO2\\_Sensor/](https://wiki.seeedstudio.com/Grove-CO2_Sensor/) (accessed Nov. 17, 2023).

[31] “Gravity: Analog ph sensor/meter kit v2 (Arduino & Raspberry Pi & Micro:bit compatible),” DFRobot, <https://www.dfrobot.com/product-1782.html> (accessed Apr. 2, 2024).

## Appendix

### Appendix A:

#### A1: Calculation of total food waste from 2018 to 2022

- Total food waste in 2018 = 763 ('000 tonnes)

- Total food waste in 2022 = 813 ('000 tonnes)

To find the rise in total food waste generated:

$$\text{Rise} = \text{Total food waste in 2022} - \text{Total food waste in 2018}$$

$$= 813 - 763$$

$$= 50 ('000 tonnes)$$

To find the percentage rise:

$$\text{Percentage Rise} = (\text{Rise} / \text{Total food waste in 2018}) * 100$$

$$= (50 / 763) * 100$$

$$\approx 6.55\%$$

*Figure 81: Total Food waste Calculation*

## A2: Evaluation of hawker centre's contribution to overall food waste generated

Total food waste per hawker centre per day = 813,000 tonnes / 365 days ≈ 2227.4 tonnes

Total food waste from all hawker centres = 2227.4 tonnes \* 110 hawker centres ≈ 245,014 tonnes

Total Singapore = 813,000 tonnes

Proportion of food waste generated by hawker centres = 245,014 tonnes / 813,000 tonnes ≈ 30.1%

*Figure 82: Calculation of food waste generated from hawker centre*

## Appendix B:

The assessment of moisture content entailed the use of an initially measured mass before introducing any water. Taking B1 as an illustration, where the intended moisture content addition was 20%, a minor deviation occurred during calculation, attributed to human error. The determination of the actual moisture content added followed the formula  $[(77.41 - 60.6) / 77.41]$ , and subsequent calculations adhered to a similar methodology.

### B1: Data collection of resistive sensors (Frass with cocopeat)

*Table B1: Resistive sensor in frass with cocopeat*

Target Frass Mass (g)		Resistive Sensor in Frass with Cocopeat					
Target		Measured Frass Mass (g)	60.06				
Moisture Content (%)	Mass (g)	Measured Mass (g)	Voltage Reading (V)	Analog Read	Industry Dervied	Amount of water added (g)	
0	60	60.06	0	1023	0.000	0	
20	75	77.41	3.74	765.204	22.413	17.35	
40	100	100.99	3.8	777.48	40.529	40.93	
50	120	120.49	3.9	797.94	50.154	60.43	
60	150	150.65	3.95	808.17	60.133	90.59	
70	200	200.63	3.96	810.216	70.064	140.57	
80	300	300.06	4.02	822.492	79.984	240	

### B2: Data collection of resistive sensors (Frass without cocopeat)

**Table B2: Resistive sensor in frass without cocopeat**

Resistive Sensor & Frass without Cocopeat						
Target Frass Mass (g)	60	Actual Frass Mass (g)	60.19			
Target		Measured			Industry Dervied	
Moisture Content (%)	Mass (g)	Measured Mass (g)	Voltage Reading (V)	Analog Read	Moisture Content (%)	Amount of water added (g)
0	60	60.19	0	1023	0.000	0
20	75	75.05	3	613.8	19.800	14.86
40	100	101.57	3.56	728.376	40.740	41.38
50	120	120.83	3.63	742.698	50.186	60.64
60	150	150.6	3.73	763.158	60.033	90.41
70	200	200.32	3.81	779.526	69.953	140.13
80	300	300.53	3.83	783.618	79.972	240.34

### B3: Data collection of capacitive sensors (Frass with cocopeat)

**Table B3: Capacitive sensor in frass with cocopeat**

Capacitive Sensor in Frass with Cocopeat						
Target Frass Mass (g)	60	Measured Frass Mass (g)	60.06			
Target		Measured			Industry Dervied	
Moisture Content (%)	Mass (g)	Measured Mass (g)	Analog Read	Moisture Content (%)	Moisture Content (%)	Amount of water added (g)
0	60	60.06	570	0	0.000	0
20	75	77.41	475.26	26	22.413	17.35
40	100	100.99	411.33	33	40.529	40.93
50	120	120.49	314.65	65	50.154	60.43
60	150	150.65	315.6	60	60.133	90.59
70	200	200.63	300.64	64	70.064	140.57
80	300	300.06	282.75	75	79.984	240

### B4: Data collection of capacitive sensors (Frass without cocopeat)

**Table B4: Capacitive sensor in frass without cocopeat**

Capacitive Sensor in Frass without Cocopeat						
Target Frass Mass (g)	60	Actual Frass Mass (g)	60.19			
Target		Measured			Industry Dervied	
Moisture Content (%)	Mass (g)	Measured Mass (g)	Analog Read	Moisture Content (%)	Moisture Content (%)	Amount of water added (g)
0	60	60.19	579	0	0.000	0
20	75	75.05	474.26	26	19.800	14.86
40	100	101.57	361.47	47	40.740	41.38
50	120	120.83	296.5	50	50.186	60.64
60	150	150.6	287.52	52	60.033	90.41
70	200	200.32	278.62	62	69.953	140.13
80	300	300.53	277.71	71	79.972	240.34

## Appendix C:

C1: Testing of the moisture and temperature sensors positions

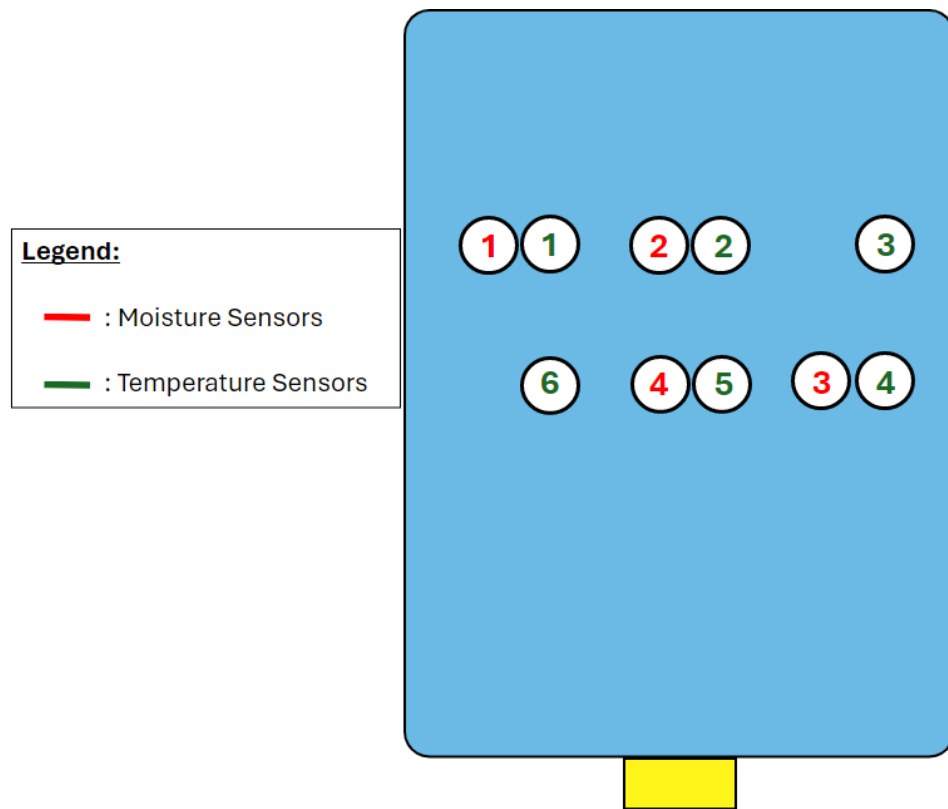


*Figure 83: Sensors positions (Moisture and Temperature sensors)*

## Appendix D:

D1: A schematic diagram of all sensors connected

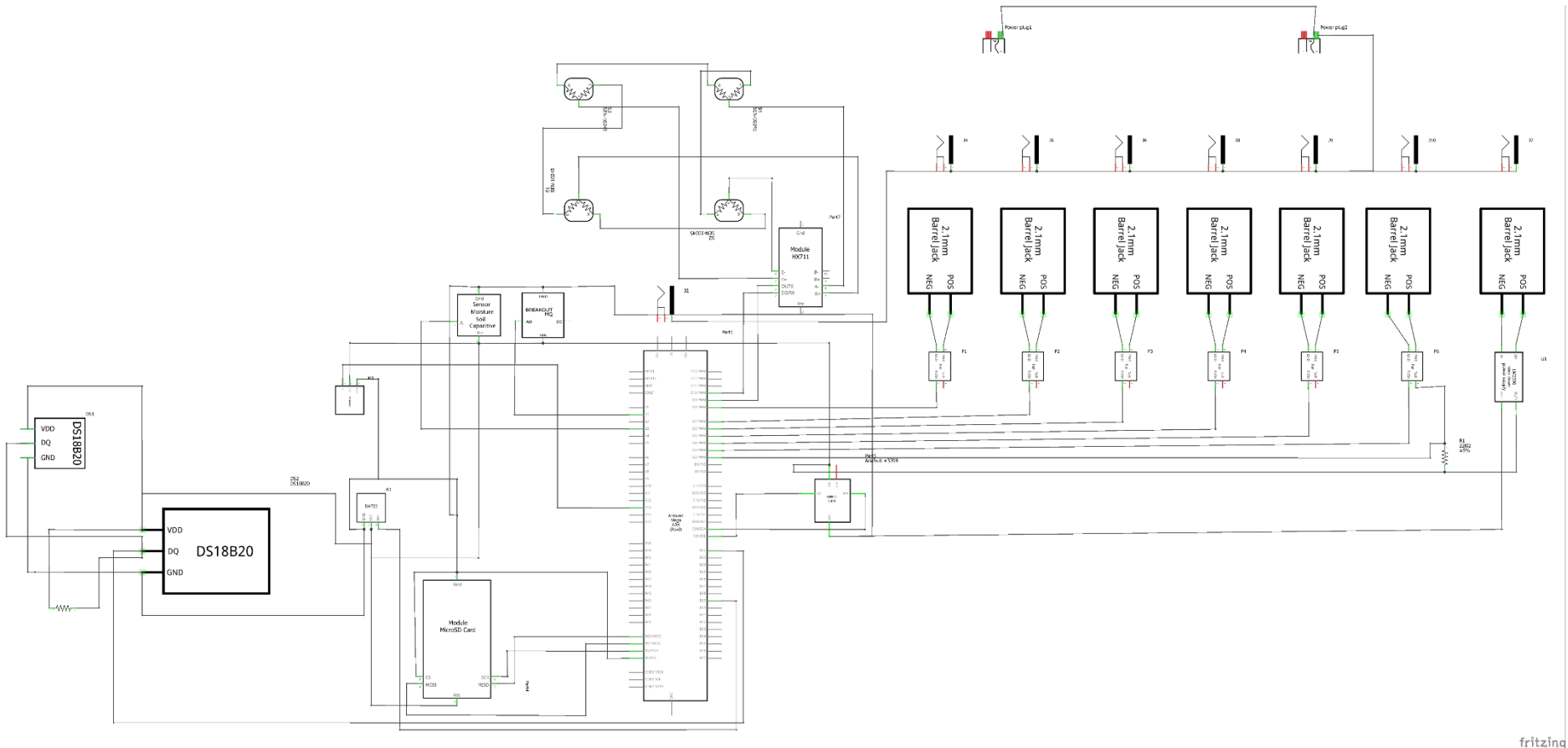


**Figure 84: Schematic Diagram**

## Appendix E:

### E1: Parameter Monitoring and Adjustment Chart for BSFL Bioconversion Process

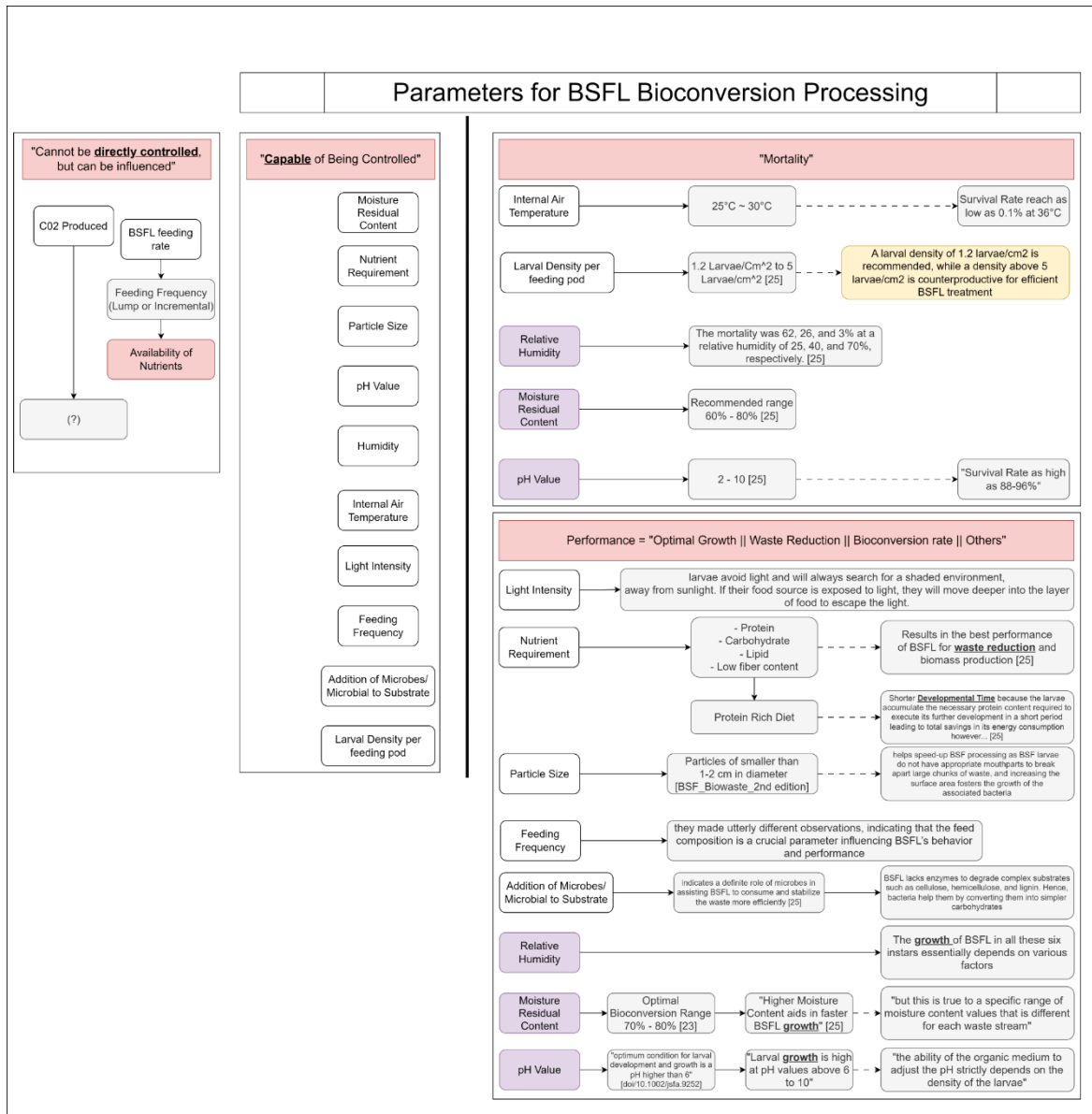
Scale up Version						
Parameters	Before Bio-conversion		Bioconversion Process		After Bio-conversion	
	Electronics	Human	Electronics	Human	Electronics	Human
Residual Moisture Content	X	Measure Adjust	Monitor Indication for Harvest	X	X	Measure Prevent spoilage
pH Value	X	X	Monitor Indication for Harvest	X	X	X
Relative Humidity (Air)	X	X	Monitor Adjust	X	X	X
Internal Air Temperature	X	X	Monitor Adjust	X	X	X
Temperature in the substrate	X	X	Monitor Adjust	X	X	X
Light Intensity	Measure Indicate the presence of light.	Adjust Check that the system is fully close	Monitor Notify BSFL Harvester	X	X	X
Larval Density per feeding container	X	Adjust Human will manually insert BSFL into Feeding pod	X	X	X	X
Gas Emission CO2	X	X	Monitor Indication for Harvesting	X	X	X
Methane CH4	X	X	Monitor Ensure no Gas build up	X	X	X
Ammonia NH3	X	X	Monitor Ensure no Gas build up	X	X	X
Mass of Food Waste	X	Measure Weight-Based Measurement	X	X	Measure Weight-Based Measurement	X

Research						
Parameters	Before Bio-conversion		Bioconversion Process		After Bio-conversion	
	Electronics	Human	Electronics	Human	Electronics	Human
Moisture Content of the Substrate	X	Measure Adjust	Monitor Indication for Harvest	X	X	Measure Prevent spoilage
pH Value	X	X	Monitor Indication for Harvest	X	X	X
Relative Humidity (Air)	X	X	Monitor Adjust	X	X	X
Internal Air Temperature	X	X	Monitor Adjust	X	X	X
Temperature in the substrate	X	X	Monitor Adjust	X	X	X
Light Intensity	Measure Indicate the presence of light.	Adjust Check that the system is fully close	Monitor Notify BSFL Harvester	X	X	X
Larval Density per feeding container	X	Adjust Human will manually insert BSFL into Feeding pod	X	X	X	X
Gas Emission CO2	X	X	Monitor Indication for Harvesting	X	X	X
Methane CH4	X	X	Monitor Ensure no Gas build up	X	X	X
Ammonia NH3	X	X	Monitor Ensure no Gas build up	X	X	X
Mass of Food Waste	X	Measure Weight-Based Measurement	X	X	Measure Weight-Based Measurement	X
Air Flow Rate	X	X	Monitor Data Collection	X	X	X

Figure 85 Chart for BSFL Bioconversion Process

## E2: Overview of Controllable and Influential Parameters in BSFL Bioconversion Process



**Figure 86: Controllable and Influential Parameters**